NASA CR-50992

NUCLEAR
SPACE
UNDERSEAS
INDUSTRIAL

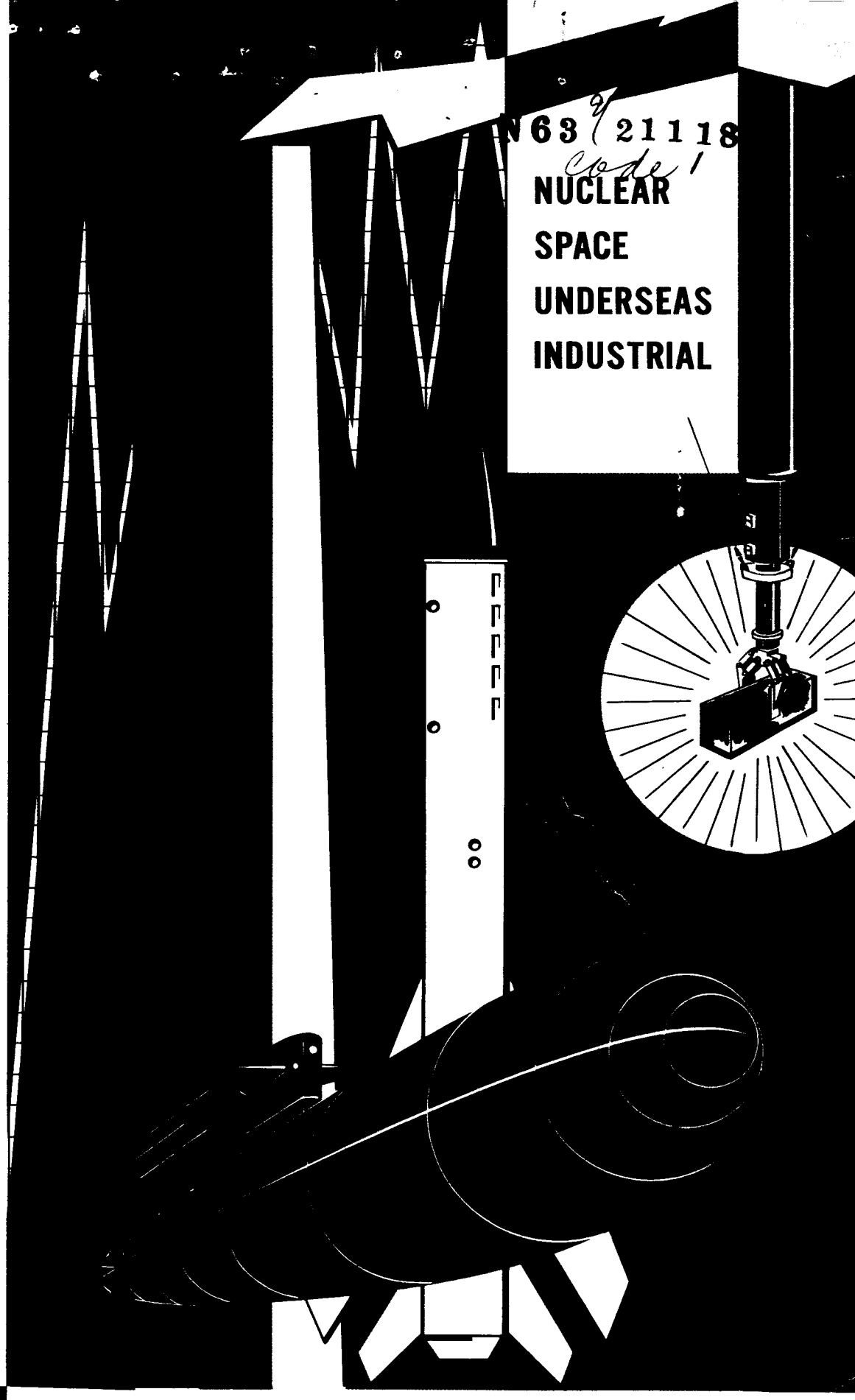

General Mills

REPORT

SQT-7190

FINAL REPORT

LUNAR TV CAMERA MANIPULATOR

(NASA CR-50992) OTS: $12.00 ph, $5.18 mf

Prepared For

JET PROPULSION LABORATORY
California Institute of Technology
Pasadena, California

(JPL Contract No. N-29999)

General Mills' Project 31102

(JPL Contract N-29999; Gen. Mills Proj. 31102)

Prepared by: F. Grimm and
R. Sullivan [1960] 166 p 13 refs

Approved by Harold E. Froehlich
Harold E. Froehlich
Head, Oceanographic &
Space Engineering Section

Electronics Group
GENERAL MILLS, INC.
Automatic Handling Equipment Department
419 North Fifth Street
Minneapolis 1, Minnesota

TABLE OF CONTENTS

LIST OF ILLUSTRATIONS

LIST OF TABULATIONS

1.0 SCOPE

This report is the final technical report under contract N29999 with the Jet Propulsion Laboratory (JPL).

It covers in detail the technical aspects of the work conducted under the contract and such administrative information and decisions as are necessary to understand and to some extent justify the technical approach and the special features of the equipment as delivered to JPL.

2.0 SUMMARY

The work under this contract started as a broad study program directed toward collecting, organizing, and integrating technical information which would be pertinent to and useful in the design of space and lunar manipulators and actuators. It was to include the basic study of motors, brakes, clutches, gears, position indicators, limit switches, lubrication means, temperature control schemes, efficiency, performance, and structura analysis and fabrication means to insure the design of manipulators possessing:

1. The highest degree of reliability.
2. The lightest weight.
3. The lowest possible power consumption.

Shortly after the start of the work, the program was re-directed to one of hardware procurement. A three motion lunar TV camera manipulator in accordance with JPL preliminary specification was mutually agreed upon as being the hardware objective of the program.

This manipulator was to be designed with the best existing components and knowledge available at that time. Special problems created by the lunar environment such as "cold welding", lubrication, brittle fracture of metals at low temperature, and problems created by the temperature extremes of the lunar day and night were to be avoided if possible or solved by the best possible means.

In conference, it was mutually agreed to eliminate concern for both manipulator and TV camera electrical leads in-so-far as providing special slip rings or other means to house the wires in a final clean design.

It was agreed to eliminate the manipulator folding requirement for in flight manipulator storage in an attempt to keep the program within the budget.

A considerable exchange of technical information between GMI and JPL took place at this time to take advantage primarily of JPL's latest thoughts with respect to some of the basic problem areas and to encorporate possible solutions thereto into the basic design of the manipulator.

Some of the consulting personnel at JPL were:

Messrs. Lewis, Barlow, McCreary, Graham, Misculin, Kohorst Meyser, and Adams.

Drawing AL229866 is the TV camera manipulator that JPL and GMI mutually agreed to design and build. Detailed analysis during the design phase of the program brought out several deficiencies in the design as presented on this drawing. Drawing 520949 is the final

assembly drawing of the manipulator as delivered.

Felt to be unique in this manipulator are:

1. The automatic control of temperature.
2. The compactness, efficiency, and low weight of the actuators for their torque output.
3. The means of providing lubrication.

3.0 LUNAR ENVIRONMENT

The lunar manipulator will be subject to three environmental conditions which are detrimental to most materials: 1. extreme heat and cold; 2. high vacuum; and 3. micrometeorite bombardment. During a lunar day which lasts approximately two weeks, the surface of the moon reaches +273°F, and during the two week night period, the temperature falls to -243°F. Observations made during an eclipse of the moon have shown that the temperature falls 200°F in 2 hours. This indicates that the outer layer of material convering the moon has a very high emissivity which approaches that of a black body. A rapid temperature drop is also an indication of shallow heat penetration.

An early investigation by two French researchers, Lyot and Dollfus, found the moon's atmosphere to be 3×10^{-8} atmospheres by volume with the use of a coronagraph. This atmosphere was believed to be composed primarily of SO_2 which has a high molecular weight and is produced by volcanic action as well as the heating of meteorites. The escape velocity of gas on the moon is 1.5 miles per second.

A later investigation by the Mullard Radio Astronomy Observatory,

Cambridge, England places the density of the moon's surface at approximately 2×10^{-13}, assuming that about one molecule in a thousand is ionized. Taking 22 seconds of arc as the upper limit of the angle of refraction, observations showed that it is unlikely that the density of the moon's atmosphere is greater than 6×10^{-13} of the density of the earth's atmosphere at normal temperature and pressure. These observations provide a measurement over a thousand times more sensitive than the upper limit derived by Dollfus from optical measurements.

No information was available on the extent of micrometeorite bombardment on the surface of the moon. A polished metal surface will undergo an emissivity change when roughened by micrometeorite bombardment. However, it is shown in the section on thermal analysis that a manipulator having a low conductivity insulation blanket is practically insensitive to micrometeorite bombardment.

4.0 GENERAL DESIGN PHILOSOPHY

Manipulator reliability was of greatest importance; second to this was a requirement of low power consumption. Although compactness of design and low weight were considered to be important, it was mutually agreed, not to go to the weight saving extremes such as scrolling out the interior of gears and other unusual means, such as using beryllium, which might ultimately be used but would be too costly for this program.

For the most part, the above philosophy was followed. The sequence of events, the timing of the program, and the available

funds did interact to a degree such that a departure from the above philosophy was found to be necessary in the Boom Elevation Drive Assembly as shown double actual size on GMI Drawing 520865. This actuator is considerably over designed for the TV camera manipulator. This came about as follows: A manipulator layout was made early in the program to obtain approval of what was to be built. This original layout utilized a boom elevation gear assembly which proved to be inadequate from a planet bearing load capability. This was discovered during the analytical gear and bearing analysis and after the complex housing had been designed and released for fabrication. Rather than redoing the housing to fit an enlarged gear assembly, the entire actuator was thoroughly reanalized, redesigned, and rearranged to fit within the original housing. This approached resulted in an actuator having very high torque capacity for its size, considerably more than required by the TV camera boom elevation drive, but none-the-less a development believed to be of importance for many other applications requiring high torque from a small and light actuator. A secondary benefit resulted from the redesign. Information was available on "DU" bearing material at that time and it was extensively utilized in the redesigned boom elevation actuator. Furthermore, the following list is indication of the improvements obtained in the redesign.

A. Clutch

Replaced friction material with DU and locked Bellville washer to shaft so that slipping occurs on two DU faces. Nut is also positively locked to shaft.

Clutch shaft now has an outboard bearing rather than a cantilevered bearing. Shaft is supported by roller bearings with one ball bearing a DU washer absorbing any axial load.

B. Idler Shaft

Shaft is now supported by two wide spread roller bearing with DU thrust washers.

C. First Gear Reduction

First gear reduction is most critical from a wear and dynamic load standpoint. A large first reduction permitted the use of a hard pinion against a softer gear thereby increasing pinion life.

D. Output Planetary

New design permitted the use of larger teeth (16 DP) as a result of a lower ratio on this stage. Pinion diameter increased from ½ inch to 3/4 inches. Sun and planets have been lengthened to reduce tooth and bearing loads. Straddle supporting of planet shafts reduces deflection thereby insuring line contact of gear teeth. An appreciable safety factor against shock and inertia loads incurred by sudden stopping is now provided.

E. Sun Gear Bearings

Pilot bearings have been added to sun gears as a means of insuring line contact on teeth. Tilting or cocking of sun gears is reduced to a minimum.

F. Running Clearance of Cages

Carriers are pinned to sun gears to prevent cage assemblies from rubbing against each other. DU thrust bearings and one ball bearing

mounted in sun gears absorb any axial load.

G. Roller Bearings

Roller bearings have been substituted for ball bearing on planet gears. Radial load capacity of roller bearings is very high compared to ball bearings. With the exception of one small ball bearing, roller bearings are used throughout, end thrust being controlled by DU washers.

H. Output Shaft

Output shaft diameter has been increased from 9/16 to 1 inch. With the uncertainty of shock and inertia loads encountered when the boom strikes the mechanical stops in event of limit failure, a shaft having a high safety factor appeared necessary. A larger hub and more dowels have also been added for this purpose.

I. Limit Switches

To avoid striking the mechanical stops, the limit switches have been repositioned for finer adjustment. Slotted holes in the mounting brackets have been added to simplify adjustment.

J. Slip Rings

To avoid the possibility of the slip rings vacuum welding to the shafts, thick walled DU slip rings have been substituted for gold plated copper rings. Rubbing pressure has been increased and more evenly distributed with the use of garter springs. DU material has been described in the literature as having fairly good thermal conductivity.

4.1 Design Philosophy With Respect to Friction

Friction between moving surfaces is one of the most troublesome and undefinable problems encountered in the design of mechanisms. All surfaces, regardless of how smooth, appear as a series of peaks and valleys under sufficient magnification. [1*] The major components of frictional force for most materials are believed to be:

A. The force required to shear welded contact areas.

B. The force required to push the asperities of the surface through the other.

C. The force required to overcome the interlocking microscopic mountains and valleys of each surface.

Under the atmospheric environment, such as we have on earth, metals form an oxide layer which protects the metal and plays an important but complicating role in the frictional behavior of the materials. The oxide layer does, however, provide a plane of distinction between two flat surfaces. In a vacuum or space environment this oxide layer is usually evaporated from the metal leaving a chemically clean metallic surface. In theory, two chemically clean metallic surfaces lose their individual identity when brought together. This phenomena has been referred to as "cold welding" and designers of mechanisms for use in a space or lunar environments have been cautioned to be aware of this phenomena as it will tend to freeze practically any mechanism. Beyond this, there is little factual data

*Superscripts refer to references listed in Section 11.0.

to indicate the effect of material composition, load, speed, time, temperature, etc. The difficulty in obtaining this data is caused by the difficulty in obtaining a high vacuum on earth.

Intuitively, one suspects that higher load, identical materials, clean surfaces, higher temperatures, longer time, and forced sliding between the surfaces aggravates the problem or promotes cold welding. The engineer then, being given the task of designing equipment for an environment of unknown consequences, has several alternatives:

A. He can say it is impossible and quit.

B. He can ignore the supposed problem.

C. He can use his ingenuity in an attempt to avoid the basic problem.

D. He can use his ingenuity in an attempt to avoid the basic problem and at the same time provide (in the the design) several alternative courses of action to take advantage of additional knowledge as acquired in the months and years to come.

Obviously, since we believe in this work, the fourth choice is the proper one and is the one taken on this program.

Accordingly, the following ground rules were formulated:

A. Highest possible efficiency between contacting components is desirable as this automatically means less friction.

B. Rolling friction is preferable to sliding friction.

C. Lower operating temperatures are desired.

D. Dissimilar materials are advantageous.

E. Areas of high surface pressure should be avoided, particularly, if the local speed is also high.

These rules brought out the following general conclusions:

Gears in their order of preference as indicated by their efficiency (for a given set of conditions) are itemized below.(1)

A. Internal cycloidal tooth gears

B. External cycloidal tooth gears

C. Internal involute tooth gears

D. External involute tooth gears

E. Helical gears

F. Worm and spiroid gears

Cylindrical roller bearings are preferred over ball bearings since their contact areas are greater for a given size.

Dissimilar materials like Teflon and steel or brass and steel should be used adjacent to each other.

Solid lubricants are preferred over liquid lubricants because a liquid would not separate the surfaces in a static condition; i.e., hydrodynamic journal lubrication is dependent upon having relative motion between the components to drag the fluid in, which then separates the shaft from the journal. In any manipulator, static internal gear loads are inherently applied during manipulator down periods or in periods of standby. Time of these static applied loads could be long. It was felt to be advantageous to avoid the necessity of having to place the manipulator into a "rest" rack and counterbalancing did not

appear practical.

The reported mechanical locking of thin Teflon bits to mating metal surfaces should be exploited.[1]

As much mechanism as possible should be sealed with a normal environment. In a sense, a sealed gear box in space with one atmosphere sealed in presents the same situation as trying to get a high vacuum on earth inside the gear box. We know that this latter problem is difficult, to say the least, so perhaps the sealed gear box in space will maintain somewhat of any environment for an appreciable period of time. The difference between the two cases is that space has a virtually unlimited pumping capacity on the gear box interior, none-the-less the outgassing of the gear box interior can conceivably take an appreciable period of time. Perhaps a slow outgassing ingredient can be added if necessary.

Mechanisms employing large steps in speeds and/or loads or transmittal of loads by flexing materials should be avoided, as power losses (or friction losses) equal the summation of the products of local speed times local load. One large product in a high reduction stage can easily overshadow the summation of several small ones. Differential reducers although compact are inefficient for this reason.[3]

5.0 MANIPULATOR DESCRIPTION

Drawing 520949 in an overall layout and assembly drawing for the Lunar TV camera manipulator. It consists essentially of three actuators, supporting structure, and temperature control components. The temperature control elements are completely automatic in operation and are described in detail in Section 9.0 of this report.

The basic structure of the manipulator is of skin or shell type, surrounding the actuators, and made of copper to facilitate heat transfer to the temperature control surfaces.

There are 3 actuators in the manipulator, 2 are almost identical and provide torque for the camera pan and camera tilt functions. The third is the boom elevation actuator and is shown double actual size on drawing 520865. Components in this actuator are:

A. A DC brake with powdered iron brake disk.

B. Globe Motor FCL75A219.

C. An adjustable mechanical friction type clutch located between the spur and planetary gear stages.

D. Five gear stages, two spur and three planetary each with pitch and face width required for the design torque output of 5000# in.

E. An output shaft which drives:

   a. A position sensing pot (Spectrol Miniature Pot #140 with 500 ohms resistance)

   b. Two limit switches

F. Flange type support with bearing material to allow relative movement between the gear head and housing for the temperature extremes encountered in service.

G. A bellows type seal seals the volume of an inside the copper housings and permits shaft rotation by means of a carbon filled teflon seal riding against a lapped seal face which is attached to the actuator output shaft.

H. Ball bearings in the motor are Barden bartemp bearings. These bearings have ball retainers made from Teflon filled with molybdenum disulphide.

I. Planet bearings, three in each output stage planet gear, are of the cylindrical roller type giving the highest possible capacity for the available space.

J. Planet gears are supported at both sides or "cage supported" to eliminate possible misalignment under load.

K. Planet gears are teflon coated for dry lubrication and are spaced laterally by "DU" material.

L. Gear pitch ranges from 64 at the high speed end to 16 and the low speed end.

M. The motor has a 300 series stainless steel housing and windings of Anaconda ML insulated magnet wire with Herox impregnated varnish.

N. The output shaft is integral with the output planet cage which allows a wide support for the highly loaded overhung output load. These latter bearings are made from "DU" material and give a very rigid support to the output shaft.

O. Planet cage location is provided by small roller bearings and lateral spacing by "DU" thrust bearing material.

The actuators for the camera pan and tilt functions are shown double actual size on drawing 229871. Components in this actuator are:

A. A DC brake with powdered iron brake disk

B. Globe Motor FC75A220

C. An adjustable mechanical friction type clutch located between the motor and gears

D. Five constant pitch planetary gear stages

E. An output shaft which drives:

a. A position sensing pot (Spectrol Miniature No. 140 with 500 ohms resistance.

b. Two limit switches and activating plungers.

F. A flange type actuator mounting plate is provided near the right end

G. A bellows type seal, seals the volume of air inside the copper housings and permits shaft rotation by means of a carbon filled teflon seal riding against a lapped seal face integral with the actuator output shaft.

H. Ball bearings in the motor are Barden "bartemp" bearings. These bearings have ball retainers made from Teflon filled with molybdenum disulphide.

I. Ball bearings in each planet gear are gold plated for dry lubricants.

J. Planet gears are teflon coated for dry film lubrication.

K. Spacing between planet carriers is provided by a ball located on the center axis of the gear reducer, one between each sun gear and the adjacent carrier.

L. Planet gears are cantilever supported on hardened pins pressed into the planet gear carriers.

M. Motors have housings of 300 series stainless steel and windings of Anaconda ML insulated magnet wire with Herox impregnated varnish.

6.0 SPECIFICATIONS AND COMPONENT PROCUREMENT

6.1 JPL Preliminary Specifications for TV Camera Manipulator Study

The first need for an articulated TV camera mount will probably be on a vehicle which is soft landed on the Lunar surface. The configuration of such a vehicle is not now definitely known. Various contractors are studying the problem. For the purpose of designing a TV boom, the following information can be assumed. As more detailed facts become available, they will be forwarded.

The vehicle will operate during both the lunar day and the lunar night. This means that the temperature extremes of -250°F and

+275°F must be considered. The vehicle will alight on three legs from one to four feet in length. The body of the vehicle will be a cylindrical object five feet in diameter and two feet thick. It will be oriented within 15° of horizontal. The camera should be able to scan in all directions. The sky and the landscape must be visible. The field of view must include the surface directly beneath the vehicle, as visual monitoring will be required on experiements such as the boring of a hole in the surface.

The TV camera has not yet been developed in its final form. A safe design estimate is a cylinder seven inches in diameter and sixteen inches long, weighing thirteen pounds with the center of gravity seven inches from the lens end. The camera can operate in any position. Some provision should be included to record camera orientation. The package contains the lens, the vidicon tube, the focus mechanism, and the camera electronics. Any fitting can be used to attach the camera to the boom. From fifteen to twenty leads must run through the boom to the body of the vehicle. If a magnetic vidicon tube is used, eight leads will be required from the vidicon and nine to the camera electronics package. Of these, the two focus leads will carry a watt or two of power and the six horizontal and deflection leads will total a watt of power. The coils can be designed so that this is either low current-high voltage or low voltage-high current. Of the additional leads, two are filament leads which carry 300 milliamps at 6.3V. The remainder carry only a few mills of current. Should an electro-static vidicon be used, the number of leads is reduced to

about thirteen and the power requirements drop. No shielding is required on these wires. The breadboard cameras in operation at the Jet Propulsion Laboratory are using instrument wire cables which are roughly the size of a pencil and extremely flexible. In addition, if a Zoomar lens is employed, a control cable will be necessary. The control cable on present commercial Zoomar units is a four-lead, shielded .225 inch diameter cable. Low rates of scan (one frame per second typical) will be used to reduce TV power transmission power requirement. This means that camera scanning will be of a start-stop nature. Angles of view will, of course, vary according to the lens being used. (Typical values are 60° for wide angle, 10° for normal, and 1° for telephoto.) With a Zoomar lens the angle will vary, so a completely flexible scan capability should be built into the boom.

6.0 Manipulator Target Specifications

It was desired by JPL to endeavor to design the equipment for a lunar environment for a total mission life of 10,000 hours (1 plus year). The equipment was to operate during a lunar night if possible.

The following manipulator specifications were arrived at by estimating the manipulator component weight (earth weight was used because of the desirability of having sufficient torque for testing on earth), internal friction, and camera coverage desired. Since the environmental effects on the manipulator are unknown (JPL is currently attempting to establish this) these target specifications are for a normal room environment. Duty cycle specifications were arrived by

attempting to anticipate a programming sequence for a TV camera manipulator photographing and transmitting to earth a panoramic sequence of picutres of the lunar landscape.

Manipulator Target Specifications

	Speed RPM	Torque Lb-In	Travel Degrees	Duty Cycle Time
Boom Elevate	.59	543	±90	1 min on; 10 min off
Camera Pan	.60	49	±180	2 secs on; 20 secs off
Camera Tilt	.60	49	±180	2 secs on; 20 secs off

Reliability was stressed to be of prime importance.

6.3 Component Specifications

To meet a tight delivery schedule (6 months after JPL and GMI agreed to build a 3 motion manipulator) somewhat arbitrary specifications were established with component manufactures on a more or less give and take mutually agreeable basis. Initially, we specified an extreme environment and through the medium of long distance telephoning established what the manufacturers could expect to do on a fixed price, best effort, non-guaranteed basis. To obtain components on a guaranteed basis would have meant practically off the shelf state of the art effort which in the case of the motors in particular would have greatly reduced the manipulator performance.

The following environmental specifications were thus established:

Ambient temp $-200^{\circ}F$
$+400^{\circ}F$

Ambient pressure 10^{-1} to 10^{-2} mm Hg

6.3.1 Motors

In addition to the above environmental and life specification the following specifications were mutually agreed to by the motor manufacturer (Globe Industries, Inc.) and GMI.

Camera pan and tilt motors - FC 75A220

Torque - 1 in oz @ 10,000 to 11,500 rpm

Brake - 1/2 in oz minimum holding torque (Stopping time not critical)

Size - 1.657 inches diameter; 3 1/4 in long

Voltage - 115 volts, 400 cycles, 3 phase

High starting torque required

High reliability of prime importance

Reversible

Duty cycle - 2 secs on; 20 secs off

Boom elevate motor - FCL 75A219

Torque - 3 in oz @ 10,000 to 11,500 RPM

Brake - 1 in oz minimum holding torque (Stopping time not critical)

Size - 1.675 inches diameter; 3 3/4 in long

Voltage - 115 volts, 400 cycles, 3 phase

High starting torque required

High reliability of prime importance

Reversible

Duty Cycle - 1 min on; 10 min off

Several trial windings were made by Globe to determine torque and speed before fabricating the motors. The highest starting torque for each of the two four motor series were chosen. These values for the selected motors were:

	Torque (in oz)		Power (watts)	
	Starting	10,000 rpm	Starting	Running
FCL75A219	10.6	3	160	35
FCA220	4	1	57	16

With these values thus established the remaining manipulator parts were designed and detailed.

6.3.1.1 Motor Winding

Anaconda ML magnet wire was specified for use in the actuator motors on the basis of its reported[1] superior overload resistance, its exceptional chemical stability, and its high operating temperature without outgassing. Ceramic impregnated and glass insulated windings were considered but eliminated on the basis of conversations with several manufacturers who had experience with winding motors with these special materials. ML magnet wire is coated from a solution of an ML polymer, a new chemical developed by Du Pont. This polymer reportedly represents a great improvement in heat resistance compared to presently used organic coatings. (Field trials, up to one year in September 1960) reportedly have proved the outstanding thermal resistance of this wire. Herox dipping varnish, which is based on the same chemical polymer as ML, was used to insure chemical capatibility between the wire insulation and varnish.

6.3.2 Bearings and Lubrication

Bearing selection for the manipulator was governed largely on the availability of special types from the bearing manufactures and/or the adaptability of the bearing to be lubricated by special means. Twenty-eight bearing manufacturers were interrogated for their recommendations in the use of bearings under vacuum conditions for a +400 degree F to -200 degree F temperature range. No manufacturer would guarantee their product for this environment, insufficient lubrication being the primary reason. Approximately 15 manufacturers of lubricants were interrogated about their product. No liquid lubricant was found to be serviceable at the -200°F temperature specification. Several bearing manufacturers had tried the various dry films such as molybdenum disulphide without success. Dry films of molybdenum disulphide were also stated to be adversely affected by most other lubricants and were finally excluded from further consideration for this reason. Ceramic bearings were excluded on the basis of their fragility, limited experience, and long delivery.

The following bearings and dry lubricant material seemed to offer the best possible chances of success and were incorporated into the design.

Manufacturer	Product	Use
New Hampshire	Gold plated ball bearings	Planet gear bearings in pan & tilt actuators
Barden Corporation	Ball bearing with filled Teflon keeper	For very light loads only. Used in motors & high speed shaft support in pan & tilt actuators

Dupont Company	Teflon material	Coating gear teeth (all planet & spur gears) Powder dust Liquid spray
Glacier Metal Company	DU-material*	Bushings & Thrust applications in boom elevation actuator.
Norma Hoffman	Cylindrical Roller Bearings	Planet gear bearings in boom elevation actuator

*Described in Section 6.3.4.1.

Other standard bearings were utilized as necessary to complete the manipulator design. Once it has been determined which bearing and lubricant is satisfactory, hopefully by the tests now being conducted at JPL, special bearing designs and sizes will be fabricated by industry. This will give the designer a choice of selection not now available.

6.3.3 Actuator Seal

Hermetic sealing of the actuators although very desirable presented design difficulties beyond the scope of current practice; therefore the best possible moving face seal arrangement was sought. Successful sealing is dependent upon several factors such as:

surface finish

clearance

deflection under load

temperature

face loading

speed of rotation

wear rate

duty cycle

A bellows type seal was selected on the basis of its ability to maintain face loadings at the temperature extremes and after considerable wear of the seal face has taken place. Carbon filled teflon was selected on the basis of reported favorable outgassing characteristics, its usability at the temperature extremes, and the low friction coefficient, especially the static coefficient, and low wear rate. The Hydrodyne Corporation machines these bellows seals and fabricated the three seals (one on each actuator output shaft) for the lunar TV camera manipulator. They were purchased to the same environmental specification as previously given for the bearings and motors.

6.3.4 Component Materials

The temperature environment necessitated a close examination of the materials comprising the manipulator. Cold brittleness was to be avoided and minimum expansion-contraction between adjacent materials is desirable. Hardenable steels were necessary to carry the loads and impart good wear resistance to various parts.

Copper was selected as the structural sheet material on the basis of its ability to rapidly transmit heat to the temperature control surfaces and its expansion coefficient being nearly equal to that of 300 series stainless steel. Motor housings are of 300 series stainless steel to minimize distortion over the wide temperature spectrum. Most gears, planet cages, and cases are of 17-4PH

stainless steel, selected because various hardnesses can be achieved at moderately low temperatures with little distortion. The three sun gears in the boom elevation actuator are case hardened high nickel 9310 steel. These gears are stressed the highest of any parts in the manipulator and accordingly have the toughest core (even at low temperature) and hardest case that we could employ.

6.3.4.1 DU Bearing Material

Du is a prefinished high performance bearing material used for bushings, thrust washers, hemispherical cups and slides. No lubricant is needed with any of the various bearing styles. DU material possesses the following properties:

1. The bearing surface exhibits frictional and wear resistance properties comparable with those of a lubricated whitemetal bearing.
2. It can be used at temperatures from -200° to +280°C (-328°F to 536°F) with substantially unchanging frictional and wear resistance properties.
3. It will operate with heavy loads and at high speeds.
4. It is tolerant of dirty surroundings.
5. The composite material is thin; bearings are light and take up little space.
6. The bearing surface is resistant to corrosion by industrial liquids and gasses.
7. There are no static electricity phenomena.
8. Unaffected by gasoline, industrial alcohol and other solvents.

9. Smooth sliding; no high breakaway friction.

10. High strength.

DU is made up of three layers; a backing strip of steel, tin plated to protect it from atmospheric corrosion; a middle layer of porous tin bronze (made by sintering on to the steel backing a layer of spherical bronze powder) filled solidly with a mixture of PTFE (Polytetrafluoroethylene called Teflon by Du Pont) and fine lead powder; an overlay about 0.001 inches thick of the same PTFE - lead mixture. Each layer has a specific purpose.

a. The steel backing provides the structural strength needed to assure stability and lasting tight interference fit.

b. The impregnated bronze interlayer, two interlocked sponge-like networks, provides a conductive path to carry heat from the bearing surface to the housing and acts as a reservoir of the PTFE mixture to assure a constant smear of low friction, low wear, material on the bearing surface.

c. The overlay applies, during the short running-in period, a coating of the PTFE-lead mixture to the journal or other mating surface, smoothing over irregularities and imparting low-friction properties to the assembly.

The yield strength in compression is 40,000 pounds per square inch minimum. Thermal conductivity is 0.1 cal. per second per $cm^{o}C$ and coefficient of linear expansion is equal to 15×10^{-6} per ^{o}C.

Loads approaching the full yield strength can only be imposed when there is little or no movement.

At very low speeds (1 to 20 ft. per minute) and at very heavy loading (up to 36,000 pounds per square inch) the coefficient of friction is at a minimum, falling within the range of 0.05 to 0.10. Within the more normal range 10 psi to 1,500 psi or speeds from 40 feet per minute to 1,000 feet per minute, the coefficient of friction lies between 0.10 and 0.18, a range similar to the figures for conventional oil-lubricated bearing materials.

DU has a thermal conductivity equivalent to that of an oil-impregnated bearing, or about 60% that of solid bronze. The thermal expansion coefficient lies midway between that of steel or cast iron and aluminum or bronze, so that journal bearings will not lose interference fit in any normal type of housing.

As a guide to what may be expected from DU, the results of comparison tests carried out a PV = 16,000 pound per square inch x feet per minute are given in the following tabulation.

Bearing Material Tested Against Mild Steel with Ground Surface Finish of 16 Micro Inches	Testing Time, Hours	Wear at End of Test, Inches
Glacier DU	1,000	Less than 0.001
Graphite and lead bronze	158	0.010
Oil-impregnated porous bronze	105	0.010
Phenolic resin with molybdenum disulphide	73	0.005
Graphite: bearing grade	24	0.005

Woven asbestos impregnated with resin and molybdenum disulphide.....0.8.....0.005

Nylon.....0.3.....0.010

7.0 TEST DATA

7.1 Motors

The motors used on the Lunar TV Manipulator were modified Globe type FC induction motors built on a "best effort" basis to meet the following requirements.

Voltage: 115 V, 400 cycle, 3 phase

Ambient temperature: -200°F to +400°F

Ambient pressure: 10^{-1} to 10^{-2} mm of Hg

Life: 10,000 hours at rated duty cycle

The boom elevate motor is identified by Globe part number 75A219. Motors for the Camera Rotate and Camera Tilt drives are identical, and are identified by Globe part number 75A220.

Globe estimated the performance of these motors to be:

	75A219	75A220
Torque	3 in oz at 10,000 to 11,500 rpm	1 in oz at 10,000 to 11,500 rpm
Starting torque	5 to 6 in oz	$2\frac{1}{2}$ to 3 in oz
Power input	45 - 50 watts @ 3 in oz	20 watts @ 1 in oz
Starting surge	80 watts	40 watts
Duty cycle	1 min on - 10 min off	2 sec on - 20 sec off

DC holding brakes were also incorporated into these motors. For the 75A219 motor, the brake torque is 1 in oz minimum, and for the 75A220 motor the brake torque is $\frac{1}{2}$ in oz minimum. Power requirements for the brakes was estimated to be 7 to 10 watts each.

To meet the severe operating conditions, Globe used 300 series stainless steel motor housings, Bar Temp ball bearings, Anaconda ML insulated magnet wire, Herox impregnating varnish, and special brake discs consisting of a powdered iron disc against a steel disc.

No test or performance data was supplied with these motors. Globe did not have facilities for testing under the specified operating conditions.

Tests at room conditions were made by our electrical engineering section to determine the operating characteristics of the motors. This data is given in GMI drawings 520739 and 520740. Comparison of these test curves with the typical curves shown for type FC motors in the Globe catalogue indicates that the calculated efficiency is much lower than the "typical efficiency". Also, the power input indicated by the tests is approximately twice the estimated requirement.

An evaluation of the test methods was made to account for the apparent discrepancies. Investigation showed that the method of determining power input was incorrect. Normally two watt meters are used for measuring power in 3 phase circuits. The total power is the sum of the two meter readings. In the tests made, only one watt meter

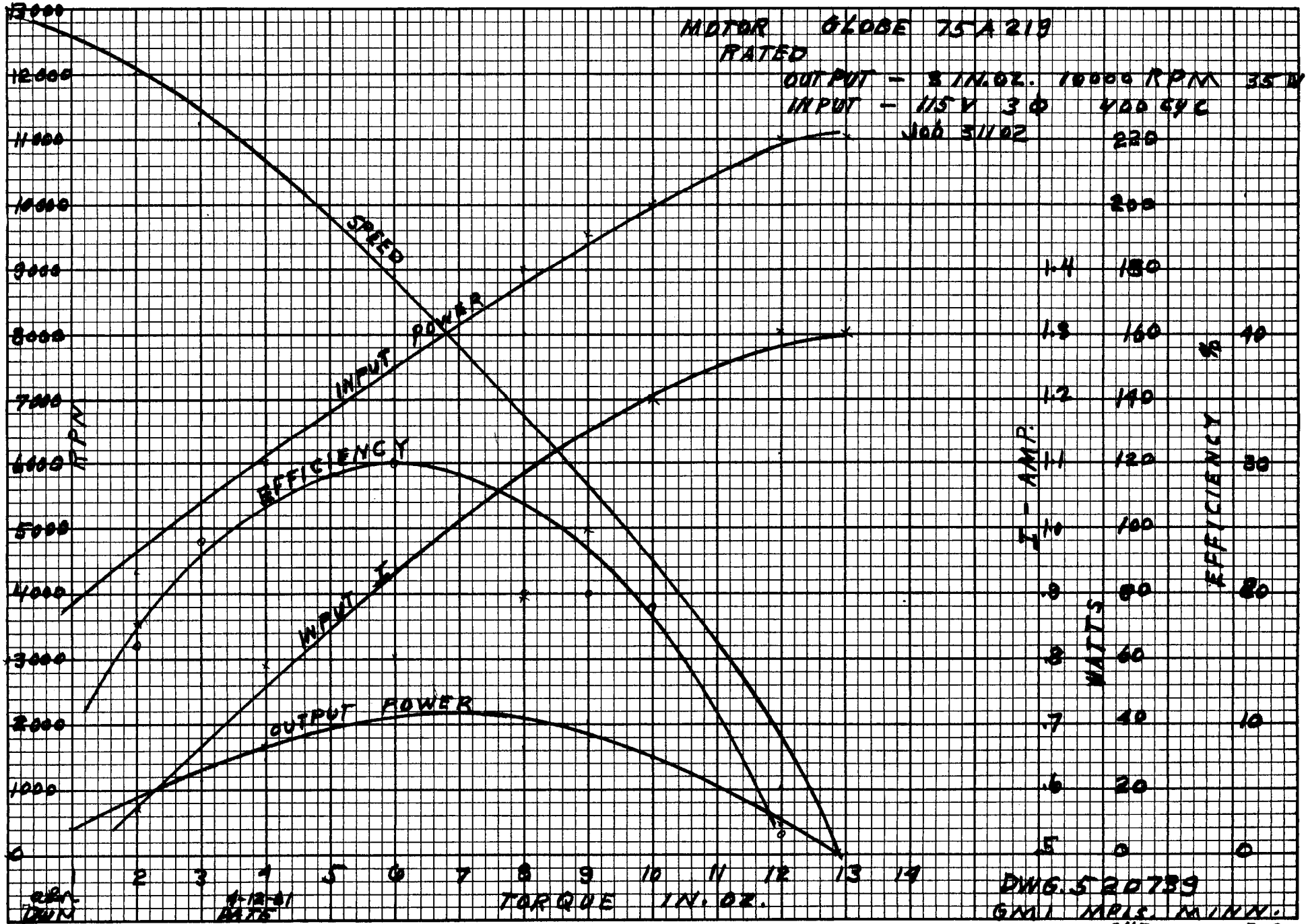
MOTOR GLOBE 75-A219
RATED
OUTPUT - 8 IN. OZ. 10000 RPM 35 W
INPUT - 115 V 3 Φ 400 CYC
.10A 3/1102
SPEED
INPUT POWER
EFFICIENCY
INPUT I
OUTPUT POWER
RPM
AMP.
WATTS
EFFICIENCY
%
TORQUE IN. OZ.
DWG. S20739
GMI MPLS. MINN.
SHEET 1 OF 2

JOHN FLUKE WATTMETER HOOK UP

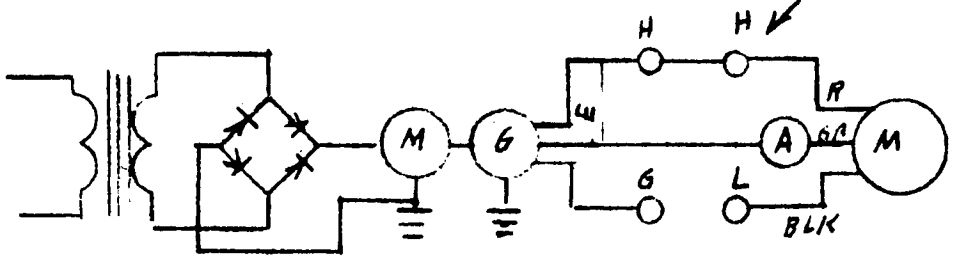

520739

SHEET OF

REVISIONS

SYM	ECO NO	DESCRIPTION	DATE	APPROVAL

OUTPUT			INPUT			FLUKE READINGS					EFF.	P.F.
WATTS	TORQUE	RPM	IA	E	VA	WATTS TOTAL	WATTS METER	I	A	E		
	#2				√3EI							
0	0	13000			100	60	80	.5		115	0	
16.3	2	12000				90	45	57			16	
23.2	3	11250				100	50			115	24	
29.	4	10500			160	120	60	.8		115	24	.75
44.6	6	9900			160	150	75	8		115	30	.94
36.	8	6500			180	180	90	.9			20	1.0
32.6	9	6200				190	95	1.0			20	
32.4	10	4800				200	100	1.2			18	
8.4	12	1000				220	110	1.3			3.8	
0	B	0	1.3			220	110	1.3			0.0	

MAGNETROL DYNAMOMETER WAS USED

1294-

ADDITIVE FINISH	UNLESS OTHERWISE SPECIFIED: DIMENSIONS ARE IN INCHES TOLERANCES FRACTIONS DECIMALS ANGLES RADII	DR	ENGR	NAME	General Mills, Inc. MECHANICAL DIVISION 1620 CENTRAL AVENUE N. E. MINNEAPOLIS, MINNESOTA
		CHKD	APPD	MOTOR DATA GLOBE NO. N02 75A219	
		ORIGINAL DATE OF DRAWING 4-11-61			
MATERIAL	HEAT TREATMENT	APPLICABLE SPECIFICATIONS:		SCALE	DWG SIZE A
				UNIT WT	520739 SHEET 2 OF 2

8428 MD-9A

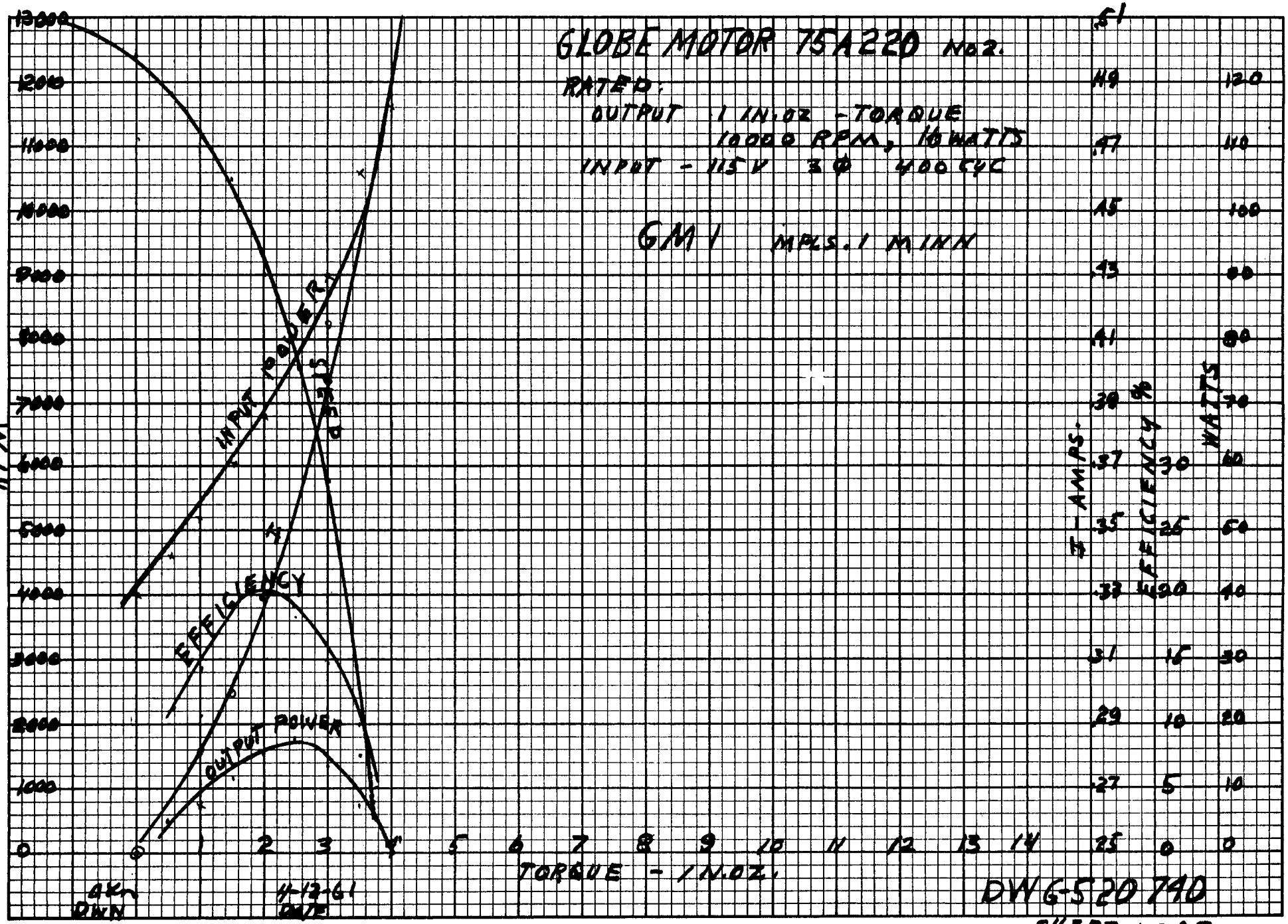
GLOBE MOTOR 75A220 No2.
RATED:
OUTPUT 1 IN.OZ - TORQUE
10000 RPM, 16 WATTS
INPUT - 115 V 3 Φ 400 CYC
GM1 MPLS. 1 MINN
RPM
AMPS.
EFFICIENCY %
WATTS
INPUT POWER
SPEED
EFFICIENCY
OUTPUT POWER
TORQUE - IN.OZ.
4K
DWN
4-12-61
DATE
DWG-520 740
SHEET 1 of 2

JOHN FLUKE WATTMETER HERE

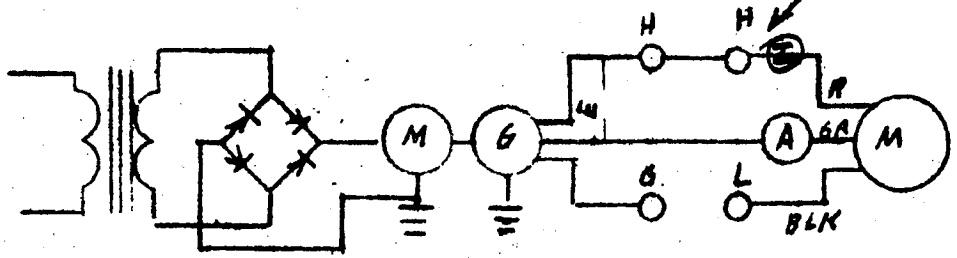

520740

SHEET 2 OF 2

REVISIONS

SYM	ECO NO	DESCRIPTION	DATE	APPROVAL

OUTPUT			INPUT			FLUKE READINGS					EFF.	PF
WATTS	TORQUE	RPM	IA	E	VA	WATTS		I	A	E	%	W/VA
					EIVS	Total	METER					
0		12500			52	40		.25		118		
9.16	½	11750			54	46	23	.26		118	12.0	85
7.6	1	11200			58	52	26	.28		115	14.6	
10.8	1.5	10500			63	60	30	.3			18	
13.4	2	9000			68	68	34	.33			20.	1.0
13.8	2.5	7500			79	78	39	.37			15	.98
13.4	3.0	5975				90	45	.42			14.8	
7.8	3.5	2000			107	106	53	.49			7.4	
2.6	3.75	1000				116	58	.53			2.5	
.86	4	200				116	58	.53				
	4	0										

$$\text{WATTS} = \frac{TN \times 746}{1008000} = \frac{TN}{1344}$$

ADDITIVE FINISH	UNLESS OTHERWISE SPECIFIED: DIMENSIONS ARE IN INCHES TOLERANCES FRACTIONS DECIMALS ANGLES RADII	DR AJM	ENGR AJM	NAME MOTOR DATA GLOBE NO. 2 75A220 3φ 400 cy.
		CHKD AJM	APPD	
		ORIGINAL DATE OF DRAWING 4-11-61		
MATERIAL	HEAT TREATMENT	APPLICABLE SPECIFICATIONS:		SCALE / UNIT WT / DWG SIZE A / 520740 / SHEET 2 OF 2

General Mills, Inc.
MECHANICAL DIVISION
1620 CENTRAL AVENUE N. E.
MINNEAPOLIS, MINNESOTA

8459 MD-9A

M

was used, and it was assumed this was $\frac{1}{2}$ of the total power. This is not true for this case as shown by the following analysis.

Measurement of Power in Three-Phase Circuits

The total power in a three-phase circuit is the sum of the powers in the individual phases and can be measured by the proper connection of watt meter in each of the phases as shown below.

The total power in the circuit is usually measured by the two-watt meter method. In the two-watt meter method, each watt meter is so connected that its current coil carries a line current, and its voltage coil is connected to a line voltage. The method is illustrated below.

In the two-watt meter method, the sum of the two meter readings is the total power. The readings of the individual meters are given by:

$$P_1 = E_{ab}\, I_{an} \cos (30^\circ + \theta) \qquad (1)$$

$$P_2 = E_{cb}\, I_{cn} \cos (30^\circ - \theta) \qquad (2)$$

where θ = phase angle

The total power (P_o) is then:

$$P_o = P_1 + P_2 \qquad (3)$$

If the load is balanced:

$E_{ab} = E_{cb} = E_L$ (line voltage)

$I_{an} = I_{cn} = I_L$ (line current)

and:

$$P_o = P_1 + P_2 = 3\ E_L = I_L \cos \theta \quad (4)$$

$\cos \theta$ = power factor

If the load is assumed to be non-reactive ($\theta = 0$):

$$P_1 = P_2 = \frac{P_o}{2}$$

However, a motor is an inductive load and has a lagging power factor (θ = negative angle). The two meter readings then will not read the same as shown by the following examples.

$\theta = -30^\circ$

$$P_1 = E\ I \cos (30^\circ - 30^\circ) = E\ I \cos 0^\circ = E\ I$$

$$P_2 = E\ I \cos (30^\circ + 30^\circ) = E\ I \cos 60^\circ = \tfrac{1}{2}\ E\ I$$

$$P_o = P_1 + P_2 = \frac{3}{2}\ E\ I$$

also:

$$P_o = 3\ E\ I \cos \theta = 3\ E\ I \cos -30^\circ = 3\ E\ I\ \frac{3}{2} = \frac{3}{2}\ E\ I$$

$\theta = -60^\circ$

$$P_1 = E\ I \cos 30^\circ = E\ I\ \frac{3}{2}$$

$$P_2 = E\ I \cos 90^\circ = 0$$

$$P_o = P_1 + P_2 = \frac{3}{2}\ E\ I$$

also:

$$P_o = 3\ E\ I \cos -60^\circ = 3\ E\ I\ (\tfrac{1}{2}) = \frac{3}{2}\ E\ I$$

$\underline{\theta = -75^\circ}$

$$P_1 = E\ I \cos -45^\circ = E\ I - \frac{.707}{2}\ E\ I$$

$$P_2 = E\ I \cos + 105^\circ = -.259\ E\ I$$

$$P_o = P_1 + P_2 = (.707 - .259)\ E\ I = .448\ E\ I$$

also:

$$Po = 3\ E\ I \cos = 75^\circ = 3\ E\ I\ (.259) = .448\ E\ I$$

From the examples shown it is obvious the one meter reading taken in the tests is not $\frac{1}{2}$ of the total power (as assumed), but is some percentage of the total power. The question is: What is the relationship between the total power and the meter reading?

Assuming P_1 was being read on the one meter used (P_1 is always positive), then:

$$f\ P_1 = P_o$$

where f - multiplier

Then from equations (1) and (4):

$$f = \frac{3\ E\ I \cos \theta}{E\ I \cos (\ 30^\circ + \ )} = \frac{3 \cos \theta}{\cos (30^\circ + \ )}$$

$\underline{\text{for } \theta = -30^\circ}$

$$P_o = \frac{3}{2}\ E\ I \qquad f = \frac{P_o}{P_1} = \frac{3}{2}$$

$$P_1 = E\ I$$

and:

$$f = \frac{(\ 3)\ (3/2)}{1} = \frac{3}{2}$$

for $\theta = -60^{\circ}$

$$P_o = \frac{3}{2} E I$$

$$P_1 = \frac{3}{2} E I$$

$$f = 1$$

and:

$$f = \frac{(\ 3)\ (\frac{1}{2})}{3/2} = 1$$

for $\theta = -75^{\circ}$

$$P_o = .448\ E I \qquad f - \frac{.448}{.707} = .634$$

$$P_1 = .707\ E I$$

and:

$$f = \frac{3 \cos (-75^{\circ})}{\cos (-45^{\circ})} = \frac{(\ 3)\ (.259)}{(.707)} = .634$$

From the preceeding analysis it is evident that if the phase angle ( ) was known, the true power input could be determined directly from:

$$P_o = 3\ E\ I \cos \theta$$

or:

$$P_o = f\ P_1 = \frac{3 \cos \theta}{\cos (\quad + 30^{\circ})}\ P_1$$

We do not know , however, we do know E I, as these values were recorded in the test. Therefore, from equation (1):

$$\cos (30^{o} + \theta) = \frac{P_1}{E\ I}$$

$$= \cos^{-1} \frac{(P_1)}{E\ I} + 30^{o}$$

Knowing θ, we can determine P_o from:

$$P_o = 3\ E\ I \cos \theta$$

and check this quantity from:

$$P_o = f\ P_1 = \frac{3 \cos \theta}{\cos (30^{o} + \ )}\ P_1$$

This method was used to revise the test data from GMI drawings 521739 and 521740 for the two motors. This data is attached in the form of data tables and performance curves.

The data and curves for the 75A220 (smaller) motor compares very well with the estimated performance and the "typical" curves in the Globe catalogue.

The data for the larger motor, 75A219, is subject to question. First, the efficiency seems rather high for this type motor. Also, the input power at 3 in oz is indicated to be 36 watts as compared to an estimated 45 to 50 watts. Finally, the "power in" curve flattens off after 8 in oz torque. This is not typical. It should be similar in shape to the "current" curve.

7.2 Actuator Tests

The Pan and Tilt Drive Assemblies (GMI drawing 229871) were mounted on the Test Fixture (GMI drawing 520165) hanger plate and the output shafts coupled to the fixture load shaft. An overhung torque load was applied to the fixture load shaft which resulted in pure torque load on the drive output shafts. The drives were

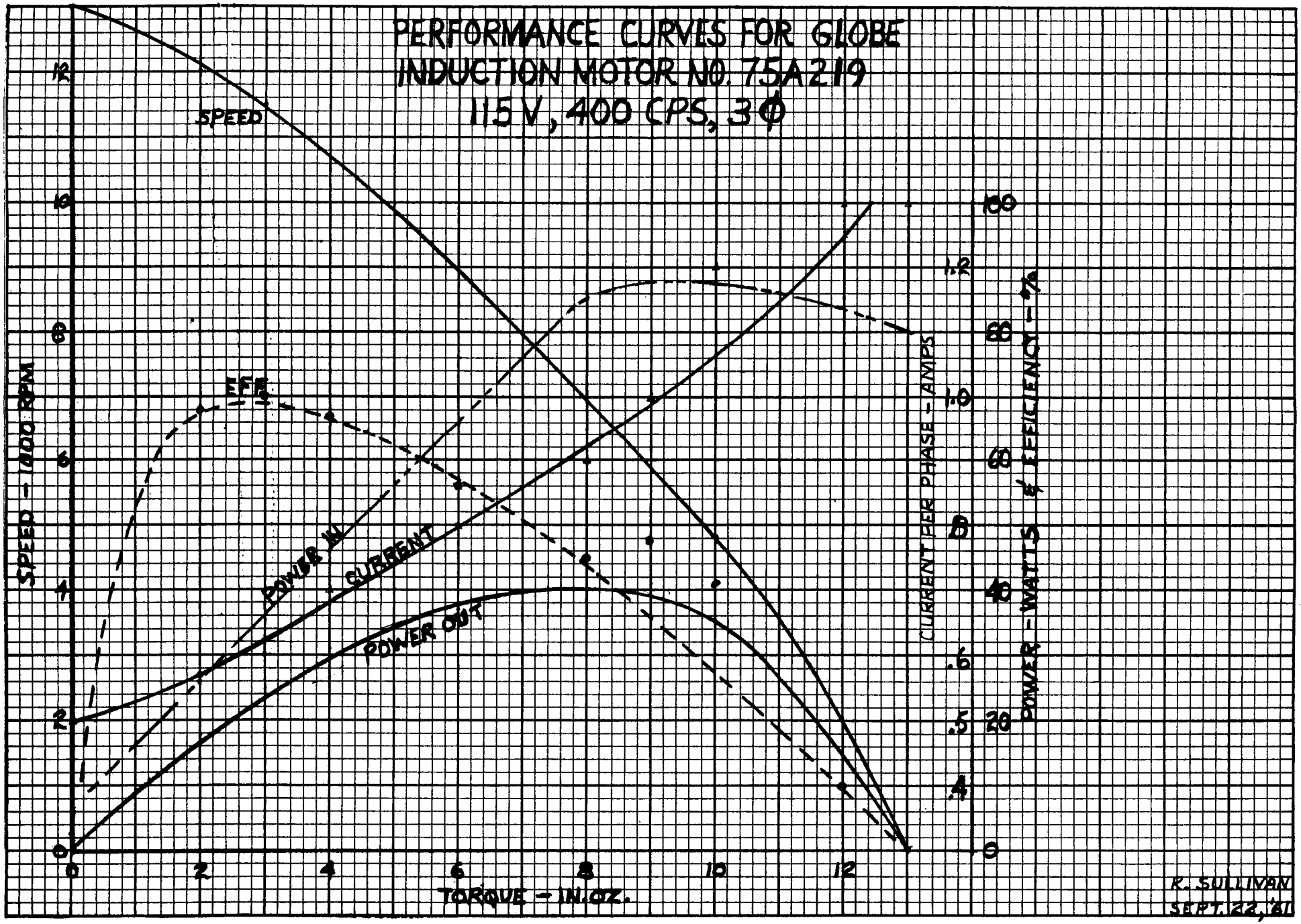
PERFORMANCE CURVES FOR GLOBE
INDUCTION MOTOR NO. 75A219
115 V, 400 CPS, 3 Φ
SPEED
EFF.
POWER IN
CURRENT
POWER OUT
SPEED - 1400 RPM
CURRENT PER PHASE - AMPS.
POWER - WATTS & EFFICIENCY - %
TORQUE - IN. OZ.
0
2
4
6
8
10
12
14
16
.4
.5
.6
1.0
1.2
20
40
60
80
100
R. SULLIVAN
SEPT. 22, '61

TEST DATA FOR GLOBE 7SA219 MOTOR

TEST DATA FROM 521739					CALCULATED DATA				REF. CALC.	
T_o IN. OZ	N_o RPM	E_L VOLTS	I_L AMPS	P_1 WATTS	P_{OUT} WATTS	$\sqrt{3} E_L I_L$ VOLT AMPS	P_{IN} WATTS	EFF. %	COS θ	f
0	13,000	115	.5	30	0	100	2.55	0	.0256	.085
2	12,000		.57	45	17.8	114	26.	68	.232	.584
3	11,200		(.62)	52	25	(123)	36	69	.292	.692
4	10,500		.8(.68)	60	31	160(136)	46	67	.342	.773
6	8400		.8	75	37	160	66	56	.416	.883
8	6500		.92	90	38.5	184	86	45	.469	.958
9	6200		1.0	95	41	200	86	48	.433	.908
10	4800		1.2(1.01)	100	35.5	240 (213)	87	41	.407	.871
12	1000		1.3(1.22)	110	8.9	260 (250)	85	10	.342	.773
13	0	115	1.3	110	0	260	78	0	.299	.703

T_o = OUTPUT TORQUE
N_o = OUTPUT SPEED
E_L = LINE VOLTAGE

I_L = LINE CURRENT
P_1 = WATTMETER READING
P_{OUT} = OUTPUT POWER

$P_{OUT} = \frac{T_o N_o}{1360}$

P_{IN} = INPUT POWER = $\sqrt{3} E I \cos\theta = f P_1$

$f = \frac{\sqrt{3}\cos\theta}{\cos(30^\circ + \theta)}$

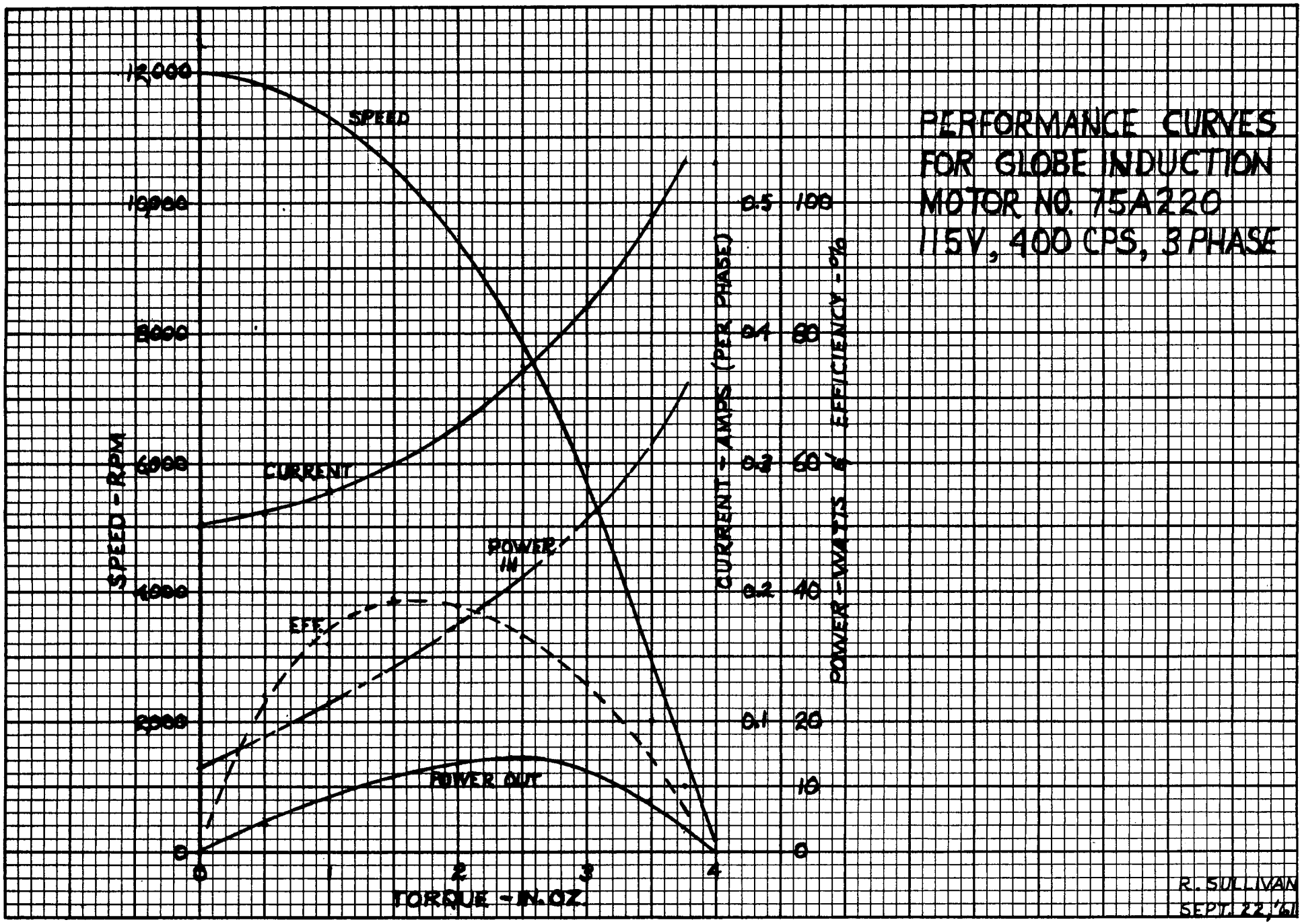
PERFORMANCE CURVES
FOR GLOBE INDUCTION
MOTOR NO. 75A220
115V, 400 CPS, 3 PHASE
SPEED
CURRENT
POWER IN
EFF.
POWER OUT
SPEED - RPM
CURRENT - AMPS (PER PHASE)
POWER - WATTS
EFFICIENCY - %
TORQUE - IN. OZ.
R. SULLIVAN
SEPT. 22, '61

TEST DATA FOR GLOBE 75A 220 MOTOR

TEST DATA FROM 521740					CALCULATED DATA				REF. CALC.	
T_o IN. OZ.	N_o RPM	E_L VOLTS	I_L AMPS	P_1 WATTS	P_{OUT} WATTS	$\sqrt{3}\,E_L\,I_L$ VOLT AMPS	P_{IN} WATTS	EFF. %	$\cos\theta$	f
0	12,500	118	.25	20	0	51	13	0	.26	.64
.5	11,750	118	.26	23	4.35	53	18	24	.34	.77
1.0	11,200	115	.28	26	8.3	56	23	36	.42	.89
1.5	10,500	115	.3	30	11.7	60	30	39	.50	1.0
2.0	9000	115	.33	34	13.3	66	35	38	.53	1.04
2.5	7500	115	.37	39	13.9	74	42.5	33	.57	1.1
3.0	5975	115	.42	45	13.3	84	52	26	.616	1.15
3.5	2000	115	.49	53	5.2	98	63	8	.643	1.19
3.75	1000	115	.53	58	2.8	106	71	4	.669	1.22
4.00	200	115	.53	58	.59	106	71	.8	.669	1.22

T_o = OUTPUT TORQUE
N_o = OUTPUT SPEED
E_L = LINE VOLTAGE
I_L = LINE CURRENT
P_1 = WATTMETER READING
P_{OUT} = OUTPUT POWER

$$P_{OUT} = \frac{T_o N_o}{1350}$$

$$f = \frac{\sqrt{3}\cos\theta}{\cos(30^\circ + \theta)}$$

P_{IN} = INPUT POWER $= \sqrt{3} E I \cos\theta = f P_1$

tested in both the horizontal and vertical mounting positions.

Test Conditions

The conditions common to all the tests were:

ambient air temperature.....approx. 85°F

power supply.....118 volts @ 400 cycles

Test #1

a. Run in air

b. Gears and bearings run dry (no teflon)

Test #2

a. Run in vacuum chamber, 25-50 microns.

b. Gears and bearings run dry

Test #3

a. Run in air

b. Planet gears teflon coated

c. Planet carriers, sun gears, and ring gears sprayed with Rulon

d. Steel balls installed between ends of sun gears and planet carriers

Test #4

a. Run in air

b. Planet gars, planet carriers, and sun gears teflon coated

c. Other moving parts (except bearings) and ring gears sprayed with Rulon

d. Steel balls installed between ends of sun gears and planet carriers

Test Results

Test No.	Drive Unit	Mounting Position	Load In.Lb.	Direction of Rotation	Current ma	Output rpm
1	pan	horiz.	none	CW & CCW	255	.6
1	pan	horiz.	45	CW & CCW	265	.6
2	pan	vert.	none	CCW	260	.6
2	pan	vert.	none	CW	255	.56
3	tilt	horiz.	none	up	250	
3	tilt	horiz.	33	up	250	
3	tilt	horiz.	44	up	250	
3	tilt	horiz.	none	down	250	
3	tilt	horiz.	33	down	255	
3	tilt	horiz.	44	down	255	
3	tilt	vert	none	up	265	
3	tilt	vert.	33	up	270-300	
3	tilt	vert.	44	up	260-290	
3	tilt	vert.	none	down	270	
3	tilt	vert.	33	down	260-300	
3	tilt	vert.	44	down	270-280	
4	pan	horiz.	0	CW	250	
4	pan	horiz.	33	CW	252	
4	pan	horiz.	44	CW	252	
4	pan	horiz.	0	CCW	257	
4	pan	horiz.	33	CCW	260	
4	pan	horiz.	44	CCW	256	
4	pan	vert.	0	CW	250	
4	pan	vert.	33	CW	250	
4	pan	vert.	44	CW	250	
4	pan	vert.	0	CCW	260	
4	pan	vert.	33	CCW	260	
4	pan	vert.	44	CCW	260	
4	pan	vert.	77	CW	255	

Starting surge was approximately 1 amp for all tests.

The boom elevation actuator was tested at room environmental conditions by a cable, drum, and hoist system. Torque outputs to 3,750 lb. in. were recorded at a current draw of .7 amperes. Its operation was extremely smooth and quiet; the brake held this load without slipping. No load motor speed was .53 rpm.

8.0 GEAR ANALYSIS

In designing the elevation drive gear reducer, three stress reducing design points were considered, (1) reduction of pitch line velocities and greater tooth accuracy where dynamic loads are the primary consideration; (2) increased size of gear teeth where transmitted loads are high compared to dynamic loads and; (3) improving line contact between meshing gear teeth by providing double end supported planet gear shafts.

The new method of gear design considers that the maximum actual load F_m on the gear tooth consists of the transmitted or useful load F_t and an increment load F_i caused by inaccuracies of the teeth, errors in spacing, tooth deflection, unbalance, and power flow fluctuation.

$$F_m = F_t + F_i$$

The increment load depends upon the masses of the moving parts and for average conditions may be expressed as:

$$F_i = \frac{v_m (C_{eb} + F_t)}{v_m + 20\sqrt{C_{eb} + F_t}}$$

where:

F_i = dynamic load in lbs

v_m = pitch line velocity in feet per minute

C = constant = 1,660,000 for 20° full depth tooth form and steel on steel

e = probable error in tooth profiles = 0.0005 inches for precision gears

F_t = transmitted load in lbs

b = face width of gear in inches

After having found the maximum actual tooth load, F_m, the tooth stress may be found from the formula:

$$S = \frac{F_m \, P_d}{b \, Y}$$

where:

S = tooth stress in pounds per square inch

P_d = diametral pitch

Y = Lewis' form factor

The above equations will be used for all of the gear calculations with the exception of the elevation drive motor pinion which is not compatible with the dynamic load formula. The elevation drive gear train is analized first beginning with the sun gear adjacent to the output shaft. As mentioned early in this report, design stresses will be based on an output torque of 5000 in - lbs which is approximately 10 times the required output torque.

8.1 Third Stage Sun Gear - Elevation Drive

Gear Data:

No. of teeth in sun gear = $N_s = 12$

Pitch dia. of sun gear = $D_s = 0.75$

No. of teeth in planet gear = $N_p = 24$

Pitch dia. of planet gear = $D_p = 1.50$

No. of teeth in ring gear = $N_r = 60$

Pitch dia. of ring gear = $D_r = 3.75$

Diametral pitch of gears = $P_d = 16$

Ratio of third stage = $R_3 = \frac{N_r}{N_s} + 1 = \frac{60}{12} + 1 = 6$

Desired torque output = 5,000 in-lbs at 0.5 rpm

Torque on sun gear per planet = $\frac{5,000}{3R_3} = \frac{5,000}{3\ (6)}$ = 277.8 in-lbs

Tooth load on sun gear per planet = $F_t = \frac{2\ (277.8)}{D_s} = \frac{2\ (277.8)}{0.75}$

F_t = 741 lbs

True pitch line velocity of sun gear when meshing with planet gear depends on rpm of planet gear about its own center. Pitch line velocity of sun gear is equal to the pitch line velocity of the planet gear about its own center.

Letting n_c = rpm of planet carrier and:

n_p = rpm of planet about its own center

$n_p = n_c \frac{N_r}{N_p} = \frac{(.5)\ (60)}{24} = 1.25$

Pitch line velocity = $v_m = (.262)\ (n_p)\ (D_p) = (.262)\ (1.25)\ (1.5)$

v_m = .491 fpm

$$F_i = \frac{v_m\ (C_{eb} + F_t)}{v_m + 20\sqrt{C_{eb} + F_t}}$$

$$= \frac{(.491)\ (1,660,000 \times .0005 \times 1.0625 + 741)}{.491 + 20\sqrt{1,660,000 \times .0005 \times 1.0625 + 741}}$$

F_i = 1.0 lbs

This shows that dynamic loads at low rpm are insignificant.

$F_m = F_t + F_i = 741 + 1 = 742$ lbs.

$S = \frac{F_m\ P_d}{b\ Y} = \frac{742\ (16)}{1.0625\ (.245)} =$

S = 45,600 pounds per square inch, which is a safe working stress for the third stage sun gear.

Since the third stage sun gear is the most highly stressed gear, the following curve has been plotted to show the tooth stress

at lower torque outputs such as 500 inch-pounds which is the torque required to raise the television camera within the earth's gravitational field.

8.1.1 Second Stage Sun Gear - Elevation Drive

Gear Data:

No. of teeth in sun gear = $N_s = 12$

Pitch dia. of sun gear = $D_s = 0.50$

No. of teeth in planet gear = $N_p = 39$

Pitch diameter of planet gear = $D_p = 1.625$

No. of teeth in ring gear = $N_r = 90$

Pitch dia. of ring gear = $D_r = 3.75$

Diametral pitch of gears = $P_d = 24$

Ratio of second stage = $R_2 = \frac{N_r}{N_s} + 1 = \frac{90}{12} + 1 = 8.5$

Torque on sun gear per planet = $\frac{5,000}{3R_2 R_3} = \frac{5,000}{3(8.5)(6)} = 32.7$ in-lbs

Tooth load on sun gear per planet = $F_t = \frac{2\ (32.7)}{D_s} = \frac{2\ (32.7)}{0.5}$

$F_t = 131$ lbs

$n_c = R_3\ (0.5) = 6\ (0.5) = 3$ rpm

$n_p = n_c \frac{N_r}{N_p} = \frac{3\ (90)}{39} = 6.9$ rpm

$v_m = (.262)\ (n_p)\ (D_p) = (.262)\ (6.9)\ (1.625)$

$v_m = 2.94$ fpm

$$F_i = \frac{v_m\ (C_{eb} + F_t)}{v_m + 20\sqrt{C_{eb} + F_t}}$$

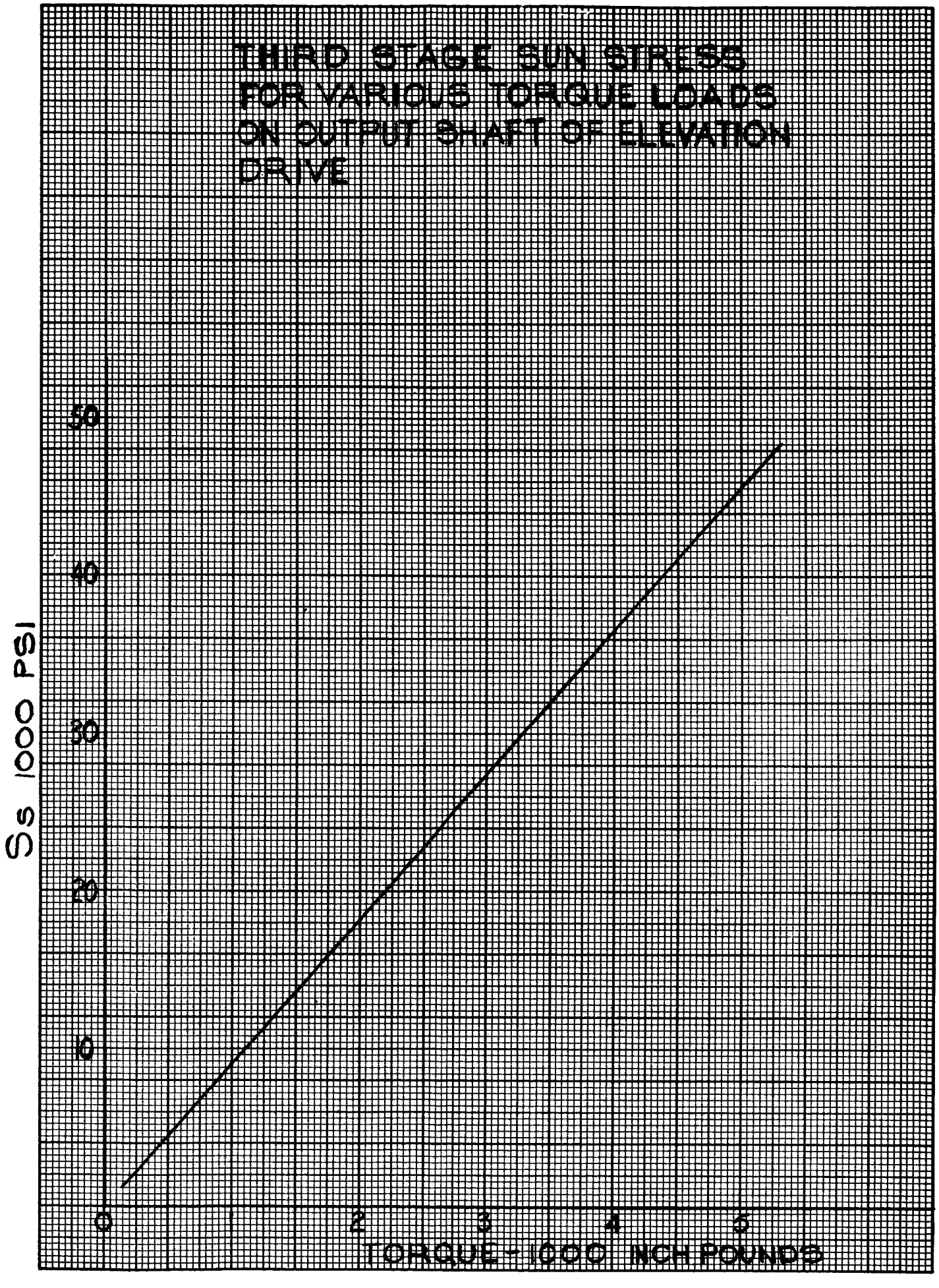
THIRD STAGE SUN STRESS
FOR VARIOUS TORQUE LOADS
ON OUTPUT SHAFT OF ELEVATION
DRIVE
50
40
30
20
10
0
S_S 1000 PSI
1
2
3
4
5
TORQUE - 1000 INCH POUNDS

$$F_i = \frac{2.94\ (1{,}660{,}000 \times .0005 \times .34375 + 131)}{2.94 + 20\sqrt{1{,}660{,}000 \times .0005 \times .34375 + 131}}$$

$F_i = 3$ lbs

$F_m = F_t + F_i = 131 + 3 = 134$ lbs

$$S = \frac{F_m P_d}{b\ Y} = \frac{134\ (24)}{(.34375)\ (.245)} = 38{,}190$$

S = 38,190 lbs per square inch

8.1.2 First Stage Sun Gear - Elevation Drive

Gear Data:

No. of teeth in sun gear = $N_s = 12$

Pitch dia of sun gear = $D_s = 0.50$

No. of teeth in planet gear = $N_p = 39$

Pitch dia of planet gear = $D_p = 1.625$

No. of teeth in ring gear = $N_r = 90$

Pitch dia of ring gear = $D_r = 3.75$

Diametral pitch of gears = $P_d = 24$

Ratio of first stage = $R_1 = \frac{N_r}{N_s} + 1 = \frac{90}{12} + 1 = 8.5$

Torque on sun gear per planet = $\frac{5{,}000}{3R_1\ R_2\ R_3} = \frac{5{,}000}{3(8.5)(8.5)(6)} = 3.84$ in-lbs

Tooth load on sun gear per planet = $F_t = \frac{2\ (3.84)}{D_s} = \frac{2\ (3.84)}{0.5}$

$F_t = 15.4$ lbs

$n_c = R_2\ R_3\ (0.5) = (8.5)\ (6)\ (0.5) = 25.5$ rpm

$n_p = n_c \frac{N_r}{N_p} = \frac{25.5\ (90)}{39} = 58.84$ rpm

$v_m = (.262)\ (n_p)\ (D_p) = (.262)\ (58.84)\ (1.625)$

$v_m = 25$ fpm

$$F_i = \frac{v_m\ (C_{eb} + F_t)}{v_m + 20\sqrt{C_{eb} + F_t}}$$

$$F_i = \frac{25\ (1{,}660{,}000 \times .0005 \times .34375 + 15.4)}{25 + 20\sqrt{1{,}660{,}000 \times .0005 \times .34375 + 15.4)}}$$

F_i = 20 lbs

$F_m = F_t + F_i = 15.4 + 20 = 35.4$ lbs

$$S = \frac{F_m\ P_d}{b\ Y} = \frac{35.4\ (24)}{.34375\ (.245)} =$$

S = 10,090 lbs per square inch

8.1.3 Second Stage Pinion and Gear - Elevation Drive

Gear Data:

No. of teeth in pinion = N_p = 12

Pitch dia of pinion = D_p = 0.5

No. of teeth in gear = N_g = 72

Pitch dia of gear = 3

Diametral pitch of gears = 24

Ratio of gear to pinion = $R_p = \frac{N_g}{N_p} = \frac{72}{12} = 6$

Torque on pinion = $\frac{5{,}000}{R_p R_1 R_2 R_3} = \frac{5{,}000}{6\ (8.5)(8.5)(6)}$ = 1.92 in-lbs

Tooth load on pinion = $F_t = \frac{2\ (1.92)}{D_p} = \frac{2\ (1.92)}{0.5}$ = 7.7 lbs

rpm of pinion = $n_p = R_p\ R_1\ R_2\ R_3\ (0.5) = 6(8.5)(8.5)(6)(0.5)$

n_p = 1300 rpm

$v_m = (.262)(n_p)(D_p) = (.262)\ (1300)\ (0.5) =$

v_m = 170.2 fpm

$$F_i = \frac{v_m\ (C_{eb} + F_t)}{v_m + 20\sqrt{C_{eb} + F_t}}$$

$$F_i = \frac{170.2\ (1{,}660{,}000 \times .0005 \times .25 + 7.7)}{170.2 + 20\sqrt{1{,}660{,}000 \times .0005 \times .25 + 7.7)}}$$

$F_i = 79$ lbs

$F_m = F_t + F_i = 7.7 + 79 = 86.7$ lbs

$$S = \frac{F_m P_d}{b\ Y} = \frac{(86.7)\ (24)}{(.25)\ (.245)}$$

S = 34,111 lbs per square inch

8.1.4 Motor Pinion - Elevation Drive

Pitch line velocity at motor input has been reduced to a minimum with a fine tooth (64 diametral pitch) motor pinion gear having a 0.375 pitch diameter. Lower pitch line velocities result in lower dynamic tooth loads which are considerably greater than transmitted loads on high speed applications. Basic dynamic gear load formulas do not hold true for gears of 24 diametral pitch and finer as determined experimentally by various gear manufacturers. Therefore to arrive at a more accurate value for a dynamic load on motor pinion teeth, it is necessary to analyze the effect of motor inertia plus tortional and transverse shaft stiffness on tooth deflection.

The third stage sun gear has the highest transmitted load, the dynamic load being insignificant because of the extremely low pitch line velocity. Gear tooth stress decreases rapidly with increase in tooth size. Therefore, the third stage planetary reduction has a 16 diametral pitch as compared to a 24 diametral pitch for the first two stages. A high overall gear reducer ratio was maintained

with the use of high spur gear ratios preceeding the planetary stages.

To insure line contact on gear teeth, all planetary gear shafts are straddle mounted. The second spur gear reduction containing the overload clutch is also straddle mounted. The motor pinion does not have an outboard bearing which is not necessary because of the light transmitted load. Its mating gear is supported by a large diameter shaft positioned by wide spread bearings.

The first stage spur gear reduction consists of a 64 diametral pitch pinion and gear, the pinion being mounted on a 10,000 rpm motor having a rated torque output of 3 inch ounces. The pinion has 24 teeth with a 0.375 inch pitch diameter, and the gear has 192 teeth and a 3 inch pitch diameter. With high speed gears it is not uncommon for dynamic loads to be four to five times the transmitted load. However with fine pitch gears of over 24 diametral pitch, formulas developed for conditions where the rotating masses are average yield dynamic loads that are 30 to 50 times the transmitted load. Experimental results by various gear manufacturers show that the life of these gears is far greater than what the dynamic load formulas indicate. More realistic values are achieved by treating the high speed, fine pitch gears as specific cases and calculating dynamic loads by going through the steps used to derive the average condition formulas. In this way, motor inertia, tortional shaft stiffness, and transverse shaft stiffness enter into the calculations.

Dynamic loads occur primarily from tooth thickness and spacing inaccuracies which cause sudden changes in backlash. A pair of gear teeth about to mesh must take up the slack before contact occurs. Consequently, the motor pinion accelerates while the driven gear decelerates, the colliding of the teeth producing an impact load. Tooth deflection, shaft windup, and shaft bending absorb the kinetic energy released when the two teeth finally contact and turn with a common velocity.

Precision gears are specified for this first spur reduction, the maximum tooth to tooth composite error being held to 0.0002 per gear. This is a radial measurement and represents the allowable center distance change for successive pairs of teeth when the gear being checked is running with a master gear. For calculation purposes this radial measurement must be put in terms of backlash variation between successive pairs of teeth. For a 20° pressure angle,

Backlash = (tooth to tooth composite error)(2) (tan 20°)

Backlash = (.0002) (2) (.3640)

Backlash = .0001456 inch per gear

For two gears:

Total Backlash = 2 (.0001456) = 0.0002912 inches

This value represents the slack that must be taken up by two teeth coming into engagement as measured along the pitch circle. From a relative velocity point of view, the driven gear may be thought of as fixed while the pinion starts from a dead stop and moves through angle θ (the angle subtended by the total backlash as measured along

the pinion pitch circle) before striking the mating tooth on the driven gear.

$$\theta = \frac{\text{total backlash}}{\text{pitch radius of pinion}}$$

$$\theta = \frac{.0002912}{.1875} = .001553 \text{ radians}$$

The peak angular velocity the pinion will achieve relative to the driven gear at time of impact is given by the equation:

$$W_f = \sqrt{2\theta A_t}$$

where:

W_f = is the final angular velocity at time of impact in radians per second.

A_t = total angular acceleration of pinion with respect to driven gear in radians per second^2

Total acceleration, A_t, is the sum of the acceleration of the pinion and deceleration of the driven gear during backlash take-up interval.

$$A_t = A_p + A_g$$

where:

A_p = angular acceleration of pinion in radians per second^2

A_g = deceleration of driven gear as referred to pinion pitch diameter in radians per second^2. When considering relative motion, the driven gear may be thought of as fixed and any deceleration of the driven gear becomes acceleration of the pinion. Deceleration of the driven

gear is transferred as acceleration to the pinion by multiplying the deceleration by the ratio of the pitch diameters.

The above acceleration must be calculated before pinion impact velocity, W_f, can be determined. A value for W_f is necessary for calculating the kinetic energy created during the acceleration period. By equating the potential energy stored in the deflected tooth plus the tortionally, transeversally strained motor shaft to the expended kinetic energy, a tooth impact load can be calculated. When impact occurs, there are undoubtedly other resilient members such as roll pins and bearing supports that absorb small quantities of kinetic energy, thereby reducing tooth impact load. However, it is felt that the tooth and motor shaft absorbthe larger portion of kinetic energy and that other points of absorption provide a safety factor for the calculations.

The pinion acceleration, A_p, is calculated by the equation:

$$T_m = \frac{I_m}{g} A_p$$

where:

T_m = output torque of motor at 10,000 rpm = 0.015625 ft-lbs

I_m = motor interia = $\frac{237.17}{10^7}$ lb-ft^2

g = acceleration of gravity = 32.2 ft/sec^2

$$A_p = \frac{T_m g}{I_m}$$

$$= \frac{(.015625)(32.2)(10^7)}{327.17}$$

$$A_p = 21{,}213 \ \frac{\text{radians}}{\text{seconds}^2}$$

Assuming the motor was operating at rated torque when the sudden change in backlash occured, the torque output of the driven gear would be eight times motor torque (gear to pinion ratio is eight to one) or 0.125 ft-lbs. When tooth contact is broken, this output load torque will become the decelerating torque on the driven gear. Actually this deceleration torque will be slightly lower than 0.125 ft-lbs because of the inertia effect of the remainder of the gear reducer. The planetary gears turn at very slow speeds and part of their inertia effect will be offset by friction. The deceleration torque of 0.125 ft-lbs represents a conservative value which will yield a slightly higher impact load than actually exists. The deceleration of the driven gear is found by the equation:

$$D_g = \frac{T_g g}{I_g}$$

where:

D_g = deceleration of driven gear in radians per second^2

T_g = deceleration torque = 0.125 ft-lbs

I_g = inertia of driven gear in lb ft^2

The inertia of the driven gear, I_g, is calculated by the equation:

$$I_g = \frac{\pi \rho \, d^4 b}{32\,(144)}$$

where: ρ is the density of steel in lbs/ cu.in. = 0.283

d = pitch diameter of driven gear in inches.

b = width of gear in inches = 0.125

$$I_g = \frac{\pi(.283)\ (3)^4\ (.125)}{(32)\ (144)}$$

$$I_g = 0.001953 \text{ lb-ft}^2$$

Substituting this value in the deceleration torque formula:

$$D_g = \frac{T_g g}{I_g}$$

$$= \frac{(.125)\ (32.2)}{.001953}$$

$$D_g = 2{,}061 \frac{\text{radians}}{\text{seconds}^2}$$

Since deceleration in the driven gear is equivalent to acceleration in the pinion from a relative motion standpoint, the equivalent acceleration, A_g, for the pinion is given by the equation:

$$A_g = \frac{d_g}{d_p}$$

where: d_g = pitch diameter of gear = 3 in.

d_p = pitch diameter of pinion = 0.375 in.

$$A_g = \frac{2{,}061\ (3)}{.375}$$

$$A_g = 16{,}488 \frac{\text{radians}}{\text{seconds}^2}$$

Substituting in the equation for total pinion acceleration:

$$A_t = A_p + A_g$$

$$A_t = 21{,}213 + 16\ 488$$

$$A_t = 37{,}701 \frac{\text{radians}}{\text{seconds}^2}$$

Peak angular velocity at time of impact can now be calculated:

$$W_f = \sqrt{2\ \theta\ A_t}$$

$$= \sqrt{2\ (.001553)\ (37{,}701)}$$

$$W_f = 10.82 \frac{\text{radians}}{\text{seconds}}$$

The kinetic energy the motor has gained during the loss of contact interval and which is also the energy that is absorbed by the pinion tooth and motor shaft when the pinion and driven gear attain a common velocity is given by the equation:

$$KE = \frac{I_m W_f^2}{2 g}$$

$$KE = \frac{237.17 (10.82)^2}{2 (10^7) (32.2)}$$

$$KE = \frac{431.2}{10^7} \text{ lb-ft}$$

or:

$$\frac{431.2 (12)}{10^7} = \frac{5174}{10^7} \text{ lb-in}$$

Figure 1 is an enlarged sketch of a pinion tooth striking a driven gear tooth. Had the pinion tooth overtaken the driven gear sooner, each tooth would be deflected, the amount of deflection in each tooth depending on the location of the impact point. The highest tooth stress occurs when the tip of the pinion tooth strikes the root of the driven gear tooth, thereby causing maximum deflection of the pinion tooth. The impact load, P, acts along the 20 degree pressure angle, the cantilever tooth deflection resulting from its tangential component, P_t which equals P cos 20°. The twisting torque is equal to P times the base radius, R_b.

The energy stored in the deflected tooth is given by the equation:

$$U_t = \frac{P_t^2 h^3}{GEI}$$

FIG. 1.

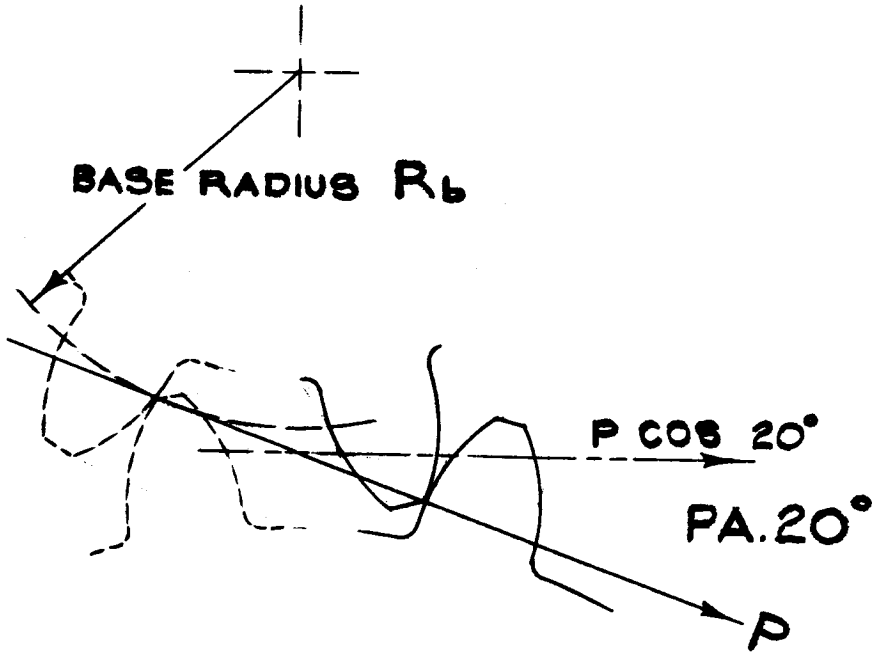

where:

h equals the full depth of the pinion tooth = 0.0364 in.

E = modulus of elasticity for steel = 29,000,000.

I = tooth sectional moment of inertia

$$= \frac{(\text{base width})\ (\text{base thickness})^3}{12}$$

$$= \frac{(.125)\ (.0245)^3}{12} = \frac{15.317}{10^8}\ \text{in}^4$$

Ut = stored potential energy in tooth in lb-in.

The energy stored in the tortionally twisted motor shaft is given by the equation:

$$U_S = \frac{(P\ R_b)^2\ l}{GI_p}$$

where:

R_b = base radius of pinion = (pitch radius) cos 20°

$$= \frac{(.375)\ (.9397)}{2} = .1762 \text{ inches}$$

l = length of motor shaft = 1 inch

G = modulus of elasticity in shear for steel = 11,500,000

U_S = stored potential energy in shaft due to twisting in lb-in

Ip = polar moment of inertia of shaft = $\frac{\pi(\text{shaft dia})^4}{32}$

$$= \frac{\pi(.25)^4}{32} = 0.0003835\ \text{in}^4$$

In addition to the shaft being tortionally twisted, it is also bent like a cantilever beam. For a cantilver with a concentrated load P at a distance l from the support (front motor bearing), the energy of strain is given by the equation:

$$U_b = \frac{P^2\ l^3}{6\ EI}$$

where:

U_b = stored potential energy in shaft due to bending in lb-in

P = impact load in lbs acting along 20° pressure angle

l = length of overhung motor shaft = 1 inch

I = shaft sectional moment of inertia

$$= \frac{\pi (\text{shaft dia})^4}{64}$$

$$= \frac{\pi (.25)^4}{64} = 0.00019175 \text{ in}^4$$

Equating kinetic energy to potential energy:

$$KE = U_t + U_s + U_b$$

$$KE = \frac{(P \cos 20^\circ)^2 h^3}{6 E I} + \frac{(PR_b)^2 l}{G I_p} + \frac{P^2 l^3}{6 E I}$$

$$\frac{5174}{10^7} = \frac{(.9397 P)^2 (.0364)^3 10^8}{6 (29{,}000{,}000) (15.317)} + \frac{(.1762 P)^2 (1)}{(11{,}500{,}000)(.0003835)}$$

$$+ \frac{P^2 (1)^3}{6 (29{,}000{,}000)(.00019175)}$$

$$5174 = 15.98 P^2 + 70.395 P^2 + 299.7 P^2$$

$$P = 3.66 \text{ lbs}$$

The kinetic energy of the motor pinion gear will increase the dynamic load of 3.66 pounds which is a result of motor armature inertia. It was seen in the above calculations that armature kinetic energy had three sources of dissipation, tooth deflection, motor shaft windup, and motor shaft bending. However, the pinion kinetic energy will not have the benefit of shaft wind up but will have shaft bending as a large dissipation source because of the equal and opposite reaction that occurs from a dynamic load on a pinion tooth. The following calculations will

deal with the additional dynamic load, P_1, resulting from motor pinion kinetic energy.

The inertia of the pinion is given by the equation:

$$I = \frac{\pi \rho l (D_1^4 - D_2^4)}{32}$$

where:

I = inertia in lb-in^2

ρ = density of steel 0.283 lbs per cu. in.

l = length of gear in inches = 0.468

D_1 - gear outside diameter in inches = 0.375

D_2 = gear bore size in inches = 0.25

$$I = \frac{\pi (.283)\ (.468)\ (.375^4 - .25^4)}{32}$$

$$= \frac{2.0633}{10^4} \text{ lb-in}^2$$

or:

$$\frac{2.0633}{144(10^4)} = \frac{1.4328}{10^6} \text{ lb-ft}^2$$

The kinetic energy is given by the equation:

$$KE = \frac{I\ W_f^2}{2\ g}$$

$$= \frac{(1.4328)\ (10.82)^2}{2\ (10^6)\ (32.2)}$$

$$= \frac{2.6046}{10^6} \text{ lb-ft}$$

or:

$$\frac{2.6046}{10^6} \times 12 = \frac{312.55}{10^7} \text{ lb-in}$$

Equating kinetic energy to potential energy:

$$KE = U_t + U_b$$

$$KE = \frac{(P_1 \cos 20^\circ)^2 h^3}{6 E I} + \frac{P_1^2 l^3}{6 E I}$$

$$\frac{312.55}{10^7} = \frac{(.9397 P_1)^2 (.0364)^3 10^8}{6 (29,000,000)(15.317)} + \frac{P_1^2 (1)^3}{6(29,000,000)(.00019175)}$$

$$312.55 = 15.98 P_1^2 + 299.7 P_1^2$$

$$P_1 = 1.00 \text{ lb}$$

This dynamic load, P_1, also acts along the 20° pressure angle and will add directly to the motor armature induced dynamic load, P. In addition to the two dynamic loads, there is a transmitted load which is added to the dynamic loads. For load addition purposes, the transmitted load is referred to the 20° pressure angle with the torque arm being the base circle radius, R_b. The transmitted load is found by the equation:

$$F = \frac{T_m}{R_b}$$

where:

F = transmitted load acting along 20° pressure angle in lbs

T_m = rated torque output of motor = 0.1875 in-lbs

R_b = base radius of pinion = .1762 in.

$$F = \frac{.1875}{.1762}$$

$$= 1.064 \text{ lbs}$$

Letting Q equal the total tooth load:

$$Q = P + P_1 + F$$

$$= 3.66 + 1.00 + 1.064$$

$$Q = 5.724 \text{ lbs.}$$

The tangential component of this tooth load, which causes the tooth to deflect like a small cantilever beam having a concentrated load at the end, is given by the equation:

$$Q_t = Q \cos 20^\circ$$

$$= 5.724\ (.9397)$$

$$Q_t = 5.38 \text{ lbs}$$

The tooth stress can now be calculated with the Lewis' formula:

$$Q_t = \frac{Sb\ Y}{D_p}$$

where:

S = tooth beam stress in lbs/in^2

b = face width of tooth = 0.125 in

Y = a constant and is called the Lewis' or form factor

For a 24 tooth, full depth 20° gear, Y = 0.337.

D_p = diametral pitch = 64

Solving for S:

$$S = \frac{Q_t\ D_p}{b\ Y}$$

$$= \frac{5.38\ (64)}{(.125)(.337)}$$

$$S = 8{,}174 \text{ lbs/in}^2$$

The stress value of 8,174 pounds per square inch is a very low operating stress and should result in a long gear life as verified by the experimental testing of various gear manufacturers. It was shown in this analysis that the dynamic load was approximately four times that of the transmitted load. However, had the motor shaft been shorter and

thicker, the value of the shaft as shock absorbing source would be lost and the dynamic load would have been considerably greater.

8.2 Fifth Stage Sun Gear - Pan and Tilt Drive

Since the last stage sun gear which is adjacent to the output shaft is the highest stressed gear, only this gear will be analized. With no theoretical load on the output shaft other than seal friction, gear stress will depend upon whatever load is imposed on reducer output shaft. A curve has been plotted showing gear stress versus torque load thereby providing a quick means for estimating gear stress when using this gear reducer on other possible applications. The gear reducer consists of five planetary stages, each having the same number of gear teeth and diametral pitch. The last stage differs from the first four stages by having a greater face width on the gears.

Gear Data:

No. of teeth in sun gear = $N_s = 15$

Pitch dia of sun gear = $D_s = 0.2344$

No. of teeth in planet gear = $N_p = 39$

Pitch dia. of planet gear = $D_p = 0.6094$

No. of teeth in ring gear = $N_r = 93$

Pitch dia. of ring gear = $D_r = 1.4531$

Diametral pitch of gears = 64

Ratio of Fifth Stage = $R_5 = \frac{N_r}{N_s} = \frac{93}{15} + 1 = 7.2$

Since the five stages have identical ratios:

$R_1 = R_2 = R_3 = R_4 = R_5 = 7.2$

Motor Data:

Torque output = .0625 in-lbs at 10,000 rpm

$$\text{Output shaft rpm} = \frac{10{,}000}{R_1\ R_2\ R_3\ R_4\ R_5} = 0.5$$

It was seen that the dynamic load, F_i, on the third stage sun gear in Elevation Drive gear reducer was insignificant. Therefore, only the transmitted load, F_t, will be considered for the Pan and Tilt fifth stage sun stage since its rpm is also very low.

Letting T_o = output shaft torque:

$$\text{Torque on sun gear per planet} = \frac{T_o}{3R_5} = \frac{T_o}{3(7.2)} = .0463\ T_o$$

$$\text{Tooth load on sun gear per planet} = F_t = \frac{2(.0463T_o)}{D_s} = \frac{2(.0463T_o)}{0.2344}$$

$$F_t = .395\ T_o$$

$$F_m = F_t + F_i = .395\ T_o + 0 = .395\ T_o$$

$$S = \frac{F_m\ P_d}{b\ Y} = \frac{.395\ T_o\ (64)}{(.26)(.289)}$$

$$S = 337\ T_o$$

The following curve is a plot of this equation which gives the stress on the sun gear teeth for various torque loads on the output shaft of the Pan and Tilt Drive.

8.3 Backlash Analysis - Elevation Drive

Theoretically speaking, gear teeth should run together without appreciable backlash. From a practical standpoint, however, this is impossible due to the following reasons: 1. Perfection in cutting and mounting is impossible because of manufacturing tolerances which should be as wide as possible to reduce costs. 2. Space between the

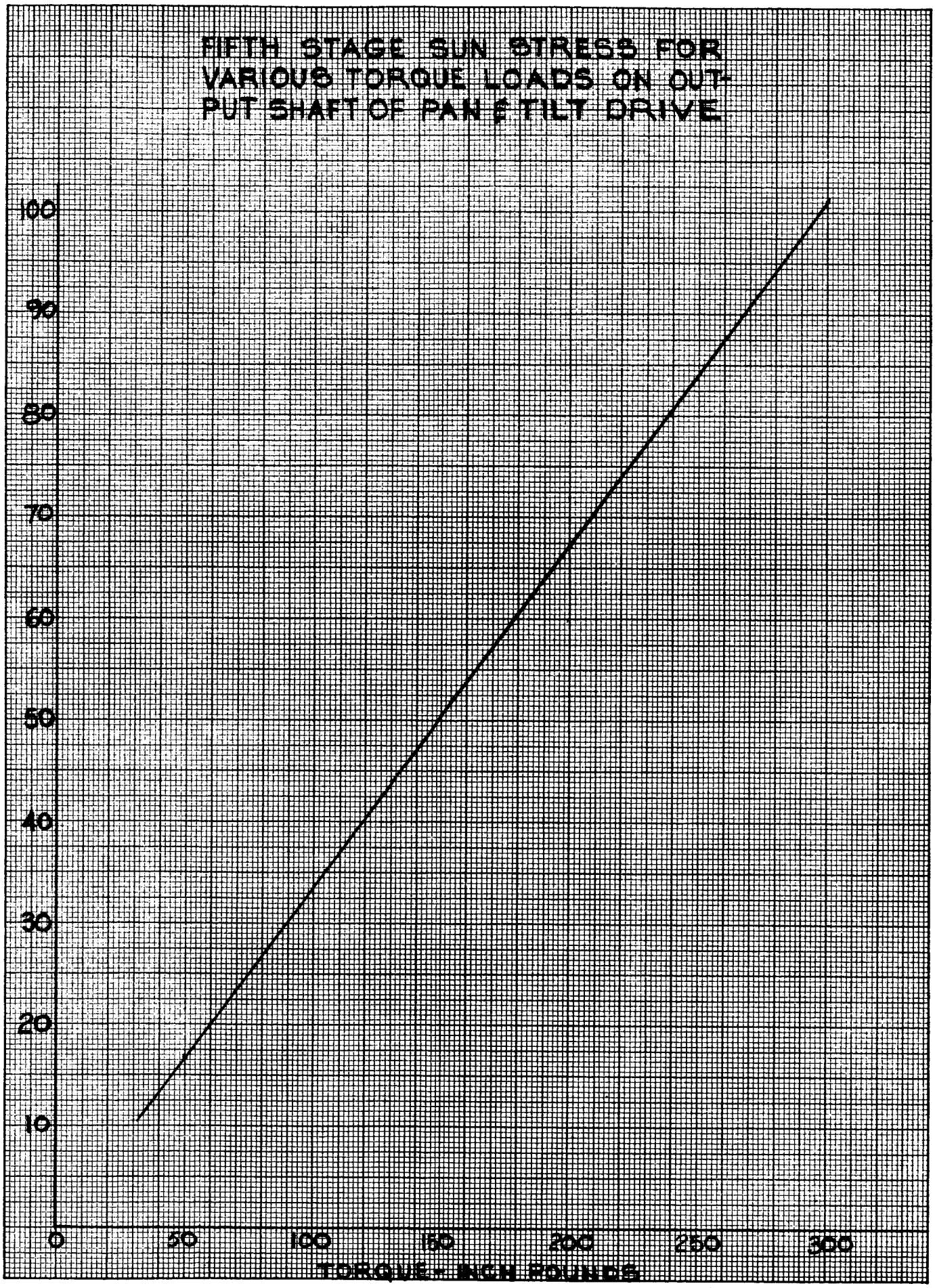
FIFTH STAGE SUN STRESS FOR VARIOUS TORQUE LOADS ON OUTPUT SHAFT OF PAN & TILT DRIVE
S_S - 1000 PSI
100
90
80
70
60
50
40
30
20
10
0
50
100
150
200
250
300
TORQUE - INCH POUNDS

teeth must be provided to aid lubrication. 3. Temperature changes due to speed and other causes affect sizes of gears and spacing of shafts on which gears are mounted. Therefore a certain amount of freedom between the teeth must be provided to avoid binding when operating. Backlash can be defined as the amount by which the width of a tooth space exceeds the thickness of the engaging tooth on pitch circles.

The degrees of rotation encountered by a gear when "taking up" backlash is given by relation:

$$\theta \text{ deg} = \frac{180}{\pi} \times \frac{2 \text{ Backlash}}{D_p}$$

The degrees of rotation for a sun gear, when taking up the backlash between itself and the planet gear, is twice this amount since the planet gear will continue to rotate until the backlash between itself and the ring gear is taken up. The total backlash of a gear reducer, as measured in terms of degrees rotation of input shaft necessary to produce movement of the output shaft, is desirable for predicting accuracy of positioning. The following tabulation shows the backlash at various points in the drive train and how backlash near the output end is magnified by the ratios of the intervening stages. The ratio referred to in the tabulation are defined as follows:

R_m = motor pinion reduction stage = $\frac{8}{1}$

R_p = 2nd pinion and gear reduction stage = $\frac{6}{1}$

R_1 = 1st planetary stage reduction = $\frac{8.5}{1}$

R_2 = 2nd planetary stage reduction = $\frac{8.5}{1}$

Calculations are based upon an average total backlash of 0.003 between mating gears.

BACKLASH TABULATION FOR ELEVATION DRIVE

Stage	Degrees Rotation	Magnification Factor	Degrees of Rotation at Input Shaft
3rd sun	0.9168	$R_m R_p R_1 R_2$ = 3468	3179.0
2nd sun	1.3752	$R_m R_p R_1$ = 408	561.0
1st sun	1.3752	$R_m R_p$ = 48	66.0
2nd pinion	0.6876	R_m = 8	5.5
motor pinion	0.9168	1	0.9
		TOTAL	3812.4 deg.

Converting this figure to revolutions:

$$\frac{3812.4^\circ}{360^\circ} = 10.6 \text{ revolutions}$$

Therefore, the motor will make 10.6 revolutions when taking up the slack during a reversal in direction.

With an overall reduction ratio of 20,808 to 1, 10.6 revolutions of the motor is equivalent to 0.183 degrees of output shaft rotation.

$$\frac{3812.4}{20,808} = 0.183 \text{ degrees or } 10.98 \text{ minutes}$$

8.1 Backlash Analysis - Pan and Tilt Drive

The Pan and Tilt Drive consists of five planetary stages with identical reduction ratios.

$$R_1 = R_2 = R_3 = R_4 = R_5 = \frac{7.2}{1}$$

Since this drive has five planetary stages as compared to three for the Elevation Drive, the total backlash for the system is greater because of the doubling of each sun gear backlash due to additional planetary rotation. The following tabulation shows the backlash at various points in the drive train.

BACKLASH TABULATION FOR PAN & TILT DRIVE

Stage	Degrees Rotation	Magnification Factor	Degrees of Rotation At Input Shaft
5th sun	2.93	$R_1R_2R_3R_4$ = 2687.4	7883.2
4th sun	2.93	R_1 R_2 R_3 = 373.25	1094.9
3rd sun	2.93	R_1 R_2 = 51.84	152.1
2nd sun	2.93	R_1 = 7.2	21.1
1st sun	2.93	1	2.93
		TOTAL	9154.2 deg

Converting this figure to revolutions:

$$\frac{9154.2^{\circ}}{360^{\circ}} = 25.4 \text{ revolutions}$$

The motor will make 25.4 revolutions when taking up the slack during a reversal in direction.

With an overall reduction ratio of 19,349 to 1, 25.4 revolutions of the motor is equivalent to 0.473 degrees of output shaft rotation.

$$\frac{9154.2}{19,349} = 0.473 \text{ degrees or } 28.38 \text{ minutes}$$

9.0 LUNAR MANIPULATOR THERMAL ANALYSIS

9.1 INTRODUCTION

The thermal analysis of the Lunar Manipulator is concerned with the method for controlling manipulator temperature within specific limits over a period of 10,000 hours under the extreme conditions of heat and cold encountered on the surface of the moon. During a lunar day which lasts approximately two weeks, the surface of the moon reaches +273°F., and during the two week night period, the temperature falls to -243°F.

The temperature control mechanism is designed to prevent the manipulator temperature from exceeding +255°F. when the moon is at +273°F. and the sun is directly overhead. This manipulator temperature is selected on the basis that a reasonable safety factor will be provided for components such as electric motors, seals, and bearings which are purchased on a +400°F. operating specification.

The lowest temperature at which the manipulator will operate satisfactorily will have to be determined experimentally. A very low operating temperature such as -250°F. would have the advantage over a higher temperature in that no batteries would be necessary for heating the manipulator during the long lunar night. Curves have been plotted which show the cooling time in days for the manipulator to reach various subzero temperatures from the start of a lunar night. Total heat which must be added to maintain the manipulator at these temperatures during the remainder of the lunar night is also plotted.

Two methods are presented in this analysis for controlling manipulator temperature. The first method employs radiative techniques and involves both polished metal and white coated surfaces. The second method is concerned with both conductive and radiative techniques and involves high performance insulation along with a small white coated surface. Superinsulations have been developed by National Research Corporation and Linde Corporation. Both insulations are comprised of multiple parallel reflective shields, the Linde insulation having a low conductivity filler between the shields. This analysis will be concerned with the NRC insulation since it has no filler material which could shift about during high acceleration periods.

Regardless of which method is used for controlling heat absorption and heat loss, it is necessary to have a small portion of the manipulator area coated with a special film which can dissipate heat rapidly and at the same time block most of the impinging solar radiation. A flat white paint will absorb approximately 80% of incident long wave length radiation and 35% of short wave length radiation. Extremely high temperatures are necessary for short wave emission, a good example being the sun which is at 10,000°F. The normal emissivity factor for a body represents the percentage of incident long wave length radiation the body will absorb as well as the percentage of heat the body can radiate compared to a black body at the same temperature. Therefore, flat white paint will emit 80% as much heat as a black body at the same temperature. The solar emissivity factor of a body represents only the percentage of incident solar radiation the body will absorb as compared to a black body.

Calculations show that the white area dissipates approximately two thirds of the total manipulator heat input. To maintain a maximum temperature of $+255^{\circ}F$. with a polished metallic surface, it is necessary to coat 8% of the total manipulator area white.

With the ability of the white area to radiate heat easily, it is necessary to cover this area during the lunar nights. A light weight bimetal controlled shield provides a simple means for automatically covering the white area. To conserve heat, the shield will completely cover the white area whenever the manipulator temperature falls below $+50^{\circ}F$. Having an early covering of the white area will increase the time interval for the manipulator to reach its lowest operating temperature.

The lunar manipulator is designed to position a television camera which is connected to the manipulator by means of shafts and bearings. The television camera is analyzed from the standpoint of maximum camera temperature, assuming it is perfectly insulated from the manipulator, and also heat input to manipulator when a conduction path is provided. Means for reducing heat loss from the manipulator by way of the camera is also studied.

The Lunar Manipulator Thermal Analysis is divided into five sections (1) Polished Metal Temperature Control (2) Thermal Insulation Temperature Control (3) Partial Insulation and Polished Metal Temperature Control (4) Television Camera Temperature Analysis and (5) Bimetal Spring Control Mechanism.

9.2 POLISHED METAL TEMPERATURE CONTROL

The calculations in this section are based on a gold plated surface and a white coated area having emissivities which are determined experimentally by the University of California Jet Propulsion Laboratory. Other finishes such as polished steel, copper, aluminum, and silver have been analyzed. Gold is considered the best finish because of its low emissivity for both short and long wave length radiation plus its high resistance to oxidation. The plating technique consists of polishing the manipulator base metal (electrolytic copper is used for this purpose because of its high thermal conductivity) to a 16 R.M.S. micro-finish followed by a bright nickel plating .0003 to .0005 thick. A gold plating .000030 to .000050 thick is deposited on the nickel and requires no polishing.

Flat white paint with a titanium dioxide base has excellent emissivity characteristics, the base being a strong binder which prevents volitization of the paint in a high vacuum. However, JPL stated that the majority of white paints turn yellow under ultra violet radiation and lose their ability to reflect solar radiation. It was suggested that a "Rokide A" spray coating be used rather than white paint. This coating has emissivity characteristics similar to white paint and is a hard, crystalline refractory aluminum oxide. It has high resistance to excessive heat, abrasion and corrosion.

The manipulator is placed in a cantilever position for calculation purposes. In this position the sun can strike a maximum amount of area, resulting in maximum heat input to the manipulator. Calculations

may be simplified, without any appreciable error, by substituting square corners for round corners thereby making all manipulator surfaces parallel or perpendicular to the surface of the moon. In making these substitutions, the cross section of the pan drive housing will be rectangular rather than elliptical. Both the crotch of the fork and top of the elevate drive housing will be square rather than round. The overall effect will be a slight increase in total manipulator surface area. Over two thirds of the heat input to the manipulator is a result of solar radiation and since the sun's rays are striking the manipulator in a parallel direction, heat input is the same whether the top surfaces are flat or rounded. When parallel rays strike a curved surface, the projected area is used for calculation.

Exact information concerning the radiation characteristics of the moon's surface could not be found. Temperature observations of the moon's surface during a lunar eclipse have shown that the temperature decreases rapidly, indicating an emissivity approaching that of a black body. Since it is better to design the manipulator with the ability to dissipate more heat than is necessary to maintain a specific temperature, it will be assumed that the moon's surface has emissivity characteristics equal to that of a black body, thereby transmitting a maximum amount of heat to the manipulator.

A better picture of the thermal analysis is gained by approaching the problem from a heat balance standpoint. In other words, the total heat leaving the manipulator by way of radiation is equated to the total heat received by the manipulator in the form of radiation plus internal heat supplied by the three electric motors.

Heat Radiated = Heat absorbed by Radiation + Internal Heat Added

The heat energy radiated from a surface is given by the equation

$$H_r = \phi A_1 E_1 T_1^4$$

Where H_r = radiated heat in B.t.u./hr.

ϕ = Stefan's constant = 17.3×10^{-10}

A_1 = area in sq. ft.

E_1 = normal emissivity of the particular surface. This value is 0.03 for gold and 0.80 for Rokide A. A black body has an emissivity of 1.00.

T_1 = temperature in $^{o}R = 460 + {}^{o}F$.

The radiation received and absorbed by a surface from another body is given by the equation.

$$H_a = \phi A_1 F_e F_c T_2^4$$

Where H_a = heat energy absorbed in Btu/hr.

ϕ = Stefan's constant = 17.3×10^{-10}

A_1 = area of receiving surface in sq. ft.

F_e = emissivity factor depending upon the emissivities of the two bodies. In this analysis $F_e = E_1 E_2$ where E_2 is emissivity of the moon's surface and is equal to 1.00. The emissivity factor, F_e, becomes more complicated when the radiation from one body is reflected off the second body and returns to the first body.

F_c = Configuration factor. This factor is 1.00 for the bottom surfaces of the manipulator and 0.5 for the vertical or side surfaces. See Figure 2. and Figure 3. for the derivation of these values.

T_2 = temperature of body emitting radiation in ^{o}R.

Figure 2. A. shows a small area dA located a distance h over one corner of a large area having length a and width b. The configuration factor represents the extent the two areas can "see" each other. If dimensions a and b are infinite making the distance h insignificant in comparison, then the infinite area will intercept one fourth of all the radiation leaving dA. Therefore the configuration factor, F_c, is equal to 0.25. This is confirmed by the following equation given in "Heat and Mass Transfer" by Eckert and Drake.

$$F_c = \frac{1}{2\pi}\left[\frac{a}{\sqrt{a^2+h^2}}\tan^{-1}\frac{b}{\sqrt{a^2+h^2}} + \frac{b}{\sqrt{b^2+h^2}}\tan^{-1}\frac{a}{\sqrt{b^2+h^2}}\right]$$

When a and b are infinite, the equation reduces to

$$F_c = 0.25$$

If the large area extends in all directions from dA (Figure 2.B.) such that all radiation leaving dA is intercepted by the large area, then the configuration factor is equal to four times 0.25 or 1.00. The underside of the manipulator with respect to the moon's surface meets this condition and therefore has a configuration factor of 1.00.

FIG.2.

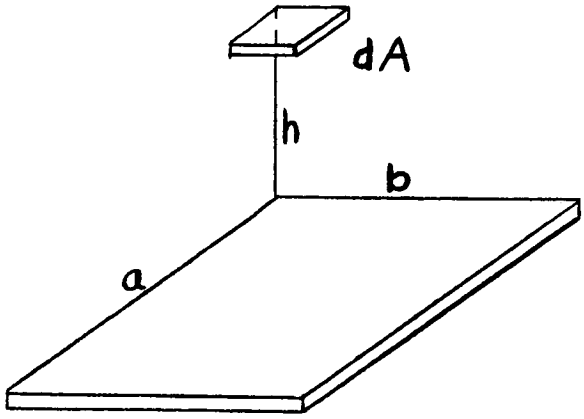

A.

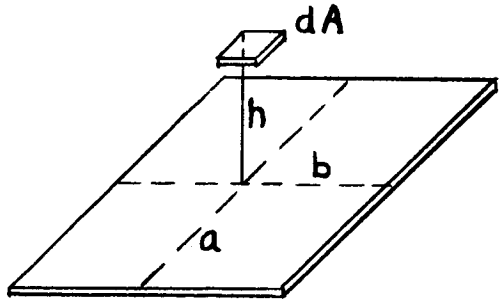

B.

Figure 3. A. shows a small area dA located perpendicularly over one corner of a large area. If dimensions a and b are infinite making the distance h insignificant, then the infinite area will intercept one fourth of all the radiation leaving dA. The configuration is 0.25. This is confirmed by the equation given in "Heat and Mass Transfer" by Eckert and Drake.

$$F_c = \frac{1}{2\pi}\left[\tan^{-1}\frac{b}{h} - \frac{h}{\sqrt{a^2+h^2}}\tan^{-1}\frac{b}{\sqrt{a^2+h^2}}\right]$$

When a and b are infinite, the equation reduces to

$$F_c = 0.25$$

If the large area extends an infinite distance in front of and to the sides of dA (Figure 3.B) such that one half of all the radiation leaving dA is intercepted by the large area, then the configuration factor is equal to two times 0.25 or 0.50. The sides of the manipulator with respect to the moon's surface meets this condition and therefore have a configuration factor of 0.50. The other half of the heat energy being radiated from the manipulator side walls is directed toward outer space.

The equation for calculating solar heat input to the manipulator differs from the basic equation in that a temperature and configuration factor are not necessary. The sun's radiation intensity is given as 420 Btu/ft^2/hr. This is the heat absorbed by a one square foot black body area placed perpendicular to the sun's rays. Other surfaces will absorb a percentage of this amount depending upon their solar emissivities. Gold has a solar emissivity of 0.30 and Rokide \ an emissivity of 0.35. Con-

FIG. 3.

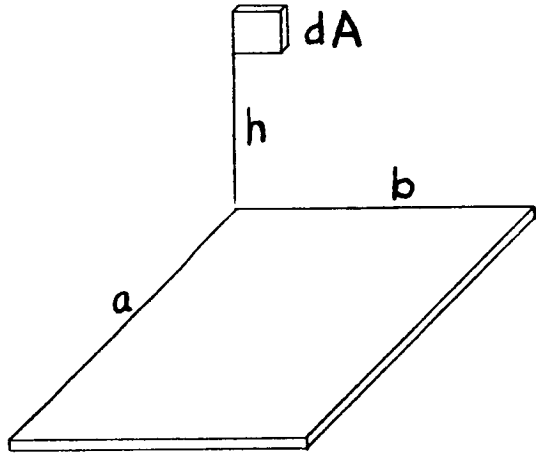

A.

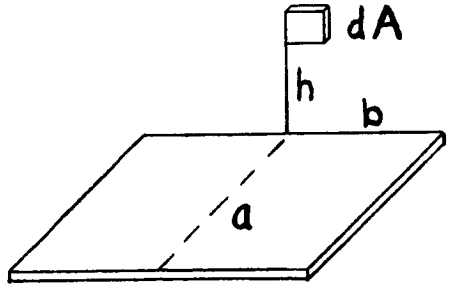

B.

figuration factors are unnecessary because of the parallel geometry of the sun's rays, thereby permitting the use of projected areas. The equation for calculating solar heat input is

$$H_s = 420\ A_1\ E_s$$

Where H_s = heat energy absorbed in Btu/hr.

A_1 = projected area of receiving surface in sq. ft.

E_s = solar emissivity

= 0.3 for gold and 0.35 for Rokide A

The square feet of white area (Rokide A) necessary to prevent the manipulator temperature from exceeding 255°F may be calculated by equating heat output to heat input and solving for the white area, A_w. Since the manipulator is constructed with electrolytic copper which has a very high thermal conductivity, it is assumed the entire manipulator, including the white area, will be at 255°F. The elevate drive motor, which has the highest horse power rating and is the only motor carrying a theoretical load, is located in the section of the manipulator containing the white area. This will tend to create a temperature uniformity, as the internal heat addition is an appreciable amount.

The heat output is calculated separately for the top gold surfaces, top white surface, side surfaces, and bottom surfaces. This gives a better perspective as to what each surface is contributing to the overall thermal balance. Likewise, the heat absorbed is calculated separately for each of these surfaces.

Heat radiated by top gold surfaces

$$H_{r_1} = \phi A_t E_g T^4$$

Where A_t = total top surface area having gold plating = .858 sq. ft.

$$H_{r_1} = \frac{17.3}{10^{10}} (.858)(.03)(460 + 255)^4 = 11.64 \text{ Btu/hr.}$$

Heat radiated by top white surface

$$H_{r_2} = \phi A_w E_w T^4$$

Where A_w = area of white surface and is unknown.

$$H_{r_2} = \frac{17.3}{10^{10}} (A_w)(.80)(460 + 255)^4 = 361.7\ A_w \text{ Btu/hr.}$$

Heat radiated by side surfaces

$$H_{r_3} = \phi A_s E_g T^4$$

Where A_s = total side area which includes all areas perpendicular to surface of moon that are uncovered = 2.06 sq. ft.

$$H_{r_3} = \frac{17.3}{10^{10}} (2.06)(.03)(460 + 255)^4 = 27.9 \text{ Btu/hr.}$$

Heat radiated by bottom surfaces

$$H_{r_4} = \phi A_b E_g T^4$$

Where A_b = total bottom surface area that is uncovered when the manipulator is in a cantilever position = .90 sq. ft.

$$H_{r_4} = \frac{17.3}{10^{10}} \quad (.90)(.03)(460 + 255)^4 \quad = 12.2 \text{ Btu/hr.}$$

Heat absorbed by top gold surfaces

$$H_{s_1} = 420 \; A_t \; E_{g_s}$$

Where E_{g_s} = solar emissivity for gold = .3

$$H_{s_1} = 420 \; (.858)(.3) = 108.1 \text{ Btu/hr.}$$

Heat absorbed by top white surface

$$H_{s_2} = 420 \; A_w \; E_{w_s}$$

Where E_{w_s} = solar emissivity for Rokide A = .35

$$H_{s_2} = 420 \; A_w \; (.35) = 147 \; A_w \text{ Btu/hr.}$$

Heat absorbed by side surfaces

$$H_{a_3} = \phi \; A_s \; F_e \; F_c \; T_2^4$$

Where T_2 = temperature of moon = $733^\circ R$

$= 460 + 273^\circ F$

$$= \frac{17.3}{10^{10}} \quad (2.06)(.03 \times 1)(.5)(733)^4 = 15.43 \text{ Btu/hr.}$$

Heat absorbed by bottom surfaces

$$H_{a_4} = \phi \; A_b \; F_e \; F_c \; T_2^4$$

$$= \frac{17.3}{10^{10}} \quad (.90)(.03 \times 1)(1)(733)^4 = 13.48 \text{ Btu/hr.}$$

Internal Heat Added

Elevate Motor - 1/15 H.P.

Cycle time - 1 minute on and 10 minutes off

Pan Motor - 1/30 H.P.

Cycle time - 2 seconds on and 20 seconds off.

Tilt Motor - 1/30 H.P.

Cycle time - 2 seconds on and 20 seconds off.

With each motor running 6 minutes out of every hour and assuming 40% efficiency (60% of output going into heat)

$H_i = (1/30 + 1/30 + 1/15)\ (.60)\ (42.418)\ (6) = 20$ Btu/hr.

Where 42.418 is a conversion factor from hp to Btu/min. 1 hp =42.418 Btu/min.

Equating the heat output to the heat input and solving for A_{w_s}

$$H_{r_1} + H_{r_2} + H_{r_3} + H_{r_4} = H_{s_1} + H_{s_2} + H_{a_3} + H_{a_4} + H_i$$

$$11.64 + 361.7\ A_w + 27.9 + 12.2 = 108.1 + 147\ A_w + 15.43 + 13.48 + 20$$

$$214.7\ A_w = 105.27$$

$$A_w = 0.49 \text{ ft. of white area}$$

$H_{r_2} = 361.7\ (.49) = 177.34$ Btu/hr.

$H_{s_2} = 147\ (.49) = 72.07$ Btu/hr.

The results of these calculations are summarized as follows:

	Heat Radiated (Btu/hr.)	Heat Absorbed (Btu/hr.)	
Top Gold	11.64	108.1	solar
Top White	177.34	72.07	solar
Sides	27.90	15.43	
Bottom	12.20	13.48	
Internal Heat		20.00	
Total	229.08 Btu/hr	229.08 Btu/hr	

It is noted in this tabulation that the white area dissipates approximately 75 per cent of the total heat input which is primarily solar radiation.

As mentioned before, the lowest temperature at which the manipulator will operate must be determined experimentally. However in the event the manipulator cannot be allowed to cool below -100°F for example, it will be necessary to know the rate of internal heat addition necessary to maintain -100°F and also the total quantity of heat required for a lunar night. The following calculations determine the rate of heat input at various subzero temperatures.

The procedure for calculating heat input rate at 0°F will be shown, the results for the other subzero temperatures being tabulated.

Heat radiated by top gold surfaces at 0°F.

$$H_{r_1} = \phi\, A_t\, E_g\, T_1^4$$

Where $T_1 = 460^\circ R = 460 + 0^\circ F$

$$H_{r_1} = \frac{17.3}{10^{10}} (.858)(.03)(460)^4 = 1.99 \text{ Btu/hr.}$$

Heat radiated by top white surface

$$H_2 = \phi\, A_w\, E_g\, T_1^4$$

Where E_g is substituted for E_w since white area is now covered with a gold shield.

$$H_2 = \frac{17.3}{10^{10}} (.49)(.03)(460)^4 = 1.13 \text{ Btu/hr.}$$

Heat radiated by side surfaces

$$H_{r_3} = \phi\, A_s\, E_g\, T_1^4$$

$$= \frac{17.3}{10^{10}} (2.06)(.03)(460)^4 = 4.78 \text{ Btu/hr.}$$

Heat radiated by bottom surfaces

$$H_{r_4} = \phi A_b E_g T_1^4$$

$$= \frac{17.3}{10^{10}} (.90)(.03)(460)^4 = 2.09 \text{ Btu/hr}$$

Heat absorbed by top gold surfaces

$$H_{s_1} = 0$$

Manipulator is in shade.

Heat absorbed by top white surface

$$H_{s_2} = 0$$

Manipulator is in shade.

Heat absorbed by side surfaces

$$H_{a_3} = \phi A_s F_e F_c T_2^4$$

Where T_2 = temperature of moon = $217^\circ R$

$$= 460 + (-243^\circ F)$$

$$H_{a_3} = \frac{17.3}{10^{10}} (2.06)(.03 \times 1)(.5)(217)^4 = .118 \text{ Btu/hr.}$$

Heat absorbed by bottom surface

$$H_{a_4} = \phi A_b F_e F_c T_2^4$$

$$= \frac{17.3}{10^{10}} (.90)(.03 \times 1)(1)(217)^4 = .103 \text{ Btu/hr.}$$

Equating the heat output to the heat input and letting I equal the internal heat which must be added to maintain $0^\circ F$,

$$H_{r_1} + H_{r_2} + H_{r_3} + H_{r_4} = H_{s_1} + H_{s_2} + H_{a_3} + H_{a_4} + I$$

$$1.99 + 1.13 + 4.78 + 2.09 = 0 + 0 + .118 + .103 + I$$

$$I = 9.77 \text{ Btu/hr.}$$

The terms H_{a_3} and H_{a_4} in the above equation represent the heat added to the manipulator by the moon in Btu per hour.

Moon heat addition rate $= H_{a_3} + H_{a_4}$

$= .118 + .103 = 0.221$ Btu/hr.

It is not surprising that the moon adds so little heat to the manipulator since the moon is at -243°F. This heat addition rate is constant regardless of what subzero temperature the manipulator is at, assuming a constant emmissivity for the gold plating.

The internal heats necessary to maintain various subzero temperatures are tabulated as follows:

Subzero Temperature, °F	Internal Heat Addition Rate, Btu/hr.
0	9.77
-50	6.10
-100	3.54
-150	1.84
-200	0.80
-250	0.211
-300	(-.075)

It is noted in this tabulation that for subzero temperatures below -250°F, the small amount of heat supplied by the moon becomes significant. At some point between -250° and -300°F the heat lost by radiation is equal to the heat added by radiation from the moon.

Before the total quantity of heat necessary to maintain the manipulator at various subzero can be calculated, the cooling time for the manipulator to reach these subzero temperatures must be determined.

Cooling is accomplished in two stages, the white area being uncovered during the first stage from $+255^{\circ}F$ to $+50^{\circ}F$ and covered during the second stage from $+50^{\circ}F$ to the subzero temperature under consideration. The time equation is greatly simplified by not including the moon's heat input to the manipulator of 0.221 Btu per hour. As shown in the above tabulation, this figure is insignificant at temperatures above $-200^{\circ}F$.

Another assumption is made which will cause the calculations to show a faster cooling time during the first stage. The white area is gradually covered as the manipulator cools from $255^{\circ}F$ to $50^{\circ}F$ resulting in a highly complex radiation exchange between the shield and the white area with part of the radiation escaping to outer space. For calculation purposes it is assumed the white area remains totally uncovered from 255° to $+50^{\circ}F$, at which point the white area is rapidly covered with no significant temperature change.

The time equation is derived as follows:

Let dQ be a small amount of heat loss (in Btu) during a small interval of time dt (in hours).

Then $dQ = U\,d\,t$

Where U is the total rate of heat loss in Btu per hour at corresponding manipulator temperature T.

Since the total rate of heat radiated by the manipulator is the sum of the rates for the top gold area, top white area, side area, and

bottom area

$$U = H_{r_1} + H_{r_2} + H_{r_3} + H_{r_4}$$

$$= \phi A_t E_g T^4 + \phi A_w E_w T^4 + \phi A_s E_g T^4 + \phi A_b E_g T^4$$

$$U = (\phi A_t E_g + \phi A_w E_g + \phi A_s E_g + \phi A_b E_g) T^4$$

Letting $M = \phi A_t E_g + \phi A_w E_w + \phi A_s E_g + \phi A_b E_g$

$$U = MT^4$$

Then $dQ = MT^4 \, dt$

To solve the differential equation it is necessary to put T in terms of Q which is done as follows using the total heat content relationship.

$$H = wc\,T$$

Where H = total heat content of the manipulator in Btu.

w = weight of manipulator in lbs.

c = specific heat in Btu/^{o}F. lb.

T = absolute temperature in ^{o}R.

If H_p equals peak heat content at time t = 0, the remaining heat content H following an amount of leakage Q is $H_p - Q$ or

$$H = H_p - Q$$

The corresponding temperature is

$$H = H_p - Q = wcT$$

or

$$T = \frac{H_p - Q}{wc}$$

Substituting in the differential equation,

$$dQ = M \left(\frac{H_p - Q}{wc} \right)^4 \quad dt$$

$$\frac{dQ}{(H_p - Q)^4} = \frac{M}{(wc)^4} \quad dt$$

Integrating

$$\frac{1}{3(H_p - Q)^3} = \frac{M}{(wc)^4} \quad t + C$$

When $t = 0$

$Q = 0$

$$C = \frac{1}{3 H_p^{\,3}}$$

$$T = \frac{(wc)^4}{3M} \left[\frac{1}{(H_p - Q)^3} \quad \frac{1}{H_p^{\,3}} \right]$$

Since Q is the difference between the peak heat content H_p and the heat content H_T at some manipulator temperature T, the equation may be written

$$t = \frac{(wc)^4}{3M} \left[\frac{1}{H_T^{\,3}} - \frac{1}{H_p^{\,3}} \right]$$

Where t is the time in hours for the manipulator to drop from a peak heat content H_p to a lower heat content H_T.

Using this equation, the cooling time for the manipulator to drop from 255°F to +50°F may be calculated. With a specific heat of 0.091 Btu per °F. lbs. for copper and a manipulator weight of 32 lbs, at 255°F.

$$H_p = wcT = 32\ (.091)(255 + 460) =$$

$$H_p = 2082 \text{ Btu.}$$

at + 50° F,

$$H_T = wcT = 32\ (.091)(50 + 460) =$$

$$H_T = 1485 \text{ Btu.}$$

$$M = \phi A_t E_g + \phi A_w E_w + \phi A_s E_g + \phi A_b E_g$$

$$= \frac{17.3}{10^{10}} \left[(.858)(.03) + (.49)(.80) + (2.06)(.03) + (.90)(.03) \right]$$

$$M = \frac{.8763}{10^9}$$

$$t_1 = \frac{\left[(32)(.091)\right]^4}{3\left(\frac{.8763}{10^9}\right)} \left[\frac{1}{(1485)^3} - \frac{1}{(2082)^3} \right]$$

$$t_1 = 5.3 \text{ hrs.}$$

The same equation is used to calculate the cooling time for the manipulator temperature drop from +50°F to various subzero temperatures. The M term in the equation will have a different value as a result of the covering of the white area by a gold plated shield. The peak heat content H_p will be at +50°F since the time count will start at this point. The time period for dropping from +50°F to 0°F is calculated as follows:

$$H_p = wcT = 32\ (.091)(50 + 460) = 1485 \text{ Btu}$$

at $0^{\circ}F$

$$H_T = wcT = 32\ (.091)(0 + 460) = 1340 \text{ Btu}$$

$$M = \phi\, A_t\, E_g + \phi\, A_w\, E_g + \phi\, A_s\, E_g + \phi\, A_b\, E_g$$

$$= \frac{17.3}{10^{10}} \left[(.858)(.03) + (.49)(.03) + (2.06)(.03) + (.90)(.03) \right]$$

$$M = \frac{.2236}{10^9}$$

$$t_2 = \frac{\left[(32)(.091)\right]^4}{3\left(\frac{.2236}{10^9}\right)} \left[\frac{1}{(1340)^3} - \frac{1}{(1485)^3} \right]$$

$$t_2 = 11.8 \text{ hours}$$

The number of hours required for the manipulator temperature to drop from $+255^{\circ}$ F to $0^{\circ}F$ is the sum of the hours for the first stage plus the second stage or

$$t_o = t_1 + t_2$$

$$= 5.3 + 11.8$$

$$t_o = 17.1 \text{ hours}$$

The cooling times in hours and days for the manipulator to drop from $255^{\circ}F$ to various subzero temperatures are tabulated as follows:

Subzero Temperature, $^{\circ}F$	Hours	Days
0	17.1	.71
-50	35.5	1.48
-100	65.7	2.74
-150	118.1	4.92
-200	219.6	9.15
-250	442.7	18.44
-300	1033.3	43.0

The total heat input in Btu or watt-hrs. to maintain various subzero temperatures following the cooling period can now be calculated. Using -100°F as an example, it is noted in the tabulation that the cooling time is 65.7 hours. Since a lunar night is approximately 2 weeks or 336 hours long, the manipulator must be heated for 336 minus 65.7 or 270.3 hours. From the tabulation on internal heat addition rates for various subzero temperatures, it is seen that 3.54 Btu per hour are necessary to maintain -100°F. Therefore:

Total Heat $3.54\ (336 - 65.7)$

$3.54\ (270.3)$

956.8 Btu.

Since 1 watt hr. = 3.413 Btu

Total Heat in watt-hr. $= \frac{956.8}{3.413}$

$= 280.3$ watt-hr.

Total heat inputs for several subzero temperatures are given in the following tabulation.

Subzero Temperature °F	Heat Input, Btu	Heat Input watt-hrs.
0	3115	913
-50	1833	537
-100	957	280
-150	401	117
-200	93	27

It is seen in the above tabulation how desirable it would be for the manipulator to be operative at temperatures below -150°F. The next section of this report will be an analysis of the thermal insulation method for controlling manipulator temperature. Similar tabulations will be made so that a series of curves can be plotted comparing the polished metal type of control to the thermal insulation method.

9.3 THERMAL INSULATION TEMPERATURE CONTROL

Two types of superinsulation are currently under development in this country. The Linde Corporation's SI-4 consists of multiple parallel reflective shields spaced by transparent, low conductivity filler. National Research Corporation's NRC-2 also has laminated parallel shields but does not contain the low conductivity filler. The superinsulations are most effective under a high vacuum which minimizes gas conduction and prevents the laminates from contacting which would generate more thermal paths.

Very little information is available concerning the physical properties of the superinsulations, as patent rights are still pending. The thermal insulation effect of these materials is given as an apparent conductivity k. The following tabulation gives the apparent conductivities and densities of the superinsulations as compared to three other common insulations.

Material	Apparent Conductivity (Btu/hr ft. ^{o}F)	Density (lb/ft^3)
NRC-2	2.3×10^{-5}	3.2
SI-4	2.5×10^{-5}	4.7
Perlite	58×10^{-5}	8.0
Vacuum (1 inch)	62×10^{-5}	
Asbestos	8900×10^{-5}	29

The insulation thermal analysis will be based upon the NRC-2 insulation with an aluminum coated outer surface. Since no information is available on the outer surface emissivities for the insulation, text

book emissivities will be adjusted to more realistic values, the proportionate increase being the same as the recommended increase for gold. Text book comparisons between gold and aluminum show the emissivities for gold being approximately half of the emissivities for aluminum. Since the practical emissivities for gold are 0.03 normal and 0.3 solar, the corresponding aluminum emissivities would be 0.06 normal and 0.6 solar.

The thermal analysis for insulation involves both radiation and conduction. The outer skin of the insulation is quite active in absorbing and reradiating heat, reaching temperatures close to 500°F when exposed to the sun. Because of the extremely low thermal conductivity of the insulation, only a negligible amount of heat is conducted to the manipulator. Of the total heat dissipated by the white area, four per cent is conducted heat, the remainder being heat absorbed by the white areas when exposed to the sun plus internal heat supplied by the electric motors.

The two unknowns in the heat balance equation are the insulation skin temperature, T_s, and square feet of white area, A_w. The heat balance equation differs from the heat balance equation for polished metal in that a heat conduction term is added. The heat conducted to the manipulator by the hot outer skin of the insulation is given by the equation:

$$H_c = \frac{k \ A_i \ (T_s - T_m)}{x}$$

Where H_c = heat conducted into manipulator in Btu/hr.

A_i = Total insulation skin area in sq. ft.

T_s = Skin temperature in $^oR = 460 + {}^oF$

T_m = Manipulator temperature in $^oR = 460 + {}^oF$

k = thermal conductivity of insulation in Btu/hr ft^2 $^oF/ft$.

x = insulation thickness in ft. = $\frac{.1875}{12} = .0156$ ft.

Equating the heat output from the manipulator to the heat input,

Heat radiated by white area = Solar heat absorbed by white area + Internal heat added by motors + Heat conducted into manipulator by skin of insulation.

$$\phi \ A_w \ E_w \ T_m^4 = 420 \ A_w \ E_{w_s} + 20 + \frac{k \ A_i \ (T_s - T_m)}{x}$$

$$\frac{17.3}{10^{10}} A_w \ (.80)(460 + 255)^4 = 420 \ A_w \ (.35) + 20 + \frac{2.3 \ (3.82)(T_s - 715)}{105 \ (.0156)}$$

It is seen the equation contains two unknowns, A_w and T_s. Fortunately the heat conducted into the manipulator from the hot skin is negligible compared to the large amount of heat being absorbed and

radiated by the skin. Therefore, the skin temperature may be calculated using the radiation formulas developed in the previous section, noting that no white area is attached to the skin for heat dissipation purposes.

Equating heat radiated from skin to heat absorbed by skin,

Top skin radiation + Side skin radiation + Bottom skin radiation = Top skin solar input + Side skin moon input + Bottom skin moon input

$$\phi A_t E_a T_s^4 + \phi A_s E_a T_s^4 + \phi A_b E_a T_s^4 = 420 A_t E_{a_s} + \phi A_s F_e F_c T_2^4 + \phi A_b F_e F_c T_2^4$$

$$\frac{17.3}{10^{10}} (.858)(.06) T_s^4 + \frac{17.3}{10^{10}} (2.06)(.06) T_s^4 + \frac{17.3}{10^{10}} (.90)(.06) T_s^4 = 420 (.858)(.6)$$

$$+\frac{17.3}{10^{10}} (2.06)(.06 \times 1)(.5)(733)^4 + \frac{17.3}{10^{10}} (.90)(.06 \times 1)(1)(733)^4$$

Solving for T_s,

$T_s = 912^{\circ}$ R or 452°F

Putting the skin temperature back into the above equation and solving for the individual surface heat exchanges, the large quantity of heat being absorbed and reradiated by the skin becomes apparent. The results are tabulated as follows:

	Heat Radiated (Btu/Hr)	Heat Absorbed (Btu/Hr)
Top skin	61.6	216.2
Side skin	147.8	30.8
Bottom skin	64.6	27.0
TOTAL	274.0	274.0

With a value for skin temperature, the heat balance equation for the manipulator may be solved for the square feet of white area A_w.

$$\frac{17.3}{10^{10}} A_w (.80)(460 + 255)^4 = 420 A_w (.35) + 20 + \frac{2.3 (3.82)(912 - 715)}{10^5 (.0156)}$$

$$361.64 A_w = 147 A_w + 20 + 1.11$$

$$A_w = .09835 \text{ sq. ft.}$$

A tabulation of the individual terms in the above equation found by substituting the value for A_w back into the equation shows what little heat is conducted into the manipulator compared to the solar heat absorbed by the white area and the internal heat generated by the electric motors.

	Heat Output (Btu/hr.)	Heat Input (Btu/hr.)
Radiated by white area	35.57	
Solar heat absorbed by white area		14.46
Internal heat added by motors		20.00
Conducted heat from hot skin of insulation		1.11
TOTAL	35.57	35.57

In studying the results of the last two tabulations it is seen why the skin temperature reaches 452°F. With 274 Btu per hour entering the skin, only 1.11 Btu per hour is conducted through

the insulation to the manipulator. Therefore only 0.098 sq. ft. of white area is needed for heat dissipation as compared to 0.49 sq. ft. for polished metal. The primary advantage of insulation over polished metal will be seen in the following calculations which deal with the quantity of heat necessary to maintain various subzero temperatures.

The heat balance equation for low temperature equilibrium differs considerably from that of the polished metal equation. Insulation skin temperature levels off between -200 and -250°F as a result of the small quantity of heat received from the manipulator and the moon. When equilibrium is reached at a specified subzero temperature, the heat being radiated from the skin is equal to the heat conducted to the skin from the warmer manipulator plus the heat the skin receives from the moon. Since the only way heat can escape from the manipulator is by conduction to the skin, the internal heat which must be added to maintain a specified subzero temperature is exactly equal to the conducted heat loss. To find the internal heat added, it is necessary to determine insulation skin temperature, as the heat conducted depends upon the difference in temperature between the skin and the manipulator.

The procedure for calculating the heat input rate at 0°F. will be shown, the results for the other subzero temperatures being tabulated.

Heat radiated from skin = Heat conducted from manipulator + Side skin moon input + Bottom skin moon input

$$\phi A_i E_a T_s^4 = \frac{k A_i (T_m - T_s)}{x} + \phi A_s F_e F_c T_2^4 + \phi A_b F_e F_c T_2^4$$

$$\frac{17.3}{10^{10}} (3.82)(.06) T_s^4 = \frac{2.3 (3.82) (460 - T_s)}{10^5 (.0156)} + \frac{17.3}{10^{10}} (2.06) (.06 \times 1) (.5) (217)^4 + \frac{17.3}{10^{10}} (.90) (.06 \times 1) (1) (217)^4$$

$$\frac{3.964}{10^{10}} T_s^4 = .005632 (460 - T_s) + .2370 + .2071$$

$$T_s = 252.5^\circ \text{ R or } -207.5^\circ \text{F}$$

The necessary rate of internal heat in btu per hour may now be calculated by substituting 252.5°F for T_s in the above equation and finding the value for the heat conduction term of the equation.

$$I = \frac{k A_i (460 - T_s)}{x}$$

$$= \frac{2.3 (3.82) (460 - 252.5)}{10^5 (.0156)}$$

$$I = 1.17 \text{ Btu per hr.}$$

The internal heat rates necessary to maintain various subzero temperatures are tabulated as follows:

Manipulator Temperature °F	Skin Temperature ° F	Internal Heat Addition Rate (Btu per Hr.)
0	(-207.5)	1.17
-50	(-216.9)	.94
-100	(-227.4)	.72
-150	(-239)	.50
-200	(-252)	.29
-250	(-267)	.09

The method for determining the total quantity of heat added internally for maintaining various subzero temperatures is similar to the polished metal method. The cooling time for the first stage temperature drop from 255°F to +50°F is calculated using the same formula developed for the polished metal. With the white area covered, resulting in a conductive form of heat loss, the second stage temperature drop from +50°F to a minimum operating temperature is calculated with a logarithmic equation.

Calculations for the first stage may be greatly simplified by assuming all of the heat leaves the manipulator via the white area. It is noticed in the heat balance tabulation for insulation that the conductive heat exchange between the manipulator and outer skin is negligible compared to the heat radiated from the white area. The amount of white area necessary with insulation is approximately

one fifth of the white area for polished metal resulting in a considerably longer first stage time period. The first stage cooling time is calculated as follows:

$$t = \frac{(wc)^4}{3M}\left[\frac{1}{H_T^3} - \frac{1}{H_p^3}\right]$$

Where $M = \phi\ A_w\ E_w = \frac{17.3}{10^{10}}(.0983)(.80)$

$$= \frac{.136}{10^{9}}$$

The other terms in the equation are the same as for the first stage drop in the polished metal method.

$$t_1 = \frac{\left[(32)(.091)\right]^4}{3\left(\frac{.136}{10^9}\right)}\left[\frac{1}{(1485)^3} - \frac{1}{(2082)^3}\right]$$

$t_1 = 34.3$ hrs.

The calculations for the second stage temperature drop from +50°F to a minimum operating temperature may be simplified by assuming the skin temperature is constant, resulting in a slightly shorter cooling time. The justification for this assumption may be seen in the last tabulation. It is noticed the skin temperature has total variation of only 50°F for a corresponding manipulator temperature variation of 250°F. Since the outer skin of the insulation is extremely thin, the heat content of the skin is very low, resulting in a very rapid skin temperature drop when the

manipulator enters the shade. Therefore, in calculating the cooling time for a temperature drop from +50°F to -100°F for example, it is assumed the skin temperature will instantly drop to its equilibrium temperature of -227.4°F.

The time equation for the second stage is derived as follows:

Let dQ equal a small amount of heat loss (in Btu) during a small interval of time dt (in hours).

Then

$$dQ = Udt$$

Where U is the total rate of heat loss in Btu per hour at corresponding manipulator temperature T. Since heat is lost by conduction only,

$$U = \frac{k\,A\,(T - T_s)}{x}$$

$$dQ = \frac{k\,A_i\,(T - T_s)}{x}\,dt$$

Where T_s is the equilibrium skin temperature for the subzero temperature for which the cooling period is being calculated in °R.

To solve the differential equation it is necessary to put T in terms of Q. Referring to the derivation of the time equation for polished metal,

$$T = \frac{H_p - Q}{wc}$$

Substituting,

$$dQ = \frac{k\ A_i}{x}\left[\frac{H_p - Q}{wc} - T_s\right] dt$$

$$dQ = \frac{k\ A_i}{xwc}\left[H_p - Q - wcT_s\right] dt$$

$$\frac{dQ}{\left[(H_p - wcT_s) - Q\right]} = \frac{k\ A_i}{xwc}\ dt$$

Integrating,

$$-\log\left[(H_p - wcT_s) - Q\right] = \frac{k\ A_i}{xwc}\ t + C$$

When $t = 0$

$$Q = 0$$

$$C = -\log (H_p - wcT_s)$$

$$t = \frac{xwc}{k\ A_i}\ \log\left(\frac{(H_p - w\ c\ T_s)}{(H_p - w\ c\ T_s - Q)}\right)$$

Since Q is the difference between the peak heat content H_p and the heat content H_T at some manipulator temperature T, the equation may be written

$$t = \frac{xwc}{k\ A_i}\ \log\left(\frac{(H_p - w\ c\ T_s)}{(H_T - w\ c\ T_s)}\right)$$

Where t is the time in hours for the manipulator to drop from a peak heat content H_p to a lower heat content H_T.

The cooling time for the temperature drop from + 50°F to 0°F will be calculated, the results for the other subzero temperatures being tabulated.

$$t_2 = \frac{(.0156)\ (32)(.091)}{\left(\frac{2.3}{10^5}\right)\ 3.82} \log \left(\frac{1485 - (32)(.091)(460 - 207.5)}{1340 - (32)(.091)(460 - 207.5)} \right)$$

$$t_2 = 517 \log \left(\frac{1485 - 735}{1340 - 735} \right)$$

$$t_2 = 110.8 \text{ hours}$$

The number of hours required for the manipulator temperature to drop from + 255°F. to 0°F. is the sum of the hours for the first stage plus the second stage or:

$$t_o = t_1 + t_2$$

$$= 34.3 + 110.8$$

$$t_o = 145.1 \text{ hours}$$

The cooling time in hours and days for the manipulator to drop from 255°F to various subzero temperatures are tabulated as follows:

Subzero Temperature (°F)	Hours	Days
0	145.1	6
-50	277	11.5
-100	437	18.2
-150	642	26.8
-200	945	39.4
-250	1552	64.7

The total heat input in Btu or watt-hrs. to maintain various subzero temperatures following the cooling period may now be calculated using the same method employed for polished metal. Referring to the above tabulation and also the tabulation listing internal heat addition rates for an insulated manipulator,

Total heat for 0°F $= 1.17\ (336 - 145.1)$

$= 223$ Btu

or $\frac{223}{3.413} = 65.3$ watt-hr.

Total heat input to maintain -50°F $= .94\ (336 - 277)$

$= 55$ Btu

or $\frac{55}{3.413} = 22.6$ watt-hr

No heat addition is necessary for the other subzero temperatures as the cooling time is longer than the lunar night.

9.4 PARTIAL INSULATION AND POLISHED METAL TEMPERATURE CONTROL

Smooth, unbroken surfaces having one plane of curvature such as the ellipsoidal shaped portion of the pan drive housing are easily insulated compared to irregular surfaces with sharp corners. If it proves infeasible to insulate the entire manipulator without considerable redesign, then the question arises whether it would be worthwhile to insulate part of the manipulator. For this study the ellipsoidal shaped portion of the pan drive housing has been selected as the area to be insulated. This area has 0.95 square feet which is approximately twenty-five per cent of the total manipulator area.

Equating the heat output to heat input for a partially insulated manipulator:

Heat radiated by gold area	+ Heat radiated by white area	= Solar heat absorbed by gold area	+ Solar heat absorbed by white area	+ Moon heat absorbed by gold area
		+ Heat conducted into manipulator from hot skin of insulation	+ Internal heat added by motors	

The heat conducted into the manipulator from the hot skin of the insulation is negligible as shown by previous calculations (1.11 Btu per hour for a total skin area of 3.82 square feet), and therefore this term in the equation will be eliminated. Because of the numerous terms in the equation (heat radiated by the gold area is subdivided into top, side, and bottom; and moon heat input to gold is subdivided into side and bottom), each term will be calculated separately, after

which the reduced terms will be substituted in the heat balance equation which is then solved for the number of square feet of white area, A_w.

Heat radiated by top gold surface

$$H_{r1} = \phi\ A_t\ E_g\ T^4$$

Where $A_t = .858 - .282 = .576$ sq. ft.

$$H_{r1} = \frac{17.3}{10^{10}} (.576)(.03)(460 + 255)^4 = 7.81 \text{ Btu/hr.}$$

Heat radiated by side gold surface

$$H_{r2} = \phi\ A_s\ E_g\ T^4$$

Where $A_s = 2.06 - .386 = 1.674$ sq. ft.

$$H_{r2} = \frac{17.3}{10^{10}} (1.674)\ (.03)\ (460 + 255)^4 = 22.7 \text{ Btu/hr}$$

Heat radiated by bottom gold surface

$$H_{r3} = \phi\ A_b\ E_g\ T^4$$

Where $A_b = .90 - .282 = .618$ sq. ft.

$$H_{r3} = \frac{17.3}{10^{10}} (.618)\ (.03)\ (460 + 255)^4 = 8.37 \text{ Btu/hr.}$$

Heat radiated by white surface

$$H_{r4} = \phi\ A_w\ E_w\ T^4$$

$$H_{r4} = \frac{17.3}{10^{10}} (A_w)\ (.80)\ (460 + 255)^4 = 361.7\ A_w \text{ Btu/hr.}$$

Solar heat absorbed by gold area

$$H_{s1} = 420\ A_t\ E_{g_s}$$

Where $A_t = .858 - .282 = .576$ sq. ft.

$$H_{s1} = 420\ (.576)\ (.3) = 72.58 \text{ Btu/hr.}$$

Solar heat absorbed by white surface

$$H_{s_2} = 420\ A_w\ E_{W_s}$$

$$Hs_2 = 420\ A_w\ (.35) = 147\ A_w\ \text{Btu/hr}$$

Moon heat absorbed by side gold area

$$Ha_3 = \phi\ A_s\ Fe\ Fc\ T_2^4$$

Where $A_s = 2.06 - .386 = 1.674$ sq. ft.

$$Ha_3 = \frac{17.3}{10^{10}} (1.674)(.03 \times 1)(.5)(733)^4 = 12.54 \text{ Btu/hr.}$$

Moon heat absorbed by bottom gold area

$$H_{a4} = \phi\ A_b\ Fe\ Fc\ T_2^4$$

Where $A_b = .90 - .282 = .618$ sq. ft.

$$Ha_4 = \frac{17.3}{10^{10}} (.618)(.03 \times 1)(733)^4 = 9.25 \text{ Btu/hr}$$

Internal heat added by motors

$$H_i = 20 \text{ Btu/hr.}$$

Equating heat output to heat input,

$$H_{r_1} + H_{r_2} + H_{r_3} + H_{r_4} = H_{s_1} + H_{s_2} + H_{a_3} + H_{a_4} + H_i$$

$$7.81 + 22.7 + 8.37 + 361.7\ A_w = 72.58 + 147\ A_w + 12.54 + 9.25 + 20$$

$$214.7\ A_w = 75.49$$

$$A_w = 0.35 \text{ sq. ft.}$$

Insulating the pan drive housing reduces the white area from 0.49 square feet to 0.35 square feet.

The heat balance equation for low temperature equilibrium includes both radiation and conduction. To maintain a specified

subzero temperature, sufficient internal heat must be added to replace that lost by radiation from the polished gold areas and also the heat conducted from the manipulator to the skin of the insulation.

Equating heat output to heat input,

Heat radiated by gold including gold covered white area	+	Heat radiated by skin	=	Heat absorbed by gold from moon	+	Heat absorbed by skin from moon
				+ Internal heat added which is lost by conduction to skin of insulation.	+	Internal heat added which is lost by radiation from gold areas.

Since the manipulator is at a uniform temperature, the above heat balance equation may be separated into two equations, one for gold and one for insulation. The internal heat additions are calculated separately for each equation and then added together to give a total internal heat addition rate.

Separating the gold heat balance equation from the above equation,

Heat radiated by gold including gold covered white area	=	Heat absorbed by gold from moon	+	Internal heat added which is lost by radiation from gold area.

$$\phi A_g E_g T_1^4 = \phi A_s F_e F_c T_2^4 + \phi A_b F_e F_c T_2^4 + I_g$$

Where A_g = total gold area including covered white area

$3.82 - .95 + .35 = 3.22$ sq. ft.

A_s = side area of gold

$= 2.06 - .386 = 1.674$ sq. ft.

A_b = bottom area of gold

= .90 - .282 = .618 sq. ft.

T_2 = temperature of moon ^oR = 460 + (-243^oF)

T_1 = manipulator temperature, ^oR

The internal heat addition rate for a manipulator temperature of 0^oF will be calculated, the results of the calculations for other subzero temperatures being tabulated.

$$\frac{17.3}{10^{10}}(3.22)(.03)(460)^4 = \frac{17.3}{10^{10}}(1.674)(.03 \times 1)(.5)(217)^4 + \frac{17.3}{10^{10}}(.618)(.03 \times 1)(1)(217)^4 + I_g$$

$$7.47 = .0959 + .0707 + I_g$$

$$I_g = 7.3 \text{ Btu/hr}$$

Subzero Temperature ^oF	Internal Heat Addition Rate (I_g) for gold areas Btu/hr.
0	7.30
-50	4.54
-100	2.62
-150	1.37
-200	.596
-250	.157

Separating the insulation heat balance equation from the combined equation,

Heat radiated by skin	=	Heat absorbed by skin from moon.	+	Internal heat added which is lost by conduction to skin of insulation.

$$\phi A_i E_a T_s^4 = \phi A_s F_e F_c T_2^4 + \phi A_b F_e F_c T_2^4 + I_c$$

Where A_i = total skin area = 0.95 sq. ft.

A_s = side skin area = 0.386 sq. ft.

A_b = bottom skin area = 0.282 sq. ft.

T_s = skin temperature

I_c = internal heat added

$$= \frac{k A_i (T_m - T_s)}{x}$$

$$\frac{17.3}{10^{10}} (.95)(.06) T_s^4 = \frac{17.3}{10^{10}} (.386)(.06 \times 1)(.5)(217)^4 +$$

$$\frac{17.3}{10^{10}} (.282)(.06 \times 1)(1)(217)^4 +$$

$$\frac{2.3 (.95)(T_m - T_s)}{10^5 (.0156)}$$

$$\frac{.986}{10^{10}} T_s^4 = .0444 + .0649 + .0014 (T_m - T_s)$$

$$\frac{.986}{10^{10}} T_s^4 + .0014 T_s - .0014 T_m - .1093 = 0$$

Letting the manipulator temperature, T_m, equal 0°F or 460°R,

$$\frac{.986}{10^{10}} T_s^4 \quad .0014 T_s - .0014 (460) - .1093 = 0$$

$$T_s = 252^\circ R$$

The internal heat added, I_c, can now be calculated by solving for the value of the heat conduction term in the heat balance equation.

$$I_c = \frac{2.3 (.95)(T_m - T_s)}{10^5 (.0156)}$$

$$I_c = .0014 (460 - 252) = 0.29 \text{ Btu per hr.}$$

Values of I_c for other subzero temperature are tabulated as follows:

Manipulator Temperature °F	Insulation Skin Temperature °F	Internal Heat Addition Rate (I_c) for insulated area. Btu/hr
0	(-208)	0.29
-50	(-217)	0.23
-100	(-228)	0.18
-150	(-239)	0.12
-200	(-252)	.073
-250	(-267)	.024

The total heat addition rates, $(I_g + I_c)$, can now be calculated. At 0°F,

$$I_{tot.} = I_g + I_c$$

$$= 7.3 + .29 = 7.59 \text{ Btu/hr.}$$

This figure represents the rate at which heat must be added internally to replace that lost by radiation from the gold areas plus conduction to the insulation skin for a 0°F manipulator temperature equilibrium.

Total heat addition rates for other subzero temperatures are tabulated as follows:

Manipulator Temperature °F	Total Internal Heat Addition Rate ($I_g + I_c$) Btu/hr.
0	7.59
-50	4.77
-100	2.80
-150	1.49
-200	.669
-250	.181

The total quantity of heat which must be added internally to maintain a specified subzero temperature depends upon the number of days the manipulator will be at this temperature, and therefore the cooling time to reach this temperature must first be calculated. As in the previous time calculations, cooling time covers a two stage temperature drop, the first drop being from +255°F to +50°F with the white area exposed and the second stage drop being from +50°F to the specified subzero temperature with the white area covered.

The rate of heat loss from the insulated portion of the manipulator is negligible compared to the rate of heat loss from the polished gold and exposed white area, and therefore will be disregarded during the first stage temperature drop. The procedure for calculating the first stage temperature drop is the same as for the polished gold temperature control method, the only difference being a reduction in

the extent of the gold and white areas which changes the value for M in the time equation.

$$t = \frac{(wc)^4}{3M}\left[\frac{1}{H_T^3} - \frac{1}{H_p^3}\right]$$

$$M = \phi\, A_t\, E_g + \phi\, A_w\, E_w + \phi\, A_s\, E_g + \phi\, A_b\, E_g$$

Where A_t = top gold area = .858 - .282

= 0.576 sq. ft.

A_w = white area = 0.35 sq. ft.

A_s = side gold area = 2.06 - .386

= 1.674 sq. ft.

A_b = bottom gold area = .90 - .282

= 0.618 sq. ft.

$$M = \frac{17.3}{10^{10}}\left[(.576)(.03) + (.35)(.80) + (1.674)(.03) + (.618)(.03)\right]$$

$$M = \frac{.6332}{10^9}$$

$$t_1 = \frac{\left[(32)(.091)^4\right]}{3\left(\frac{.6332}{10^9}\right)}\left[\frac{1}{(1483)3} - \frac{1}{(2082)3}\right]$$

t_1 = 7.37 hours

The same equation is used to calculate the cooling time for the manipulator temperature drop from + 500F to various subzero temperatures.

The M term in the equation will have a different value as a result of the covering of the white area by a gold plated shield. The error in using the simplified equation, which does not take into account the heat lost by conduction through the insulation or moon heat input, is very small. The reason for a small error may be seen in the tabulations on I_g and I_c where it is noted the rate of heat loss by conduction, I_c, is only four per cent of the radiation from the gold area for a manipulator temperature of $0^{\circ}F$. Since part of the heat being lost by conduction through the insulation is continually being replaced by moon heat input to the gold areas (.0959 + 0707 Btu/hr.) the rate of heat loss which is disregarded in the time formula is only 1.7 per cent of the rate of heat loss from the gold areas. Therefore, the small amount of error involved in calculating cooling times for the second stage temperature drops does not warrant the use of a more complex time equation.

$$t_2 = \frac{(wc)^4}{3M}\left[\frac{1}{H_T^3} - \frac{1}{H_p^3}\right]$$

$$M = \phi\ A_t\ E_g + \phi\ A_w\ E_g + \phi\ A_s\ E_g + \phi\ A_b\ E_g$$

Noting that the white area is covered,

$$M = \frac{17.3}{10^{10}}\left[(.576)(.03) + (.35)(.03) + (1.674)(.03) + (.618)(.03)\right]$$

$$M = \frac{.167}{10^{9}}$$

A second stage drop from +50°F to 0° is calculated as follows using the same values for H_T and H_p as found in the second stage for a completely gold manipulator.

$$t_2 = \frac{\left[(32)(.091)^4\right]}{3\left(\frac{.167}{10^9}\right)} \left[\frac{1}{(1340)^3} - \frac{1}{(1485)^3}\right]$$

$t_2 = 15.8$ hours

The number of hours required for the manipulator temperature to drop from +255°F to 0°F is the sum of the hours for the first stage plus the second stage or

$$t_o = t_1 + t_2$$

$$= 7.37 + 15.8$$

$t_o = 23.18$ hours

The cooling time in hours and days for the manipulator to drop from 255°F to various subzero temperatures are tabulated as follows:

Subzero Temperature 0°F	Hours	Days
0	23.18	0.970
-50	47.86	2.00
-100	88.23	3.68
-150	158.44	6.60
-200	294.35	12.26
-250	593	24.7
-300	1383	57.6

From the tabulation on total internal heat addition rates and the above tabulation, the total heat input in Btu and watt-hours to maintain temperature equilibrium following the cooling period can now be calculated.

Total Heat = $I_{tot.}$ (336 - t_o)

Where 336 = length of lunar night in hours.

For 0°F,

Total Heat = 7.59 (336 - 23.18)

2374 Btu.

Total Heat in watt-hr. = $\frac{2374}{3.413}$

= 695 watt-hrs.

The total heat inputs for other subzero temperatures are tabulated as follows:

Subzero Temperature °F	Total Heat Input Btu	Total Heat Input Watt-hrs.
0	2374	695
-50	1374	402
-100	694	203
-150	265	78
-200	28	8

The following tabulation compares the total heat input for a completely gold plated manipulator to the total heat input for a partially insulated manipulator, the insulated area being approximately twnety five per cent of the total area.

Subzero Temp. °F	Total Heat Input for all gold manipulator Btu	Total Heat Input for partially insulated manipulator Btu	Per cent reduction in total heat input
0	3115	2374	23.8
-50	1833	1374	25.0
-100	957	694	27.5
-150	401	265	33.9
-200	93	28	70.0

It is seen in the above tabulation that for subzero temperatures involving high total heat input, the per cent reduction in total heat input is approximately the same as the per cent of insulated area. As would be expected, the per cent reduction in total heat input increases rapidly as the cooling period approaches the length of a lunar night. When the cooling period for a partially insulated manipulator exactly equals a lunar night or 336 hours, the per cent reduction in total heat input will be equal to 100 per cent. As a conclusion to the effect of partial insulation, it may be stated that the per cent of area insulated is approximately equal to the per cent

reduction in heat input to maintain an equilibrium temperature of -100°F and above.

Tabulations on total heat input, heat input rates, and cooling time for the three methods of temperature control are presented as a series of curves. The advantage of thermal insulation over polished metal is very apparent. If experimental tests show that the manipulator can be operated at -70°F which is the lowest temperature a completely insulated manipulator will reach during a lunar night, means for adding heat internally will not be necessary. With polished gold, it is seen on the cooling time curve that the manipulator would have to operate at -232°F to avoid auxiliary heating equipment. After the minimum operating temperature has been established experimentally, the total heat input and rate of heat input can be determined from the curves.

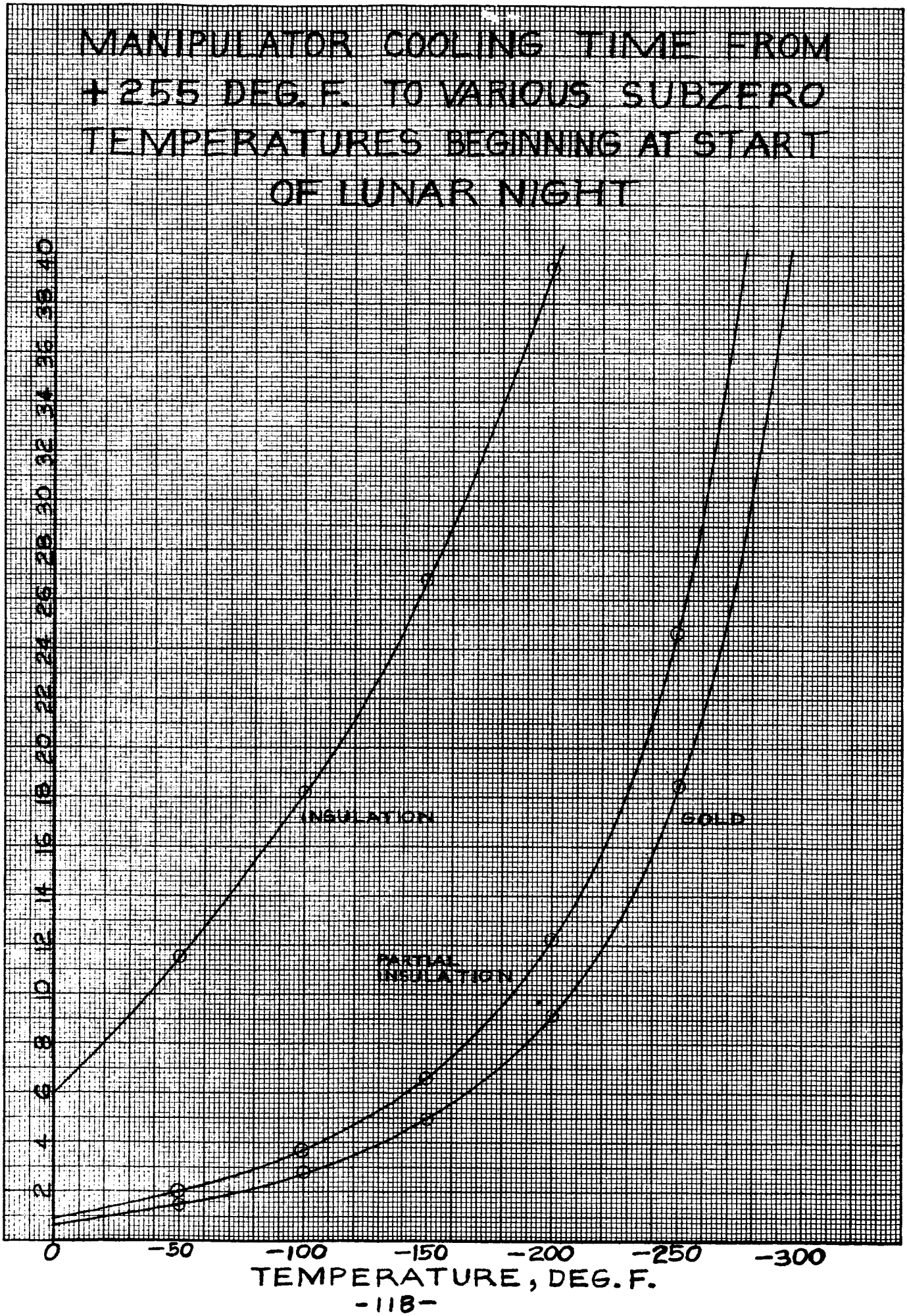
MANIPULATOR COOLING TIME FROM +255 DEG. F. TO VARIOUS SUBZERO TEMPERATURES BEGINNING AT START OF LUNAR NIGHT
COOLING TIME, DAYS
2
4
6
8
10
12
14
16
18
20
22
24
26
28
30
32
34
36
38
40
INSULATION
PARTIAL INSULATION
GOLD
0
-50
-100
-150
-200
-250
-300
TEMPERATURE, DEG. F.

RATE OF HEAT INPUT TO MANIPULATOR FOR TEMPERATURE EQUILIBRIUM AT VARIOUS SUBZERO TEMPERATURES DURING LUNAR NIGHT

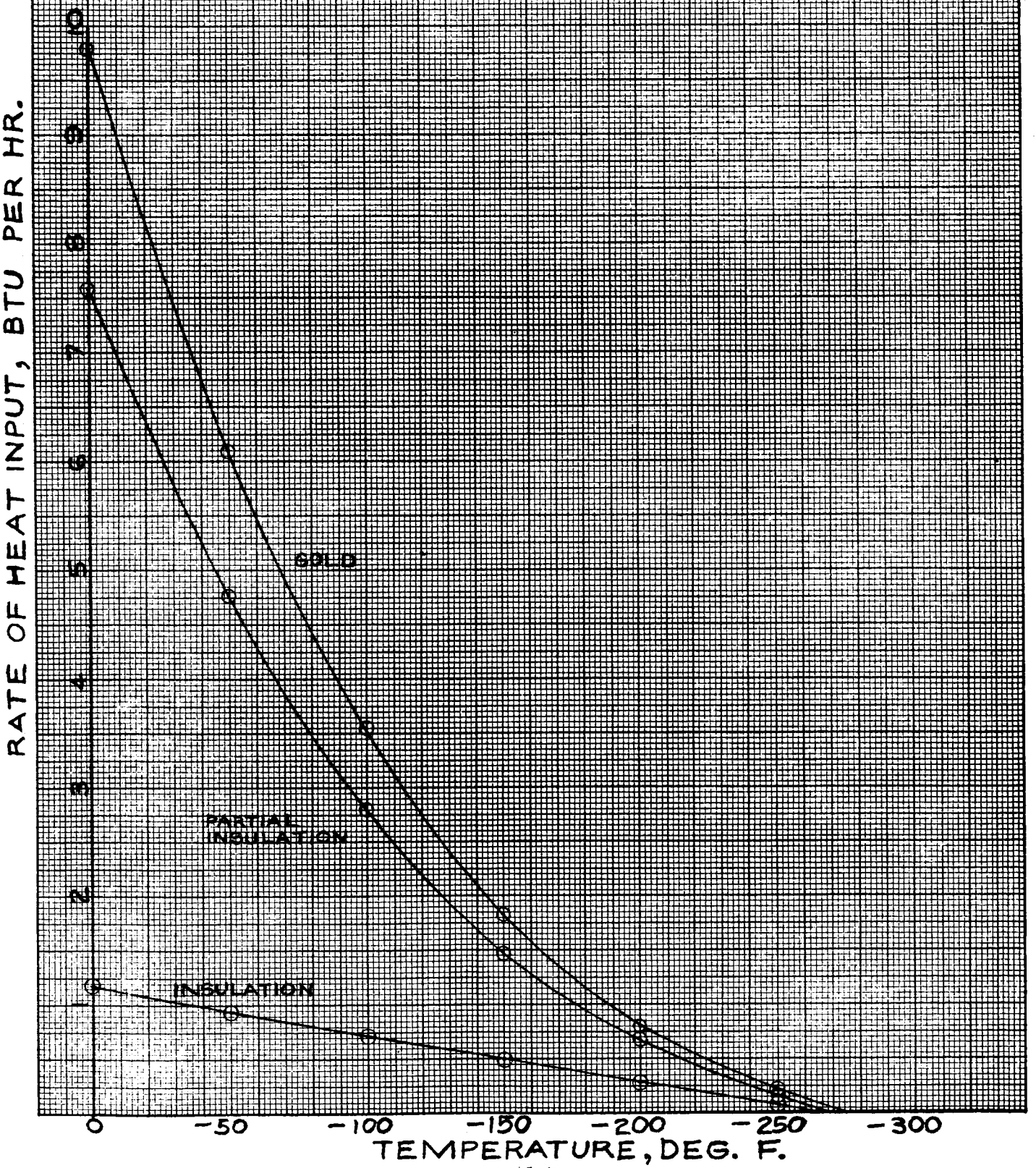

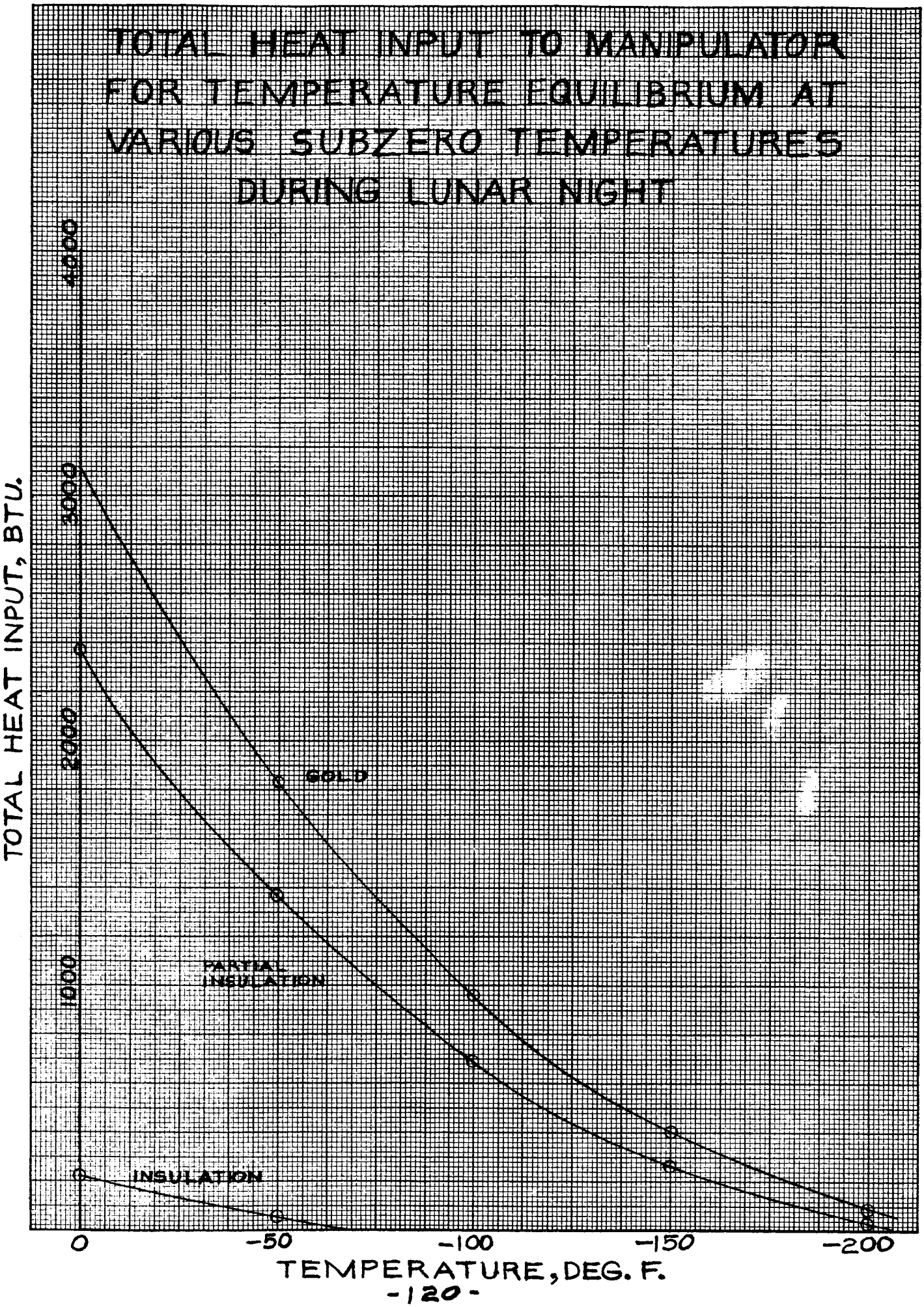
TOTAL HEAT INPUT TO MANIPULATOR FOR TEMPERATURE EQUILIBRIUM AT VARIOUS SUBZERO TEMPERATURES DURING LUNAR NIGHT
TOTAL HEAT INPUT, BTU.
4000
3000
2000
1000
GOLD
PARTIAL INSULATION
INSULATION
0
-50
-100
-150
-200
TEMPERATURE, DEG. F.

9.5 TELEVISION CAMERA THERMAL ANALYSIS

The preceding manipulator analysis is independent of the television camera. However, to avoid possible manipulator redesign when the camera is connected to the manipulator, thermal data for the camera is calculated using the radiation formulas presented in the foregoing sections. The exact lense area for the camera is not known, and therefore it is assumed to be one half of the camera end area, the camera being in the shape of a cylinder. Error in the amount of glass area assumed will not alter the results significantly, as the heat entering through the glass is approximately equal to the heat dissipated by the glass. The camera, being a potential source of heat loss for the manipulator at subzero temperatures, is assumed to be gold plated.

Both the high and low camera temperatures are calculated on the assumption the camera is perfectly insulated from the manipulator. Should it be necessary to cool the camera, a conduction path from the camera to the manipulator will be necessary, as attaching a heat dissipating area to the camera would be ineffective since the camera has no surface which is always pointed skyward. To see how effective the white area of the manipulator will be in cooling the camera, the overall conduction resistance between the camera and the white area of the manipulator is calculated. Heat conduction requires a temperature differential. To effectively cool the camera by a white area located two feet from the camera, the following calculations

show it will be necessary to operate the entire manipulator at a considerably lower temperature than 255°F. If the camera can withstand a peak temperature of approximately +300°F and a low temperature of -250°F, insulating the camera from the manipulator is the best approach.

For calculation purposes the cylindrical shaped camera is placed in a vertical position with the camera lense facing the moon. Both ends are parallel to the surface of the moon and the curved side surface is perpendicular to the moon. The heat output is calculated separately for the top gold surface, side surface, bottom glass surface, and bottom gold surface. Likewise the heat absorbed is calculated separately for each of these surfaces.

Heat radiated by top gold surface

$$H_{r_1} = \phi\, A_t\, E_g\, T_c^4$$

Where A_t is top area = 0.259 sq. ft.

T_c = camera temperature in °R

$$H_{r_1} = \frac{17.3}{10^{10}} (0.259)(.03)(T_c)^4$$

$$H_{r_1} = \frac{.1344}{10^{10}}\ T_c^4 \text{ Btu/hr}$$

Heat radiated by side surface

$$H_{r_2} = \phi\, A_s\, E_g\, T_c^4$$

Where A_s is side area = 2.25 sq. ft.

$$H_{r_2} = \frac{17.3}{10^{10}} (2.25)(.03)\ T_c^4$$

$$H_{r_2} = \frac{1.168}{10^{10}}\ T_c^4 \text{ Btu/hr.}$$

Heat absorbed by bottom glass surface

$$H_{a_3} = \phi \; A_1 \; F_e \; F_c \; T_2^4$$

$$H_{a_3} = \frac{17.3}{10^{10}} (.129)(.94 \times 1)(733)^4$$

$$H_{a_3} = 60.56 \text{ Btu/hr.}$$

Heat absorbed by bottom gold surface

$$H_{a_4} = \phi \; A_b \; F_e \; F_c \; T_2^4$$

$$H_{a_4} = \frac{17.3}{10^{10}} (.129)(.03 \times 1)(733)^4$$

$$H_{a_4} = 1.93 \text{ Btu/hr.}$$

Equating the heat radiated to the heat absorbed and solving for T_c,

$$H_{r_1} + H_{r_2} + H_{r_3} + H_{r_4} = H_s + H_{a_2} + H_{a_3} + H_{a_4}$$

$$\frac{.1344}{10^{10}} T_c^4 + \frac{1.168}{10^{10}} T_c^4 + \frac{2.097 T_c^4}{10^{10}} + \frac{.0669}{10^{10}} T_c^4 = 32.63 + 16.85 + 60.56 + 1.93$$

$$\frac{3.4663}{10^{10}} T_c^4 = 111.97$$

$$T_c = 754^\circ R$$

$$= 294^\circ F$$

It is seen the maximum camera equilibrium temperature is 294°F as compared to 255°F for the manipulator.

In calculating minimum camera equilibrium temperature, the terms on the left side of the above equation will not change. On the right side, solar heat, H_s, becomes zero when the manipulator

Heat radiated by bottom glass surface

$$H_{r_3} = \phi A_1 E_1 T_c^4$$

Where A_1 is lense area = 0.129 sq. ft.

E_1 is emissivity for glass = 0.94

$$H_{r_3} = \frac{17.3}{10^{10}} (.129)(.94) T_c^4$$

$$H_{r_3} = \frac{2.097}{10^{10}} T_c^4 \text{ Btu/hr.}$$

Heat radiated by bottom gold surface

$$H_{r_4} = \phi A_b E_g T_c^4$$

Where A_b is bottom gold area = 0.129 sq. ft.

$$H_{r_4} = \frac{17.3}{10^{10}} (.129) (.03) T_c^4$$

$$H_{r_4} = \frac{.0669}{10^{10}} T_c^4 \text{ Btu/hr.}$$

Heat absorbed by top gold surface

$$H_s = 420 A_t E_{g_s}$$

$$H_s = 420 (.259)(.3)$$

$$H_s = 32.63 \text{ Btu/hr.}$$

Heat absorbed by side surface

$$H_{a_2} = \phi A_s F_e F_c T_2^4$$

$$H_{a_2} = \frac{17.3 (2.25)(.03 \times 1)(.5)(733)^4}{10^{10}}$$

$$H_{a_2} = 16.85 \text{ Btu/hr.}$$

enters the shade and the other three terms are reduced in value as a result of the -243°F moon surface temperature.

$$\frac{3.4663}{10^{10}} T_c^4 = 0 + \frac{17.3}{10^{10}} (2.25)(.03 \times 1)(.5)(460 - 243)^4 +$$

$$\frac{17.3}{10^{10}} (.129)(.94 \times 1)(1)(460 - 243)^4 +$$

$$\frac{17.3}{10^{10}} (.129)(.03 \times 1)(1)(460 - 243)^4$$

$$T_c = 204.7^\circ R$$

$$= -255.3^\circ F \text{ minimum equilibrium temperature}$$

Referring to the maximum camera temperature heat balance equation, it is seen that the heat radiated by the camera at 294°F is 111.97 Btu per hour which is also the rate of heat being absorbed by the camera. Since the manipulator is at 255°F, heat will be conducted into the manipulator by the camera, resulting in a camera temperature drop. For a camera temperature of 255°F the theoretical rate of heat flow from the camera is the difference between the external heat absorbed (111.97 Btu/hr) by the camera and the heat it can radiate when it is at 255°F. By substituting this camera temperature in the left side of equation, the radiation rate is found as follows:

$$H_r = \frac{3.4663}{10^{10}} (460 + 255)^4 = 90.57 \text{ Btu/hr.}$$

Heat conducted to the manipulator = 111.97 - 90.57 = 21.4 Btu/hr.

Providing a heat conduction path between the camera and manipulator will increase the manipulator temperature slightly. The following calculations indicate the rate at which the white area can

dissipate camera heat. The manipulator frame is constructed with half hard, cold rolled electrolytic copper which has a high thermal conductivity. For the same weight, aluminum offers less resistance to heat flow because of larger cross-sectional areas. However, copper has a linear coefficient of expansion that is more compatible with internal steel parts.

Figure 4. shows the heat conduction path from the camera to the elevate drive housing to which the white area is attached. Average cross sectional areas are used wherever there is a tapered construction. In instances where the construction is similar to a manifold, average distances are used. Theoretically the slip rings have negligible resistance to heat flow because of the large cross sectional areas and very short lengths, and therefore are not included in the calculations. Slip ring efficiency in a vacuum will have to be determined experimentally. For conduction through solids of varying cross section and length that are arranged in series,

$$H_c = \frac{(T_1 - T_2)}{\frac{l_1}{k_1 A_1} + \frac{l_2}{k_2 A_2} + \cdots + \frac{l_n}{k_n A_n}}$$

Where H_c is the heat conducted in Btu per hour.

$(T_1 - T_2)$ is overall temperature differential in ^{o}F.

FIG. 4.

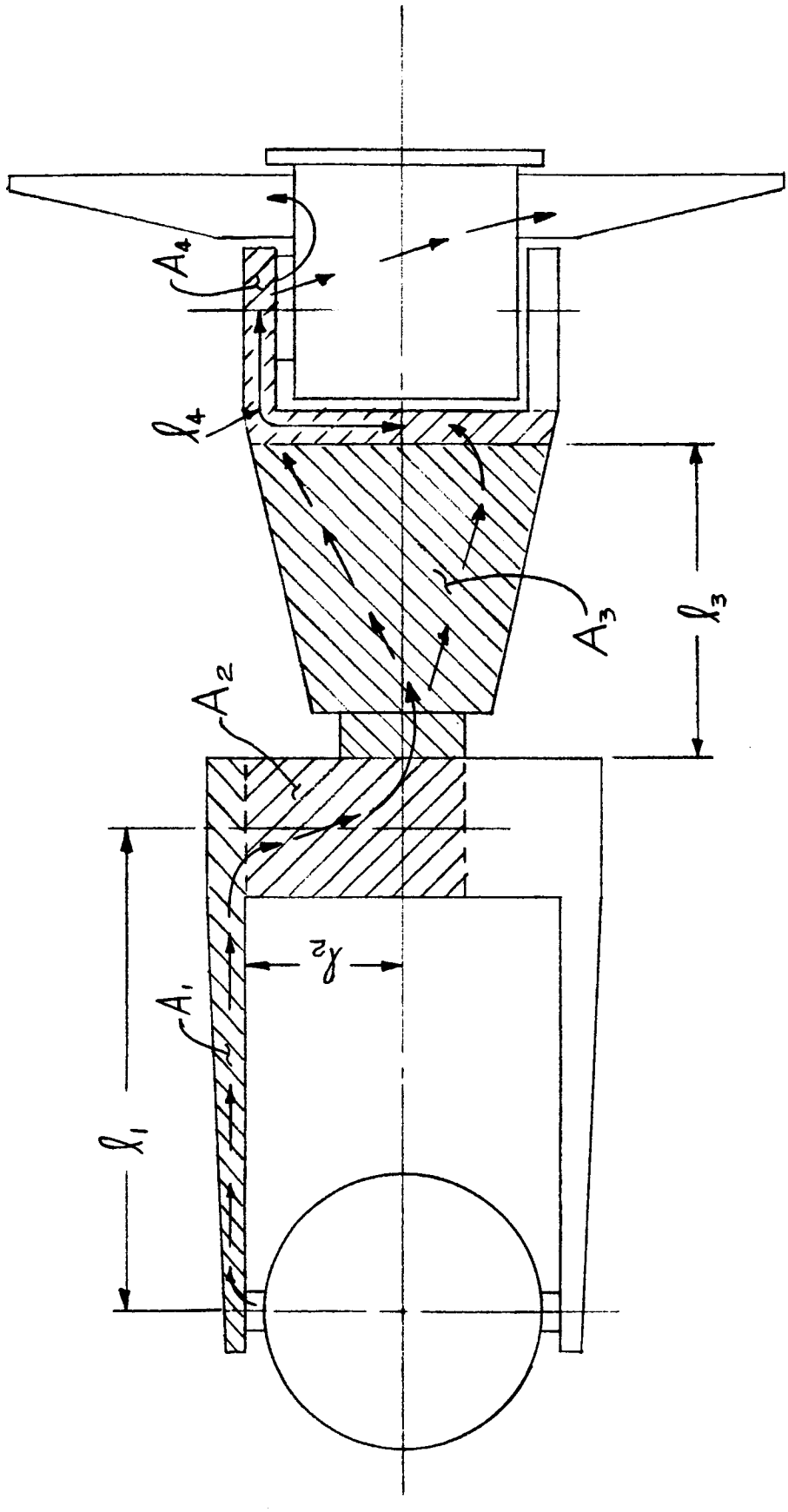

l_1, l_2, etc. are the lengths in feet of members having respective cross sectional areas A_1, A_2, etc. in square feet and thermal conductivities k_1, k_2, etc. in Btu/hr. ft^2 ^oF/ft.

$$H_c = \frac{(T_1 - T_2)}{\frac{l_1}{k_1A_1} + \frac{l_2}{k_2A_2} + \frac{l_3}{k_3A_3} + \frac{l_4}{k_4A_4}}$$

$$= \frac{(T_1 - T_2)}{\frac{.96}{225(.00265)} + \frac{.325}{225(.00431)} + \frac{.658}{225(.00542)} + \frac{.54}{225(.00488)}}$$

$$= \frac{(T_1 - T_2)}{1.61 + .335 + .540 + .4918}$$

$H_c = .34\ (T_1 - T_2)$ Btu per hr.

In examining the above conduction equation, it is seen that for every degree difference in temperature between the camera and the white area, 0.34 Btu per hour will flow to the white area. The camera equilibrium temperature may be calculated by equating the heat output from the camera to the heat input.

Heat radiated by camera at its equilibrium temperature + Heat conduced to white area = 111.97 Btu per hr.

$$\frac{3.4663\ T_c^4}{10^{10}} + .34\ (T_c - T_w) = 111.97$$

Where T_c = temperature of camera in ^oR.

T_w = temperature of white area in ^oR = $460 + 255^o = 715$

$$\frac{3.4663\ T_c^4}{10^{10}} + .34\ (T_c - 715) = 111.97$$

$$T_c = 740^\circ\ R$$

$$\text{or } 280^\circ\ F$$

It is noticed that the camera temperature will drop from 294° to 280° F when a conduction path to the manipulator is provided. This small drop in temperature does not warrant the installation of a slip ring conduction path. Should it become necessary to heat the camera during the lunar night by conducting heat from the manipulator, a conduction path must be provided. From a manipulator heat conservation standpoint, there should not be a metallic connection between the camera and the manipulator. With the camera being clamped by a ring, a band of low conductivity material inserted between the ring and camera will reduce the heat loss.

9.6 BIMETAL SPRING CONTROL MECHANISM

Until the minimum manipulator operating temperature is established experimentally, it must be assumed that the manipulator cannot be allowed to approach absolute zero and operate. Therefore heat loss during the lunar night must be kept to a minimum as the transportation of batteries to the moon for heating purposes is very costly. The white area dissipates 75 per cent of total manipulator heat, and therefore covering this area with a highly reflective shield will block the main path of heat loss. Controlling the shield by means of a bimetal spring appears to an inexpensive, reliable method requiring no electric power.

The bimetal spring mechanism is shown on drawing 520394-E. Two white Rokide A areas, totalling 0.49 square feet, are attached to the elevate drive housing. Each shield is controlled by a left and right hand wound spring rather than one long spring, thereby providing two heat conduction paths and symmetrical loading which reduces friction. Spring actuation depends primarily on heat radiation from the manipulator. To increase heat input rate to the springs, the internal surfaces surrounding the springs are not plated or polished.

Bimetal springs have a wide range of thermal conductivities. In some applications springs are heated electrically by passing current through the springs. Springs designed for this purpose have low electrical resistivity or conversely, high thermal

conductivity. The following calculations are based upon a low resistivity bimetal manufactured by the H. A. Wilson Division of Engelhard Industries called R-39.

The spring torque loads from 0 to 90 degrees in 10 degree increments are based upon the earth's gravitational pull and are calculated as follows:

Referring to Figure 5 and drawing 520394-E, point 0 represents the center of the spring which is also the pivot point for the shield. Point d is the center of gravity of the shield which weighs 10.38 ounces. Scaling drawing 520394-E,

$$\text{line } \overline{b\,d} = 3.06 \text{ inches}$$

$$\text{line } \overline{o\,b} = .43 \text{ inches}$$

Noting Figure 4,

$$\text{line } \overline{b\,c} = \overline{b\,d} \cos\theta = 3.06 \cos\theta$$

$$\text{line } \overline{a\,b} = \overline{o\,b} \sin\theta = 0.43 \sin\theta$$

Since torque load on spring equals weight of shield times distance $\overline{a\,c}$,

$$\text{Torque} = 10.38\ \overline{a\,c} \quad 10.38\ (\overline{a\,b} + \overline{b\,c})$$

$$\text{Torque} = 10.38\ (3.06 \cos\theta + 0.43 \sin\theta) \text{ oz-in.}$$

Using this equation, the torque which the spring must exert to overcome the earth's pull of gravity on the shield may be calculated. Results are tabulated as follows:

FIG. 5.

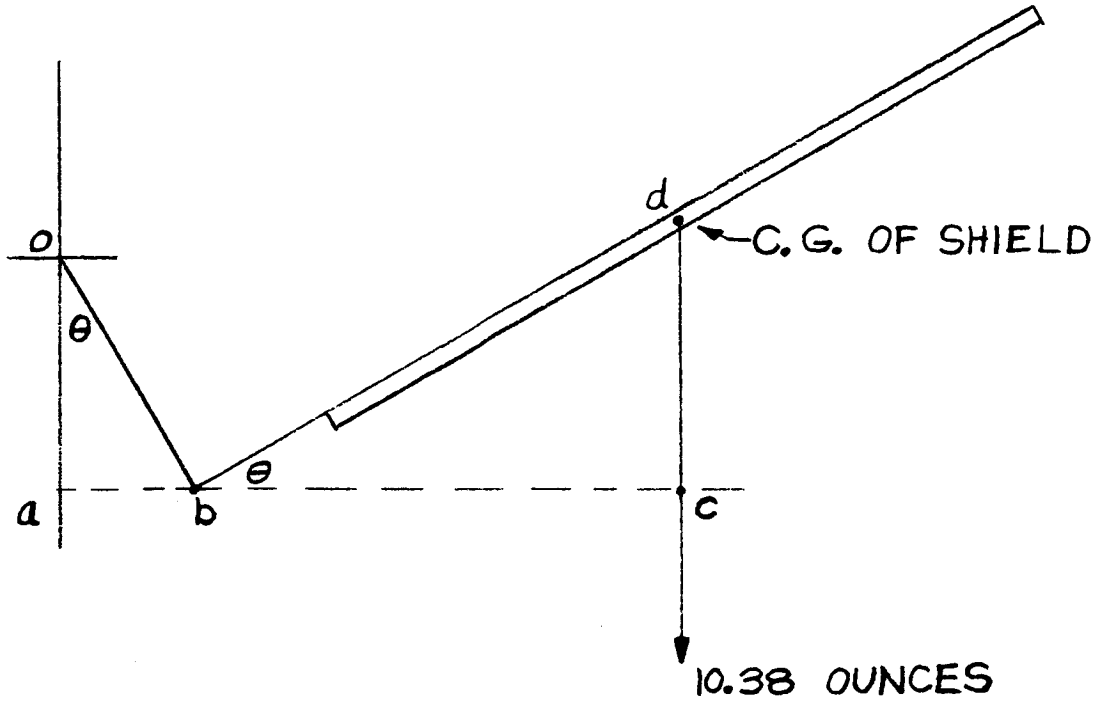

θ (degrees)	Torque oz.-in.
0	31.76
10	32.05
20	31.37
30	29.74
40	27.20
50	23.83
60	19.74
70	15.05
80	9.90
90	4.46

Referring to Figure 6.,

Spring O.D. = .80 in.

Spring Thickness = .031 in.

Mean Spring Dia. = .769 in.

$l = \sqrt{(\pi \cdot 75)^2 + (5/16)^2} = 2.377$ true length of one coil

No. of active turns at 50°F = 10

Total active length = 10(l) = 10 (2.377)

= 23.77 in.

The ideal spring thickness cannot be found directly, and therefore it is necessary to assume a thickness and solve

FIG. 6.

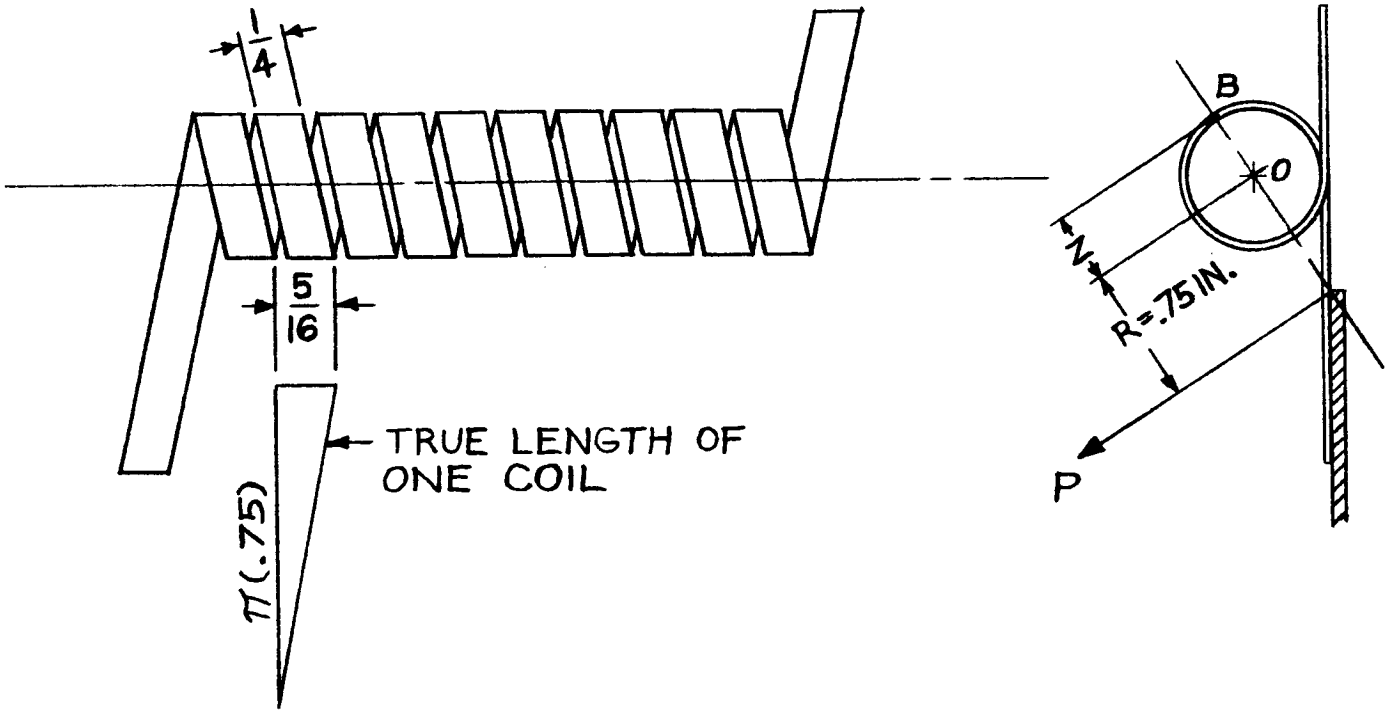

for the total angular deflection and torque per degree of rotation. Too thick a spring will not have sufficient angular rotation to move the shield through an angle of 90°, although the starting torque is very high. The optimum thickness, which is found by trial and error, is shown in the sample calculations.

$$A = \frac{T\ C\ L}{t}$$

Where A = Angular deflection in degrees

T = Temperature change in °F.

C = Spring constant for R-39 material and equals 0.00091.

L = Total active length in inches

t = optimum thickness in inches = 0.030.

$$A = \frac{(255 - 50)(.00091)(23.77)}{.030}$$

A = 148 degrees

The mechanical stiffness is given by torque rate, M_r, in oz-in. per degree rotation.

$$M = \frac{Y\ w\ t^3}{L}$$

Where Y = spring constant for R-39 material and equals 580,000.

w = spring width in inches

$$M_r = \frac{580{,}000(.25)(.030)^3}{23.77}$$

M_r = .165 oz-in./°Rot.

The above spring data was reviewed by Engelhard Industries and a stock spring thickness of 0.031 inches, an active length of 24.25 inches, and a mean diameter of 0.75 plus 0.040 minus 0.000 was recommended. The revised spring data based upon Engelhard Industries recommendations is as follows:

$$A = \frac{T\ C\ L}{t} = \frac{(255 - 50)(.00091)(24.25)}{.031} = 146 \text{ degrees}$$

$$M_T = \frac{Y\ w\ t^3}{L} = \frac{580{,}000(.25)(.031)^3}{24.25} = 0.178 \text{ oz-in/}^{o}\text{Rot.}$$

The torque that the spring is capable of exerting on the shield with a 255°F spring temperature is determined by visualizing the bimetal spring as a conventional torsion spring and noting the torque necessary to wind the spring to various angular positions starting from a free position. Therefore the torque the spring can exert on the shield, when the shield is in the horizontal position ($\theta = 0$ degrees), is found by imagining the movable end of the spring as being rotated through a 146 degree angle causing a torque build up equal to 146 degrees times the torque rate M_T. Numerically this equals 146 times 0.178 or 25.99 oz.-inches. The potential torque which the spring is capable of exerting on the shield at any angle θ may be found by the equation.

$$M = M_T\ (146 - \theta)$$

Where M is the maximum torque the spring can exert on the shield when the spring is is at 255°F.

The following tabulation shows the total potential torque of a pair of springs as compared to the theoretical load torque necessary to raise the shield at various angles of θ. The difference between the potential torque and the load torque is the reserve torque, part of which is used for overcoming friction in the shield hinge.

θ (Deg.)	Load Torque (oz.-in.)	Potential Torque (oz-in.)	Reserve Torque (oz.-in.)
0	31.76	51.98	20.22
10	32.05	48.42	16.37
20	31.37	44.86	13.49
30	29.74	41.30	11.56
40	27.20	37.74	10.54
50	23.83	34.18	10.35
60	19.74	30.62	10.88
70	15.05	27.06	12.01
90	9.90	23.50	13.60
90	4.46	19.94	15.48

From this tabulation it is seen that a 0.031 inch thick spring provides an ample reserve torque for all shield positions thereby permitting experimental testing on the earth without the aid of booster springs. On the moon the load torque will be one sixth of the earth value.

Maximum spring stress will occur when the manipulator is cooled to subzero temperatures. The white area is covered at +50°F, resulting in no further movement of the bimetal springs. The stress

at -100°F is calculated as follows to illustrate the method of calculation and to show what degree of stress can be expected at a typical subzero temperature.

The torque developed in the spring is given by the equation:

$$M = T\ Y\ C\ w\ t^2$$

Where T is the temperature differential between +50°F and -100°F. M = torque in oz-inches.

$$M = \left[\overline{50 - (-100)}\right] (580{,}000)\ (.00091)\ (.25)\ (.031)^2$$

$$M = 19.04 \text{ oz-in.}$$

Referring to Figure 6, it is seen that the torque is equal to the product P times r or:

$$P\ (r) = M$$

Where r is the lever arm in inches for a tangential turning force P about point O. On drawing 520394-E, r scales 0.75 inches.

$$P = \frac{M}{r} = \frac{19.04}{.75}$$

$$P = 25.39 \text{ oz.}$$

Maximum stress occurs at point B which has a bending moment equal to P (r + Z). Stress is given by the beam formula:

$$S = \frac{M\ (c)}{I}$$

Which for a rectangular cross section and P in ounces reduces to:

$$S = \frac{3P\ (r + z)}{8\ w\ t^2}$$

Where z = mean spring radius

Which = 0.375 inches

$$S = \frac{3\ (25.39)\ (.75 + .375)}{8\ (.25)\ (.031)^2}$$

$S = 44{,}548$ psi

As a rough guide to bimetal spring design where there is deflection restraint, the maximum safe stress as recommended by the W. M. Chase Company is 50,000 psi. Other companies such as Engelhard Industries, Inc. and Metals Controls Corporation do not suggest a maximum safe stress in their design manuals.

The following calculations illustrate the importance of enclosing the bimetal springs. A bimetal spring at 255°F will lose heat rapidly by radiation unless a cover is provided. In this application the cover, being attached to the manipulator, is at 255°F and radiates heat to the spring. Assuming that the spring is not covered and has an emissivity of 0.6 (average for rolled metals) with an external strip area of 0.0402 sq. ft., the heat radiated or lost by the spring at 50°F is:

$$H_1 = \phi\ A\ E\ T^4$$

$$= \frac{17.3}{10^{10}}\ (.0402)\ (.6)\ (460 + 50)^4 = 2.82 \text{ Btu/hr.}$$

With the white area covered by a polished gold shield, the underside of the springs are exposed to a large gold area which encloses approximately the lower half of the springs. The heat radiated to the springs per hour by this gold area is calculated by the equation:

$$H_2 = \phi\ E_g\ E_{sp} F_c\ A\ T^4$$

Where F_c = 0.5 since the springs are approximately one half enclosed.

E_{sp} = spring emissivity = 0.6

$$H_2 = \frac{17.3}{10} (.03) (.6) (.5) (.0402) (460 + 255)^4$$

$$= 0.1635 \text{ Btu/hr.}$$

Heat conducted to the spring by the gold area is:

$$H_c = \frac{k A (T_1 - T_2)}{X}$$

Where k is approximately 45 Btu/hr $ft^2{}^oF/ft$. for R-39 material.

X = one half the length of the spring in ft. The other end of the spring is also attached to a 255°F source of heat.

$(T_1 - T_2)$ = temperature differential between 255°F manipulator and the 50°F spring.

A = cross-sectional area of spring in square feet.

$$H_c = \frac{45 \frac{(.030 \times .25)}{144} (255 - 50)}{\frac{23.17}{2 (12)}}$$

H_c = .498 Btu/hr.

Total heat to spring = $H_1 + H_2$

= .498 + .1635

= 0.66 Btu/hr.

With only 0.66 Btu per hour being added to the spring which is losing heat at the rate of 2.82 Btu per hour, the spring temperature would be lower than +50°F. If the conduction rate (0.498

Btu per hour) to the spring had been considerably higher, a reflective type enclosure for preventing spring heat loss would, at first glance, appear to be the solution. However, an enclosure having a high emissivity can radiate heat to the spring at a rapid rate, thereby insuring a spring temperature which very closely parallels manipulator temperature. The net heat energy radiated from the enclosure to the spring is given by the equation:

$$H = \phi\, A_s\, F_c\, F_e\, (T_1^4 - T_2^4)$$

Where A_s = external spring surface area = 0.0402 square feet

F_e = emissivity factor = $\dfrac{1}{\frac{1}{E_c} + \frac{1}{E_s} - 1}$

Where E_c = emissivity of rolled copper = 0.6

E_s = emissivity of rolled bimetal spring = 0.6

F_c = configuration factor = 1.0 for total enclosure

T_1 = enclosure temperature in $^\circ R$ = 460 + 255°F

T_2 = spring temperature in $^\circ R$ = 460 + 50°F

$$H = \frac{17.3}{10^{10}} (.0402)\,(1) \left[\frac{1}{\frac{1}{.6} + \frac{1}{.6} - 1}\right] (715^4 - 510^4)$$

H = 5.77 Btu/hr.

It is seen that the net heat input rate to the spring by radiation is 5.77 Btu per hour as compared to 0.498 Btu per hour for conduction. Theoretically the springs are designed with ample reserve torque so that a spring temperature of 255°F will not be necessary to completely uncover the white area.

9.7 CONCLUSION

The one unknown factor which could alter the temperature equilibrium goals set forth in this analysis is micrometeorite bombardment. In this respect high performance insulation has the advantage over polished gold in that insulation ability is not entirely dependent upon the condition of the outer surface. This is very important at subzero temperatures where heat must be conserved. However, both methods require a white coated area which, if eroded, would lose the ability to reflect solar radiation, thereby causing an increase in manipulator temperature.

Elimination of the bimetal springs might be possible by having an inactive position for the manipulator such that the white area is covered by the pan drive housing when the manipulator is not in use. This is more feasible with the insulation method of temperature control since the white area is only 14 square inches as compared to 70 square inches for the polished gold method.

An insulated manipulator with the ability to operate at -70°F or lower will not require auxiliary heating during the lunar nights. If experimental tests show that the manipulator can operate at an average temperature of 300°F, then an oversize white area (approximately 20.4 square inches) will cool the manipulator when eroded from a 0.35 to a 0.9 solar emissivity. Referring to the original heat balance equation under Section 9.3:

$$\phi A_w E_w T_m^4 = 420 A_w E_{ws} + 20 + k A_i \frac{(T_s - T_m)}{x}$$

Substituting an emissivity of 0.9 for the white area for both solar and long wave length radiation (E_w = 0.9 and E_{ws} = 0.9) and also 300°F (760°R absolute) for the manipulator temperature:

$$\frac{17.3}{10^{10}} A_w (.9) (760)^4 = 420 A_w (.9) + 20$$

The conduction term is omitted since it was shown that heat conducted into the manipulator from the hot skin was negligible. With an eroded skin, the skin temperature will be cooler making this term of the equation even less significant.

Solving for A_w:

$$519 A_w = 378 A_w + 20$$

$$A_w = 0.142 \text{ sq. ft.}$$

$$A_w = 20.4 \text{ sq. in.}$$

It appears, then, that an ideal temperature control method is attainable providing the manipulator can operate between +300 and -100°F. A white area of 20.4 square inches can easily be covered by the manipulator when in an inactive position thereby eliminating bimetal springs.

The manufacturers only concern with the insulation is the high outer skin temperature which they feel will exceed 600°F. The skin has a highly reflective aluminum coating which is effective in reflecting solar radiation on cold storage tanks. On the moon the skin will not have the benefit of an air cooling medium and therefore

it would seem that a skin coating having black body characteristics would be more practical. The skin portion of the insulation facing the moon will tend to level off at moon temperature or +273°F. A black body surface facing the sun will level off at approximately +152°F. This can be shown by equating heat radiated by a black body to solar heat input to the black body or:

$$\phi \, A \, E \, T^4 = 420 \, A \, E$$

$$\phi \, T^4 = 420$$

$$\frac{17.3}{10^{10}} \, T^4 = 420$$

$$T = 702^{\circ}R$$

$$T = 152^{\circ}F$$

National Research Corporation is interested in space applications for their NRC-2 insulation and feel the insulation is rugged enough to withstand high accelerations and shock loads. Following the complex contours of the manipulator will not present any problems.

It remains to be determined how closely the temperature of the manipulator will follow the theoretical predictions given herein. To facilitate this determination, calculations as given in Section 9.4 show the anticipated effect of insulating the elliptical section of the manipulator, this section being chosen because it can be easily insulated as compared to the other manipulator components. It is recommended that after the testing of the completely polished gold manipulator is completed, the elliptical section be insulated and the manipulator retested. In this manner it is

intended that the theory presented herein can be substantiated.

Final decisions on temperature control design cannot be made until experimental tests establish maximum and minimum operating temperatures, after which reliability and weight decide the method of temperature control.

10.0 CONCLUSIONS

It is believed that the delivered manipulator represents the best stage of the art in terms of actuator design. This is especially true of the boom elevation drive assembly as meticulous care was exercised in its design to eliminate and reduce friction as well as to support loaded components in the best possible manner.

The temperature control schemes pursued in this work are thought to be unique and worthy of complete evaluation.

Fabrication difficulties with the thin copper surfaces were troublesome and not dependable. Materials with a lower, but still high, heat conduction rate (aluminum for example) should be considered for structural components. Mechanical fastening of thin sheet is probably more reliable than bonded, brazed, or welded joints.

11.0 RECOMMENDATIONS FOR TESTING AND EVALUATION

Theoretical temperature curves as presented herein should be verified by test in a lunar environmental simulator. Heat transfer between moving joints and static components should be noted. Variations from theoretical curves should be analyzed for cause.

The actuators should be tested over their entire output range from zero to stall at increments of ambient pressure and temperature comparable to a lunar environment (night and day) first without sealing the compartments and then with the compartments sealed. Duty cycles should be established by noting motor temperature rise (220^{o}C

being the upper limit).

Other lubricants (teflon powder, molybdenum disulphide, low temperature silicones) can be evaluated in the sealed enclosures if necessary or desired.

Brake and clutch performance as well as gear train measured efficiency is of great interest. The load at which the brake slips should be noted for various temperatures. Analysis of the best clutch location (motor end, output shaft end, or in between gear stages) would be welcome. The pan and tilt clutches are at the motor end and the boom elevate clutch is approximately midway in the gear train.

Determine a permissible heat conduction coefficient to allow other materials such as aluminum to be used in the outer skin.

Determine the effect during temperature change on actuator performance in bolting the actuator mounting flange to mounting surfaces having a coefficient of expansion and contraction different from that of the actuator flange. In the boom elevation drive assembly a "DU" strip was used between these materials to facilitate relative motion. Do the bolts loosen with repeated temperature cycling?

12.0 REFERENCES

1. Friction & Lubrication of Solids by Frank Phillip Boden and David Tabor, Oxford Clarendon Press - 1950

2. Exploration of the Moon, the Planets and Interplanetary Space; Report No. 30-1; Jet Propulsion Laboratory, California Institute of Technology, Pasadena, California; April 30, 1959; edited by A. R. Hibbs

3. Astronomy; Wm. Lee Kenon; Ginn & Co.; 1948

4. Popular Astronomy; 1946

5. Paris Symposium on Radio Astronomy by Bracewell; Article #6

6. Astronautica; Vol. 4-5; 1958-1959

7. Dry Bearings & Materials; Handbook No. 2; The Glacier Metal Company Limited, Alperton, Wembley, Middlesex, England

8. Heat and Mass Transfer by Eckert and Drake; McGraw Hill 1959; 2nd edition

9. Heat Transmission by W. H. McAdams; McGraw Hill 1954; 3rd edition

10. Further Studies on the Pyrolysis of Polytetrafluoroethylene in the Presence of Various Gases; Journal of Research of the National Bureau of Standards; Vol. 58, No. 6; June 1957 by J. D. Michaelsen and L. A. Wall

11. Thermal Decomposition of Polytetrafluoroethylene in Various Gaseous Atmospheres; Journal of the National Bureau of Standards; Vol. 56, No. 1; January 1956 by L. A. Wall and J. D. Michaelsen

12. Polymer Decomposition: Thermodynamics, Mechanisms and Energetics; SPE Journal, Vol. 16, No. 8, August 1960, by Leo A. Wall

13. Pyrolysis of Polytetrafluoroethylene by J. C. Siegle and L. T. Muus, Polychemicals Department, E. I. du Pont de Nemours & Co.; Inc.; Du Pont Experimental Station Wilmington, Delaware

13.0 LIST OF DRAWINGS REFERRED TO IN REPORT WHICH ARE INCLUDED IN THE FOLLOWING ENVELOPES

229866E - Lunar TV Camera Manipulator Assembly

520865D - Boom Elevation Drive Assembly

520949E - Lunar TV Camera Manipulator Assembly

229871D - Pan and Tilt Gear Box Assembly

520165R - Test Fixture Assembly

520394E - Temperature Control Mechanism